ISSUES IN CONTROL AND MONITORING OF INTELLIGENT VEHICLES

by

Li Li

A Dissertation Submitted to the Faculty of the

DEPARTMENT OF SYSTEMS AND INDUSTRIAL ENGINEERING

In Partial Fulfillment of the Requirements
For the Degree of

DOCTOR OF PHILOSOPHY

In the Graduate College

THE UNIVERSITY OF ARIZONA

2005

THE UNIVERSITY OF ARIZONA
GRADUATE COLLEGE

As members of the Dissertation Committee, we certify that we have read the dissertation

prepared by Li Li

entitled Issues in Control and Monitoring of Intelligent Vehicles

and recommend that it be accepted as fulfilling the dissertation requirement for the

Degree of Doctor of Philosophy

_____ Date: (Nov.30, 2004)
Fei-Yue Wang

_____ Date: (Nov.30, 2004)
Ferenc Szidarovszky

_____ Date: (Nov.30, 2004)
J. Cole Smith

Final approval and acceptance of this dissertation is contingent upon the candidate's submission of the final copies of the dissertation to the Graduate College.

I hereby certify that I have read this dissertation prepared under my direction and recommend that it be accepted as fulfilling the dissertation requirement.

_____ Date: (Nov.30, 2004)
Dissertation Director: Fei-Yue Wang

STATEMENT BY AUTHOR

This dissertation has been submitted in partial fulfillment of requirement for an advanced degree at The University of Arizona and is deposited in the University Library to be made available to borrowers under rules of the Library.

Brief quotations from this dissertation are allowable without special permission, provided that accurate acknowledgement of source is made. Requests for permission for extended quotation from or reproduction of this manuscript in whole or in part may be granted by the head of the major department or the Dean of the Graduate College when in his or her judgment the proposed use of the material is in the interests of scholarship. In all other instances, however, permission must be obtained from the copyright holder.

SIGNED: _____

Li Li

ACKNOWLEDGMENTS

I would like to thank my advisor, Dr. Fei-Yue Wang. Without his guidance and kindly support, I might not have the opportunity to carry out research in the field of Automated Highway Systems (AHS) and Intelligent Vehicles (IV). I would like to thank members of my committee, Dr. Szidarovszky, Dr. Zeng, Dr. Smith, and Dr. Jin. I appreciate their help in both my course work and research project.

I would like to thank all the professors of the Systems and Industrial Engineering Department. It was their guidance and support that helped me to finish these four years of tedious work. I would like to thank my friends in the University of Arizona and Tucson. Their kind encouragement and generous help makes my achievement possible and life enjoyable. I will never forget these special four years here.

Thousands of thanks to my dear parents! Their love, understanding, support and encouragement are the major motivation for me in working towards the Ph. D. degree.

TABLE OF CONTENTS

TABLE OF CONTENTS (CONTINUED)

LIST OF FIGURES

LIST OF FIGURES (CONTINUED)

LIST OF FIGURES (CONTINUED)

LIST OF TABLES

ABSTRACT

Inspired by the recent developments, we studied some recent developments and research trends in intelligent vehicle sensing and control tasks. We emphasize on advanced vehicle motion control techniques and intelligent tires. The main research motivation is to improve drivers/passengers' comfort and safety as well as highway capacity and efficiency.

In Chapter 2, we presents a review of recent developments and research trends in vehicle lateral (steering) control tasks. It is an attempt to provide a bigger picture of the very diverse, detailed and highly multidisciplinary research in this area. Based on diversely selected research, this chapter explains the initiatives and techniques for vehicle lateral (steering) control with a specific emphasis on disturbance rejection, time delay, system dynamic variation tolerance and controller saturation handling. Besides, some other related topics including vehicle lateral motion sensory and observer (virtual sensor) design are also discussed.

In Chapter 3, Lateral control of vehicles on automated highways often requires estimation of sideslip angle, yaw rate and lateral velocity, which are difficult to measure directly. Thus, several observers (virtual sensors) were developed in the last decade. To solve the unhandled estimation problem caused by dynamic model uncertainty, a robust observer using H_∞ design method is proposed in this chapter. It maintains the good disturbance rejection property that derived form previous research,

and simultaneously provides acceptable tolerance to model variance. Specially, effects of displacements of sensory, dynamics variance caused by mass/velocity/tire-road frictions change or nonlinear characteristic are studied. Simulations demonstrate the usefulness of the proposed observer.

Being parallel to frequency domain robust steering controller designs, time domain robust steering controller designs attract continuous interest in the last decade. Based on previous research results, a systematic time design framework is proposed in Chapter 4. The design task is constructed as a multi-objective optimization problem which simultaneously considers system stabilization, disturbance rejection, actuator saturation and time delay. A mixed L_1/H_∞ robust controller is finally obtained by solving a set of linear matrix equalities (LMI) that guarantee the performance requirements regarding these mentioned factors. Simulations show the effectiveness of the proposed design method.

Cooperative driving technology with inter-vehicle communication attracts increasing intentions recently. It aims to improve driving safety and efficiency using appropriate motion scheduling of all the encountered vehicles. Under cooperative driving control, the motion of individual vehicles can be conducted in a safe, deterministic and smooth manner. This is particularly useful to heavy duty vehicles, since their acceleration/deceleration capacity is relatively low. Specifically in Chapter 5, cooperative driving at blind crossings (crossings without traffic lights) is studied. A concept of safety driving patterns is proposed to represent the collision free

movements of vehicles at crossings. The solution space of all allowable movement schedules is described by a spanning tree in terms of safety driving patterns; four trajectory planning algorithms are formulated to determine the driving plans with least execution times using schedule trees. The corresponding group communication strategy for inter- vehicle networks is also analyzed. Finally, simulation studies have been conducted and results demonstrate the potentiality and usefulness of the proposed algorithms for cooperative driving at blind crossings.

Many tire fault monitors are designed nowadays because tire failure is proved to be one of the main causes of traffic accidences. However, most of them are high in manufacturing cost and unreliable. Thus Chapter 6 is devoted to solve this problem and a new practical tire fault observer is proposed. Based on the new introduced dynamic tire/road friction model that considers external disturbances, the observer estimate and track the changes of tire/road friction conditions using only vehicle track forces and wheel angular velocity information. Tire fault diagnosis is carried out as follows. Since the wheel speed sensor is one basic component of normal anti-lock brake system (ABS), the observer proposed could be easily realized in low cost within an anti-lock brake system.

CHAPTER 1 INTRODUCTION

1.1 Research Progress of Intelligent Vehicles

During the last twenty years, road traffic increases significantly, which results in frequent traffic congestions and a gradually decrease in driving safety. To handle this problem, the concepts of Intelligent Transportation Systems (ITS) had been proposed in the late 1980s and beginning of 1990s, [1]-[51].

As one component of ITS, intelligent vehicles (IV) use sensing and intelligent algorithms to “understand” environment situation around the vehicle, and either assists the driver in vehicle operations (driver assistance) or fully controls the vehicle (automation), see Larsen 1995, Shladover 1995, Ashley 1998, Martin, Marini and Tosunoglu 1999a, 1999b, Bishop 2000.

Following the success of current research, intelligent vehicle is currently viewed as the "next wave" for ITS. It is widely expected to function as the basic element to construct the whole transportation system and help it operate more effectively. On the other side, as pointed out by Vahidi and Eskandarian 2003, due to financial and practical limitations, the short-term tendency has switched from AHS to IVI, since the driver assist systems that can independently be implemented in today’s generation of cars without the costly modifications in the infrastructure. Such assist systems provide

the driver with information, warning and operational support. ACC, stop and go cruise, collision warning and collision avoidance systems are being developed in this context. When each vehicle acts the desired operations, the performance of vehicle platoon can then be improved.

Currently, this field has attracted great interests worldwide in different programs, i.e. California PATH program (i.e. Parsons and Zhang 1989, Patwardhan, Tan and Guldner 1997), Ohio State University Center for Intelligent Transportation Research (i.e. Fenton, Melocik and Olson 1976, Hatipoglu, Ozguner and Redmill 2003), The Robotics Institute of Carnegie Mellon University (i.e. Jochem, Pomerleau and Kumar et. al 1995) and Advanced Traffic & Logistics Algorithms & Systems Lab of University of Arizona (i.e. Mirchandani and Head 2001, Nobe and Wang 2001) in the United States; Daimler–Benz and MAN Project (i.e. Darenberg 1987), PROMETHEUS Program (i.e. Fritz 1995), ARGO Car project (i.e. Broggi, Bertozzi and Fascioli 1999, Broggi, Cellario and Lombardi, et. al 2003) and Project EZAuto (i.e. Sohnitz and Schwarze 1999, Simon and Becker 1999) in Europe; some programs under ITS Japan (i.e. Tsumura 1994, Tsugawa, Aoki and Hosaka et. al 1996); and a number of growing projects in China (i.e. Wang, Wang and Li et. al 2003, Wang, Tang and Sui et. al 2003, Zheng, Tang and Cheng et. al 2004).

There is no common conclusion on what functions are essential of an intelligent vehicle. In other words, researchers now argue about what vehicles can be called intelligent vehicles.

Bishop 2000 categorized the intelligent vehicles into three different levels: a) the systems which provide an advisory/warning to the driver (collision warning systems); b) the systems which take partial control of the vehicle, either for steady-state driver assistance or as an emergency intervention to avoid a collision (collision avoidance); c) the systems which take full control of vehicle operation (vehicle automation).

Generally, most researchers agree that a so called intelligent vehicle should be capable to implement function level a), because of the importance of collision avoidance. Dravidam and Tosunoglu 1999 estimated that 15% to 20% of the reported accidents involve rear-end collisions. And the National Highway Traffic Safety Administration (NHTSA) estimates that about 88% of rear-end collisions in the United States are caused by driver inattention or by vehicles following too closely. Therefore, collision warning systems is believed to be the fundamental function of an intelligent vehicle.

However, as Bishop 2000 summarized, the collision warning system itself may includes several different functions such as forward collision warning, blind spot warning, lane departure warning, lane change/merge warning, intersection collision warning, pedestrian detection and warning, backup warning, rear impact warning, and rollover warning for heavy vehicles. And to monitor the driver in case of his/her drowsy is also viewed as a special category of collision warning system. Till now, most experiment vehicles can only reach parts of the functions listed above. Thus, the strictly defined intelligent vehicle is yet to be developed.

Some researchers believed that cars won't drive themselves. For example, Jones 2002 presented his idea as follows:

"Though cars will soon be capable of doing much of what drivers do when guiding cars down a road, a car that operates without a driver's input may never see commercial production.

'New technologies are meant to complement rather than replace the driver,' said Daniel McGehee, director of the human factors research program at the University of Iowa's Public Policy Center in Iowa City. Giving the car total control, he said, raises a tangle of complex legal questions like, 'Who is responsible in the event of an accident - the driver or the carmaker? '

Other vehicle-sensing and human factors researchers, speaking under condition of anonymity, stressed the potential for crippling liability claims against auto manufacturers and makers of smart car systems.

In view of that deterrent, movie- and TV-inspired visions of a future in which cars ask only that their driver select the destination will remain confined to celluloid."

However, more other researchers aimed to build totally automatons vehicle within the next twenty years, see Simon and Becker 1999, Simon, Sohnitz and Becker et. al 2000.

Fig.1.1 shows a great commercial example designed by Technical University Braunschweig. This driving robot "Klaus" is a practical driving robot developed by German carmaker Volkswagen, which is driving a VW Multi-van on a test track. But

the cars will not be able to drive and navigate only with the robot-driver. The sophisticated car control systems and sensor technology were also used to identify the surroundings and calculate the desired course.

Figure 1.1 "Klaus," the driving robot developed by German carmaker Volkswagen, drives a VW Multi-van on a test track (from http://www.vw-personal.de/)

Besides the classification method of Bishop 2000, to detect and warn of dangerous engine status, abnormal tire pressure or other similar faults is taken as another important function of intelligent vehicle recently. For example, Pohl, Steindl and Reindl 1999, Wang, Shan and Ding et. al 2002 showed that many traffic accidences, extremely some really bad ones, were caused by tire failure.

Beyond the driving safety, the driving performance including comfort and time optimality achieved increasing research interests too; see Li and Wang 2002, Weber and Weisbrod 2003. For example, Metz and Williams 1989 investigated how to get shortest driving time for racing cars. And in the design of Li and Wang 2002, the

driver/passengers' feeling of vehicle speed are quantified and analyzed to guide the vehicle speed adjusting.

There are some other requirements of the next generation intelligent vehicles, i.e. save oil and pollution free; see Menig and Coverdill 1999. Since this topic has little to do with intelligent vehicle motion control and sensing, we will not examine them within this dissertation.

Here, we think that a general intelligent vehicle research should cover the following fields including:

(1) hardware: smart sensory, new control devices and intelligent center;

(2) software: advanced control algorithms, and intelligent decisions.

First, a vehicle is a highly complex system comprising a large number of mechanical, electronic, and electromechanical elements. To describe all the movements of the vehicle, numerous measurements and mathematical model are required. Besides real sensors, many virtual sensors (online observer or real-time estimation procedure) are proposed too.

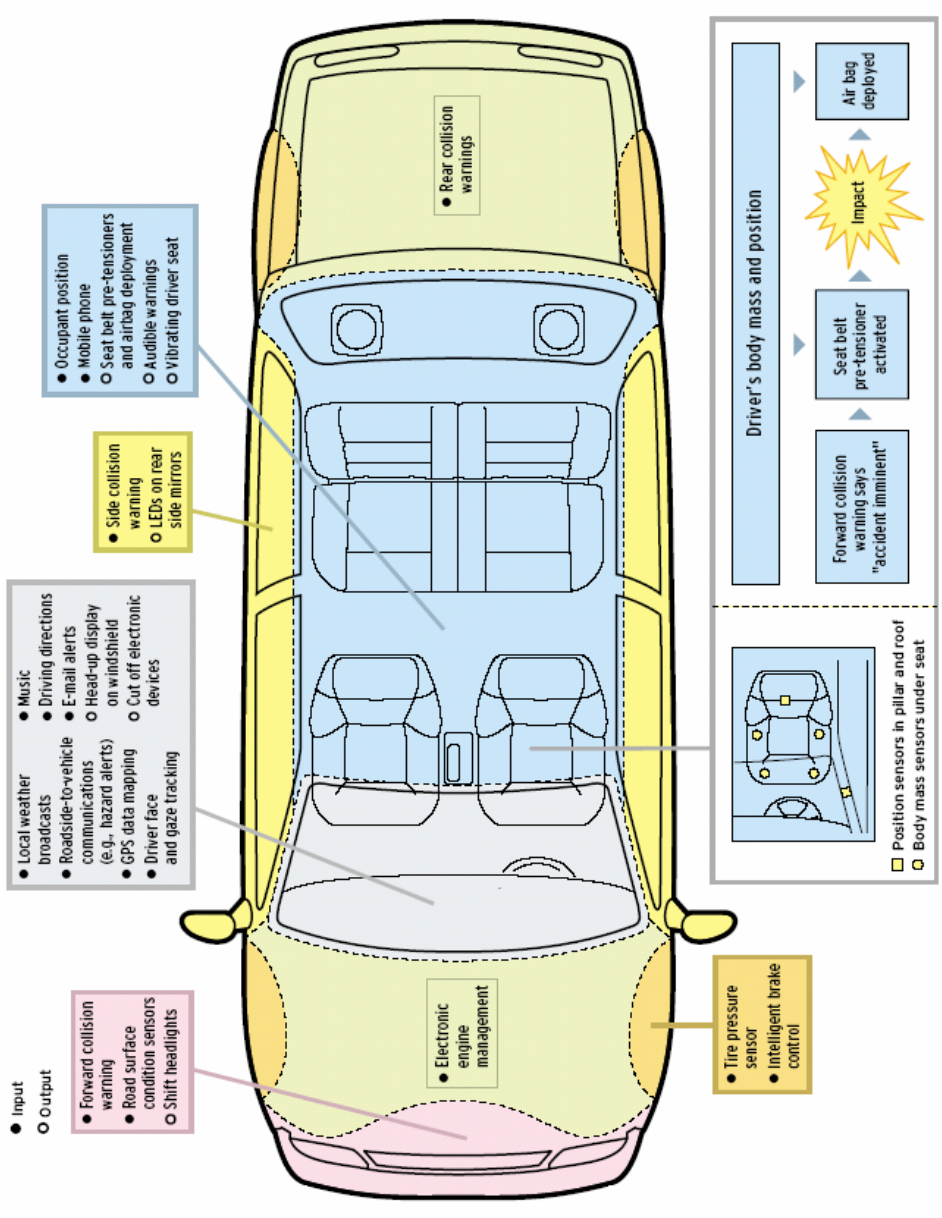

Figure 1.2 Vehicle Intelligent Sensors [19]

With the developing of sensor technology, sensor fusion of intelligent vehicle becomes a new research direction in this field. For instance, Jones 2002 arranged the intelligent sensors into several independent groups as shown in Fig.1.2. In his plan, the input data is managed from myriad sensors and used for make split-second

decisions that may involve taking control from the driver. As an example, when forward collision warning senses that a crash is imminent, data from body mass and position sensors in the cabin instantly adjust the amount of force with which air bags are deployed and seat belts are tightened. Noting that this is still a novel research direction, we will not discuss sensor fusion within this dissertation

Second, increasing requirements of safe and comfortable driving have led vehicle manufacturers and suppliers to actively pursue development programs in the so called "by-wire" subsystems. These computer-controlled subsystems include steer-by-wire, brake-by-wire, drive-by-wire and etc, which are connected through in-vehicle computer networks. A steer-by-wire system replaces the traditional mechanical linkage between the steering wheel and the road wheel actuator (e.g., a rack and pinion steering system) with an electronic connection. Because it removes direct kinematical relationship between the steering and road wheels, it enables control algorithms to help enhance driver steering command, see Claesson, Poledna and Soderberg 1998, Huh, Seo and Kim et. al 1999, Hayama, Nishizaki and Nakano et. al 2000, Yih, Ryu and Gerdes 2003.

If we take the intelligent sensors as human’s eyes and ears, the intelligent center and the intelligent controller should be considered as human’s brain and arms respectively. The intelligent center is usually a microcomputer that links all the sensors and control devices. It uses the information that is collected from the environment near the vehicle though intelligent sensors, and makes decisions of the

vehicle motion based on pre-stored control algorithms. Apparently, they are the most important electronic devices in an intelligent vehicle, see Chowanietz 1995a, 1995b, Ronald 1999, Schoner and Hille 2000, Kiencke 2001, Ribbens 2002 and Hori 2002.

Advanced control algorithms and intelligent decisions are essential for an intelligent vehicle, since it needs to help the driver to find the optimal driving plan, translate the driving demand into actual, usually complex, mechanical or electronic operations and execute them. It is also expected to be capable to detect any error driving behavior when the driver makes wrong actions, or any fault of sensors/actuators.

For example, when the intelligent center “see” a moving obstacle on the road in front of vehicle, it would invoke certain procedures to determine whether this obstacles will hinder the motion of it or not. If it decided that this obstacle would not bother its motion, it would continue its original motion. Otherwise it would either stop or steer this obstacle. Such simple control algorithms may collaborate with each other so as to implement certain complex actions. As a typical example, Fig.1.3 shows the flowchart of an intelligent vehicle’s navigation algorithm that was proposed by Simon and Becker 1999. We can see that the complex obstacle avoidance function is divided and studied as several individual and relatively simpler functions. Due to cost consideration, most researcher focus on how to implement such individual operations. In this dissertation, we will address the research advance of these simpler functions,

while the control synthesis is neglected since it is still premature and under further discussions.

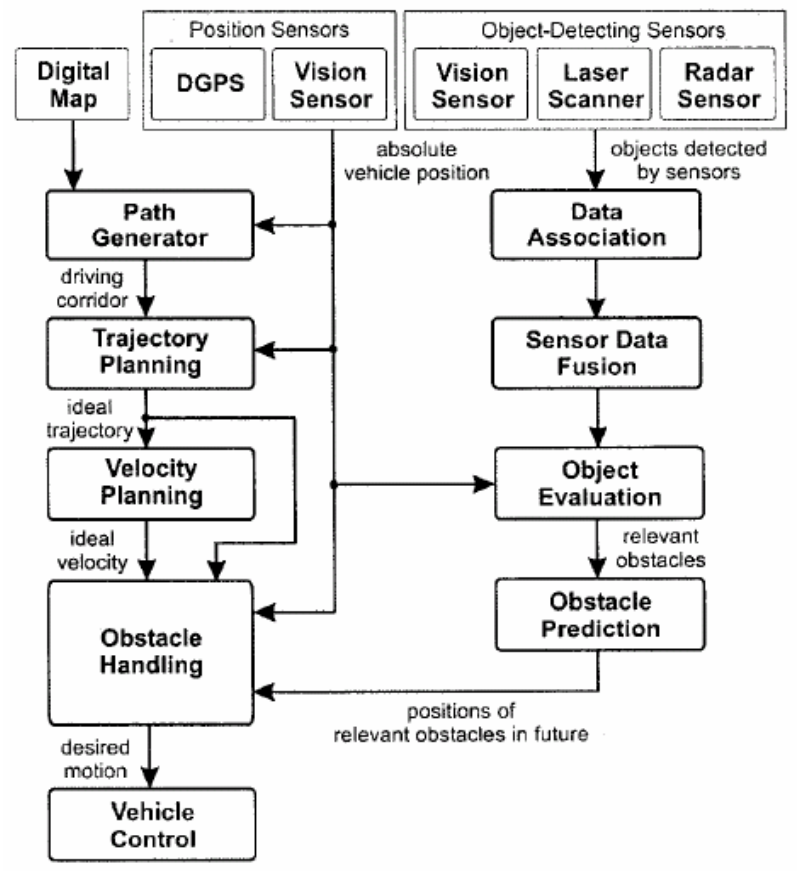

Figure 1.3 Intelligent vehicle navigation algorithm [39]

1.2 Our Efforts in Intelligent Vehicle Field

Inspired by the recent developments, we studied some recent developments and research trends in intelligent vehicle sensing and control tasks. Among the very diverse, detailed and highly multidisciplinary research in this area, we emphasize on advanced vehicle motion control techniques and intelligent tires. The main research motivation is to improve drivers/passengers' comfort and safety as well as highway

capacity and efficiency. Some research results are listed in Fig.1.4 below.

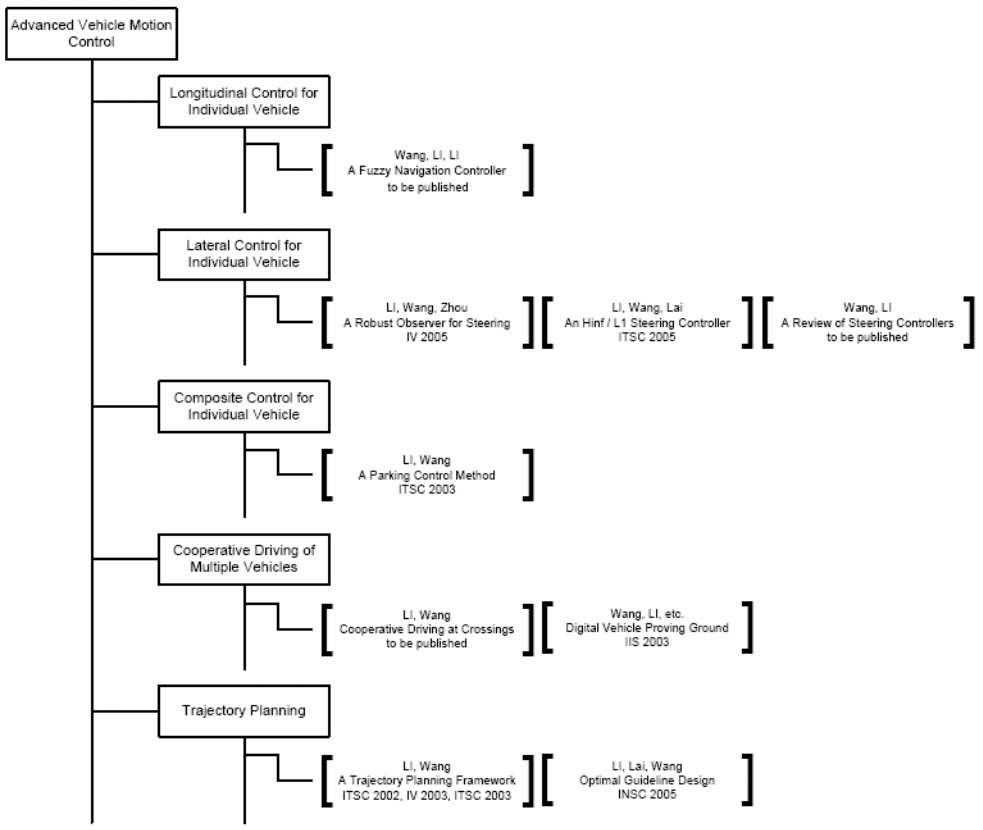

(a)

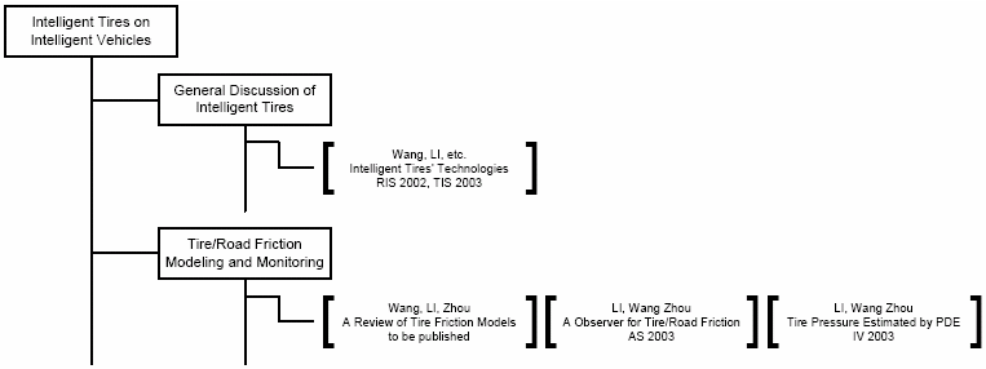

(b)

Figure 1.4 Research directions demonstrated in tree forms: (a) reports related to advanced vehicle motion control, (b) reports related to intelligent tires.

During developing process of intelligent traffic and intelligent vehicles, varied

problems emerge, which motivate an increasing amount of research on related topics. Although this dissertation tires to provide a broad overview of all the corresponding cutting-edge techniques and applications in intelligent vehicle research, we cannot discuss everything encountered in details. Thus, we mainly addressed our contributions in the rest of this dissertation.

1.3 Outline of this Dissertation

The following five chapters of this dissertation are arranged as follows.

Chapter 2 presents a review of recent developments and research trends in vehicle lateral (steering) control tasks. It is an attempt to provide a bigger picture of the very diverse, detailed and highly multidisciplinary research in this area. Based on diversely selected research, this chapter explains the initiatives and techniques for vehicle lateral (steering) control with a specific emphasis on disturbance rejection, time delay, system dynamic variation tolerance and controller saturation handling. Besides, some other related topics including vehicle lateral motion sensory and observer (virtual sensor) design are also discussed.

In Chapter 3, Lateral control of vehicles on automated highways often requires estimation of sideslip angle, yaw rate and lateral velocity, which are difficult to measure directly. Thus, several observers (virtual sensors) were developed in the last decade. To solve the unhandled estimation problem caused by dynamic model uncertainty, a robust observer using H_∞ design method is proposed in this chapter. It

maintains the good disturbance rejection property that derived form previous research, and simultaneously provides acceptable tolerance to model variance. Specially, effects of displacements of sensory, dynamics variance caused by mass/velocity/tire-road frictions change or nonlinear characteristic are studied. Simulations demonstrate the usefulness of the proposed observer.

Being parallel to frequency domain robust steering controller designs, time domain robust steering controller designs attract continuous interest in the last decade. Based on previous research results, a systematic time design framework is proposed in Chapter 4. The design task is constructed as a multi-objective optimization problem which simultaneously considers system stabilization, disturbance rejection, actuator saturation and time delay. A mixed L_1/H_∞ robust controller is finally obtained by solving a set of linear matrix equalities (LMI) that guarantee the performance requirements regarding these mentioned factors. Simulations show the effectiveness of the proposed design method.

Cooperative driving technology with inter-vehicle communication attracts increasing intentions recently. It aims to improve driving safety and efficiency using appropriate motion scheduling of all the encountered vehicles. Under cooperative driving control, the motion of individual vehicles can be conducted in a safe, deterministic and smooth manner. This is particularly useful to heavy duty vehicles, since their acceleration/deceleration capacity is relatively low. Specifically in Chapter 5, cooperative driving at blind crossings (crossings without traffic lights) is studied. A

concept of safety driving patterns is proposed to represent the collision free movements of vehicles at crossings. The solution space of all allowable movement schedules is described by a spanning tree in terms of safety driving patterns; four trajectory planning algorithms are formulated to determine the driving plans with least execution times using schedule trees. The corresponding group communication strategy for inter- vehicle networks is also analyzed. Finally, simulation studies have been conducted and results demonstrate the potentiality and usefulness of the proposed algorithms for cooperative driving at blind crossings.

Many tire fault monitors are designed nowadays because tire failure is proved to be one of the main causes of traffic accidences. However, most of them are high in manufacturing cost and unreliable. Thus Chapter 6 is devoted to solve this problem and a new practical tire fault observer is proposed. Based on the new introduced dynamic tire/road friction model that considers external disturbances, the observer estimate and track the changes of tire/road friction conditions using only vehicle track forces and wheel angular velocity information. Tire fault diagnosis is carried out as follows. Since the wheel speed sensor is one basic component of normal anti-lock brake system (ABS), the observer proposed could be easily realized in low cost within an anti-lock brake system.

CHAPTER 2 RESEARCH ADVANCES IN VEHICLE LATERAL MOTION CONTROL

This chapter presents a review of recent developments and research trends in vehicle lateral (steering) control tasks. It is an attempt to provide a bigger picture of the very diverse, detailed and highly multidisciplinary research in this area. Based on diversely selected research, this chapter explains the initiatives and techniques for vehicle lateral (steering) control with a specific emphasis on disturbance rejection, time delay, system dynamic variation tolerance and controller saturation handling. Besides, some other related topics including vehicle lateral motion sensory and observer (virtual sensor) design are also discussed.

2.1 Introduction

Increasing traffic congestion and accidents inspired the concepts of Automated Highway Systems (AHS) and Intelligent Vehicle (IV) more than twenty years ago. Among a variety of techniques that had been introduced, the concept of Advanced Vehicle Control Systems (AVCS) gets significant interests world-widely [53]-[55].

Advanced vehicle control systems help drivers by taking control of the steering, brakes and/or throttle to maneuver the vehicle in a safe sate. Thus, it is also called driver aid systems and intelligent (autonomous) driving systems in some literals. The

related technologies include smart cruise control, collision avoidance systems, and vehicle platooning, etc. On the aspects of motion control, corresponding research can be divided into three directions: lateral control, longitudinal control and their combinations.

The main task of longitudinal control is vehicle following/ tracking. It requires that an appropriate headway should be maintained between the lead vehicle and the controlled vehicle to avoid collision. The lateral control usually refers to vehicle steering control. Its prime task is path (road) following, or plainly, to keep the vehicle on the road.

From the viewpoint of steering, vehicles can be divided into two kinds: single track vehicles and track-trailers, see Fig.2.1. Track-trailer systems consist of a steering tractor and one (sometimes more than one) passive trailer(s) linked with rigid free joints. Single track vehicles usually refer to passenger cars or car-like vehicles/robots which can be viewed as a steering tractor. Single track vehicles can be further classified into two types: front steering vehicles (2WS) in which only the two front tires can be steered and full steering vehicles (4WS) of which the front and rear tires can be steered independently. Since the discussion of track-trailers steering control requires a dedicated paper due to its broad range, it is not addressed here.

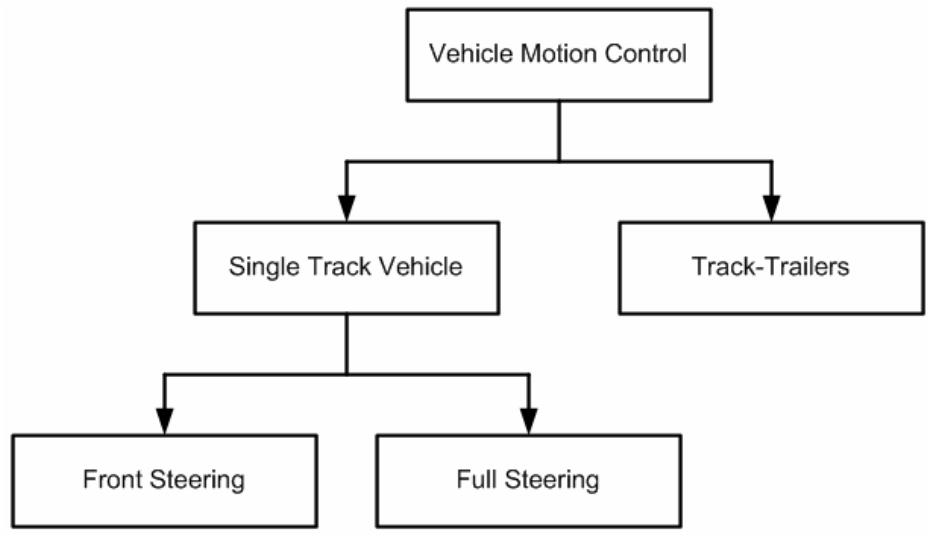

Figure 2.1 Classification of vehicle lateral motion control models.

In this chapter, we sequentially look into the following areas of vehicle lateral motion control: 1) control devices and sensory; 2) lateral motion model; 3) lateral motion observer; and 4) lateral motion controller. Only the last topic is extended and discussed in details. Specially, robust controller, sliding mode controller, adaptive controller and fuzzy controller are addressed. While it is impossible to cover the large number of publications in this area, the key findings and trends of research are included. The focus is on more recent literature since good reviews already exist on the relatively long history of the subject [77], [79], [98], [141].

2.2 Advance in Steering Control Devices

2.2.1 Steer-by-Wire

Increasing requirements of safe and comfortable driving have led vehicle

manufacturers and suppliers to actively pursue development programs in the so called "by-wire" subsystems. These computer-controlled subsystems include steer-by-wire, brake-by-wire, drive-by-wire and etc, which are connected through in-vehicle computer networks.

A steer-by-wire system replaces the traditional mechanical linkage between the steering wheel and the road wheel actuator (e.g., a rack and pinion steering system) with an electronic connection. Because it removes direct kinematical relationship between the steering and road wheels, it enables control algorithms to help enhance driver steering command [56]-[59].

For instance, Fig.2.2(b) shows a production model which was modified for full steer-by-wire capability by replacing the steering shaft with a brushless DC servomotor actuator [59]. A rotary position sensor measures the lower steering shaft angle, which is equal to the front wheel steer angle scaled by the steering ratio. An identical sensor attached to the upper steering shaft measures the hand wheel angle. The servomotor actuator specifications are chosen based on the maximum torque and speed necessary to steer the vehicle under typical driving conditions including moderate emergency maneuvers.

It was reported in [56]-[59] that the response in steer-by-wire system is more quickly and accurately than that in conventional steering system. This improves vehicle stability and provides a basis for fault detection. Moreover, it was showed in [57] and [59] that by effectively changing front cornering stiffness, the same vehicle

can be made to handle differently. Therefore, it is possible to maintain consistent handling characteristics under variable operating conditions. Nevertheless, steer-by-wire also simplifies assembly and reduces vehicle's mass. For example, in the steer-by-wire system proposed in [59], only the stock hydraulic power assist unit and rack and pinion mechanism is retained. This therefore allows flexibility in packaging.

In general, steer-by-wire system is expected to provide a better operation platform of the lateral motion controllers.

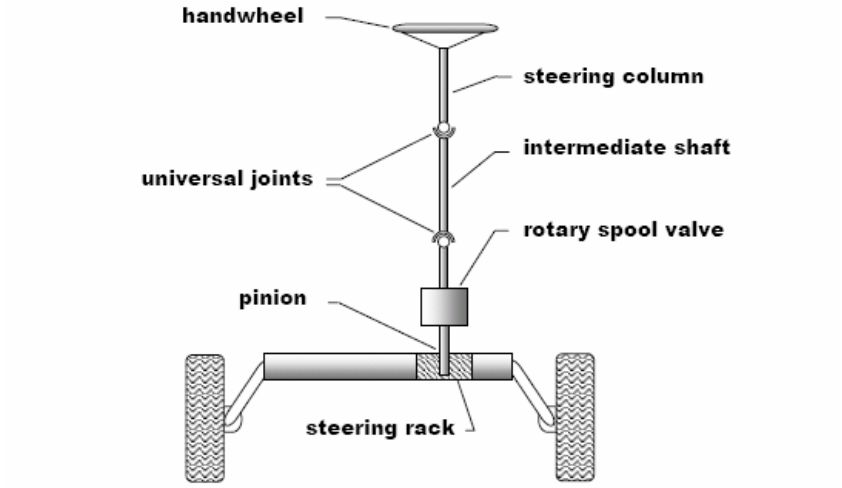

(a)

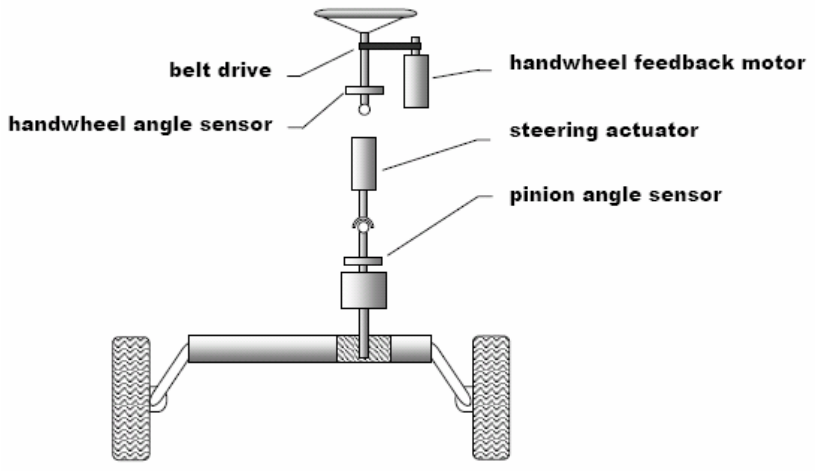

(b)

Figure 2.2 Diagram of steering systems: (a) conventional steering system, (b) steer-by-wire system [59].

2.2.2 Steering Related Sensory

Since a vehicle is a highly complex system that constitutes of varied mechanical, electronic and electromechanical elements, numerous sensors were designed and applied to measure the movement information. Concentrated on vehicle lateral motion control, position and movement information of a vehicle need to be accurately measured.

In [69], sensors for lateral control are categorized into two types: infrastructure-based and infrastructure-independent. Examples of the infrastructure-based systems include discrete magnetic reference markers and continuous magnetic tape [67]-[69]. The infrastructure-independent methods use, for example, global positioning system (GPS), inertia position system (INS), or vision system for sensing [60]-[76], [80]. However, these infrastructure-independent systems

still rely on infrastructure in the sense of reliable roadway markings in the former case, and a reliable and accurate roadway geographical information system (GIS) database.

Global positioning system (GPS), inertial navigation system (INS) and their combinations attract great interest in the last decade. The position and velocity of a vehicle can be directly measured by using global position systems [60]-[61]. It had been proven in several literals including [62]-[64] that sideslip angle, yaw rate, heading angle and position displacements can be indirectly estimated with cooperated inertial navigation system and global position systems. The newly developed fiber optic gyroscopes (FOP) are capable to measure sideslip angle, yaw rate, heading angle straightforward with high accuracy [65]-[66]. But current FOPs usually require considerable installing and maintaining cost, which prevents their widely application in the near future.

Magnetic sensing is another promising technology that has been developed recently for the purposes of vehicle position measurement and guidance. By using either magnetic tape or magnetic markers, vehicle position displacement can be gotten as well some other useful information [67]-[69]. Besides, vision sensors can also be employed to measure displacement. For example, the offset between the vehicle and curve can be accurately obtained by using the laser sensor proposed in [70]. However, measure performance of these two methods is more vulnerable to environment disturbances than that of the above two techniques, i.e. the laser sensor is sensitive to fog.

In the rest of this chapter, we assume all the information needed has already been accurately measured.

2.3 Vehicle Lateral Motion Model and Estimation

2.3.1 Bicycle Model

Lateral vehicle dynamics has been studied since the 1950s [71]-[72]. In 1956, Segel presented a vehicle model with three degrees of freedom in order to describe lateral movements including roll and yaw. If roll movement is neglected, a simple model known as "bicycle model" is obtained. This model is widely used for studies of lateral vehicle dynamics (yaw and sideslip) now. The following discussions will be primly carried out based on this model.

Suppose the vehicle is moving on a flat surface. By lumping the four wheels into one virtual wheel in the centerline of the vehicle, we can have front steering and full steering models as shown in Fig.2.3(a) and Fig.2.3(b) respectively [73]-[75].

Here Reference point ***CG*** is chosen to represent the center of gravity for vehicle body, where vehicle velocity v is defined. Symbol ***A*** and ***B*** denote the positions of front and rear tire/road interfaces respectively. Heading angle ψ is the angle from the guideline to the longitudinal axis of vehicle body ***AB***. Slide-slip angle β is the angle from the longitudinal axis of vehicle body to the direction of the vehicle velocity. δ_f is the front tires steering angle. δ_r is the rear tires steering angle. Yaw rate is denoted as r. f_f and f_r are the front and rear tire forces which are

perpendicular to the directions of tire movements, respectively. f_w is the wind forces acting on the aerodynamic center of the side surface and l_w denotes the distance between ***CG*** and aero-dynamical center of the side surface. l_{fs} and l_{rs} denotes the distances from the front and rear sensor "looking at" points to ***CG***, respectively. y_f and y_r represent the displacements from the front and rear "looking at" points to the guideline. Other variables are given in Table.2.I, in which the values are set for a city bus O 305 based on IFAC benchmark example [74]. Here, c_f and c_r denote the cornering stiffness of front and rear tires respectively, which we will use in the following Eq. (2.7)-(2.8).

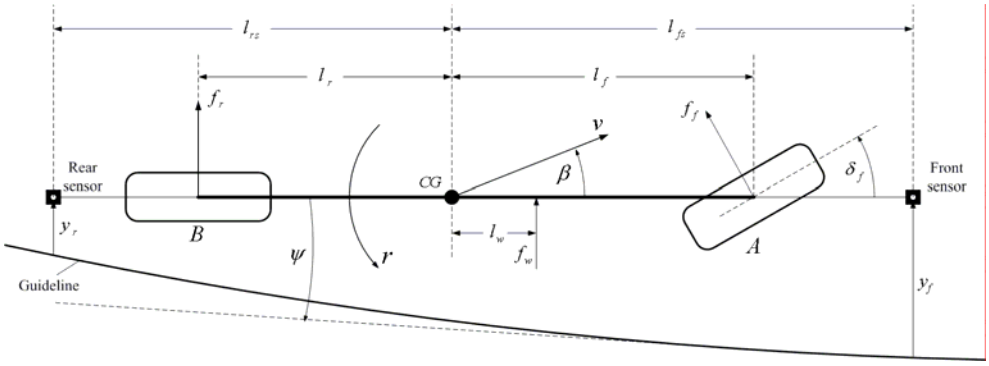

(a)

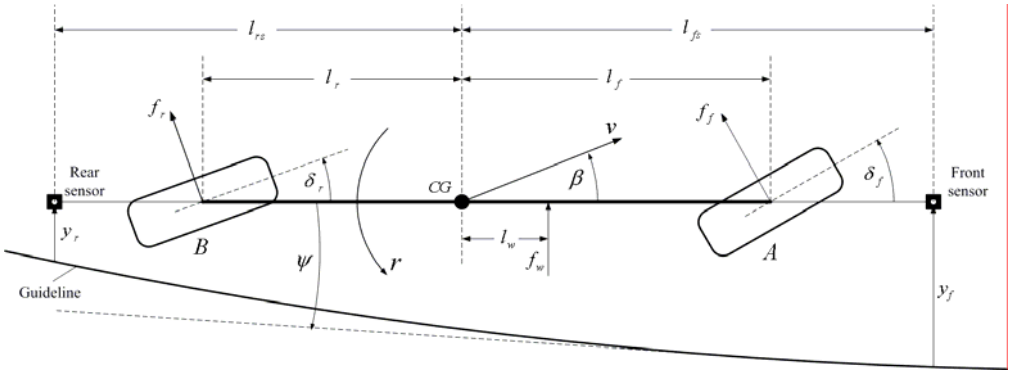

(b)

Figure 2.3 "Bicycle" steering model: front steering (a) and full steering (b).

Table 2.1 Parameters and Their Typical Values

Symbols	Typical values
Mass of the vehicle m	[9950, 16000]kg
Initial moment around z-axis I_z	[10.85, 21.7]Ns/rad
Distance from ***A*** and ***CG*** l_f	3.67m
Distance from ***B*** and ***CG*** l_r	1.93m
l_{fs}	6.12m
Stiffness coefficients of front tire c_f	198000N/rad
Stiffness coefficients of rear tire c_r	470000N/rad

Assuming that vehicle has a constant velocity, front steering model with nonlinear tire force characteristics can be described by the differential equations

$$\frac{d}{dt}\begin{pmatrix}\beta\\ r\end{pmatrix}=\begin{pmatrix}\dfrac{f_f+f_r}{mv}-r\\ \dfrac{l_f f_f - l_r f_r}{I_z}\cos\beta\end{pmatrix} \tag{2.1}$$

Using the famous "magic" formulas of tire/road friction given in [76]-[77], we have

$$f_f = D_f \sin\left\{C_f \tan^{-1}\left(B_f\left[1-E_f\right]\alpha_f + E_f \tan^{-1}\left(B_f\alpha_f\right)\right)\right\} \tag{2.2}$$

$$f_r = D_r \sin\left\{C_r \tan^{-1}\left(B_r\left[1-E_r\right]\alpha_r + E_r \tan^{-1}\left(B_r\alpha_r\right)\right)\right\} \tag{2.3}$$

$$\begin{cases}\alpha_f = \beta + \tan^{-1}\left(\dfrac{l_f}{v}\cdot r\cos\beta\right) - \delta_f\\ \alpha_r = \beta - \tan^{-1}\left(\dfrac{l_f}{v}\cdot r\cos\beta\right)\end{cases} \tag{2.4}$$

where α_f is the slip angle of front tires, α_r is the slip angle of rear tires. The coefficients B_j, C_j, D_j and E_j ($j=f,r$) in the models can be calculated in practice.

In [78], Ono, Hosoe and Tuan et. al analyzed the bifurcation phenomena in above

model (1)-(4). The vehicle unstabilization was shown to be caused by a saddle-node bifurcation which depends heavily on the rear tire side force saturation. By approximating the nonlinearities with

$$\cos\beta \cong 1,\ \ \alpha_f \cong \beta + \frac{l_f}{v}\cdot r + \delta_f,\ \ \alpha_r \cong \beta - \frac{l_f}{v}\cdot r \tag{2.5}$$

They approximated the Jacobian matrix of system model $\frac{d}{dt}\begin{pmatrix}\beta\\ r\end{pmatrix} = F(\beta, r, \delta_f)$ at equilibrium point χ_0 by the matrix

$$A_{\chi_0} = \begin{bmatrix} -\frac{c_f^* + c_r^*}{mv} & -1 - \frac{l_f c_f^* - l_r c_r^*}{mv^2} \\ -\frac{l_f c_f^* - l_r c_r^*}{I_z} & -\frac{l_f^2 c_f^* + l_r^2 c_r^*}{I_z v} \end{bmatrix} \tag{2.6}$$

where c_f^* and c_r^* are the tangents to slopes of front and rear side force characteristics at equilibrium point χ_0 respectively. The bifurcation situation around point χ_0 has been checked. It showed that the linear system should be stable at a relatively large neighborhood of this equilibrium point.

If cornering stiffness c_f^* and c_r^* is taken to be constant, we can write the linear dynamic model for front steering vehicle as

$$\begin{bmatrix}\dot\beta\\ \dot r\\ \dot\psi\\ \dot y_f\\ \dot y_r\end{bmatrix} = \begin{bmatrix} a_{11} & a_{12} & 0 & 0 & 0\\ a_{21} & a_{22} & 0 & 0 & 0\\ 0 & 1 & 0 & 0 & 0\\ v & l_{fs} & v & 0 & 0\\ -v & -l_{rs} & v & 0 & 0\end{bmatrix}\begin{bmatrix}\beta\\ r\\ \psi\\ y_f\\ y_r\end{bmatrix} + \begin{bmatrix} b_{11} & 0 & d_1\\ b_{21} & 0 & d_2\\ 0 & -v & 0\\ 0 & -vl_{fs} & 0\\ 0 & vl_{rs} & 0\end{bmatrix}\begin{bmatrix}\delta_f\\ \rho_{ref}\\ f_w\end{bmatrix} \tag{2.7}$$

Similarly, the linear dynamic model of full steering vehicle is written as

$$\begin{bmatrix}\dot\beta\\ \dot r\\ \dot\psi\\ \dot y_f\\ \dot y_r\end{bmatrix} = \begin{bmatrix} a_{11} & a_{12} & 0 & 0 & 0\\ a_{21} & a_{22} & 0 & 0 & 0\\ 0 & 1 & 0 & 0 & 0\\ v & l_{fs} & v & 0 & 0\\ -v & -l_{rs} & v & 0 & 0\end{bmatrix}\begin{bmatrix}\beta\\ r\\ \psi\\ y_f\\ y_r\end{bmatrix} + \begin{bmatrix} b_{11} & b_{12} & 0 & d_1\\ b_{21} & b_{22} & 0 & d_2\\ 0 & 0 & -v & 0\\ 0 & 0 & -vl_{fs} & 0\\ 0 & 0 & vl_{rs} & 0\end{bmatrix}\begin{bmatrix}\delta_f\\ \delta_r\\ \rho_{ref}\\ f_w\end{bmatrix} \tag{2.8}$$

where

$$a_{11} = -(c_r + c_f)/\tilde{m}v, \quad a_{12} = -1 + (c_r l_r - c_f l_f)/\tilde{m}v^2$$

$$a_{21} = (c_r l_r - c_f l_f)/\tilde{I}_z, \quad a_{22} = -(c_r l_r^2 + c_f l_f^2)/\tilde{I}_z v$$

$$b_{11} = c_f/\tilde{m}v, \quad b_{12} = c_r/\tilde{m}v, \quad b_{21} = c_f l_f/\tilde{I}_z$$

$$b_{22} = -c_r l_r/\tilde{I}_z, \quad d_1 = 1/mv, \quad d_2 = l_w/I_z$$

Here $\tilde{m} = m/\mu$ and $\tilde{I}_z = I_z/\mu$ are the normalized mass and inertia respectively, in which μ is common road adhesion factor. ρ_{ref} is the curvature of the guideline. The contribution of ρ_{ref} to y_f or y_r is sometimes neglected, since it is small.

It should be pointed out that cornering stiffness varied with several factors. One factor is that it increases with tire pressure. When the car turns, the mass transfer onto the external wheels increases tire pressure, which can lead to notable variations in cornering stiffness. Stephant, Charara and Meizel showed in [79] that such variations are normally less than 10% and still tolerant for most robust steering controllers.

Full steering vehicles outperform front steering vehicles in handling and stability significantly [145]. Usually, when the vehicle enters the curved path, the rear wheel will first steer in the opposite direction to the front wheel in order to generate sufficient yaw motion to follow the desired yaw rate. After that, the rear wheel steers will synchronize with the front wheel to keep the yaw rate with desired value and also control the lateral motion for path tracking. Since most controller design methods can be applied to both situations without extreme modifications, we will not emphasis the difference between front steering vehicles and full steering vehicles in the rest of this

chapter.

The design specifications of steering controller are primarily given in terms of maximal displacement from the guideline and maximal steering angle and steering angle rate. For instance, the benchmark problem mentioned in [74] mainly requires

1) the steering angle is limited as

$$\left\|\delta_f\right\| \le 40 \text{ deg} \tag{2.9}$$

2) the steering angle rate is limited as

$$\left\|\dot{\delta}_f\right\| \le 28 \text{ deg/ } s \tag{2.10}$$

3) The displacement from the guideline must not exceed 0.15m in transient state and 0.02m in steady state;

4) The lateral acceleration must not exceed 2m/s for passengers comfort. The ultimate limit is 4m/s.

Generally, "bicycle" model grasps the prime characteristics of vehicle steering movement and yields a relatively simple linear model for analyzing. Thus it was widely used in steering controller design in the last decade.

2.3.2 Other Vehicle Lateral Motion Models

Besides the "bicycle" model, there were some other dynamic models that had been proposed and analyzed. These models usually set up the direct relationships of

vehicle longitudinal and lateral speeds in terms of steering angle. Many of them also considered some unhandled factors that are left untouched in "bicycle" model. For instance, the vehicle dynamics in [80] tried to incorporate vehicle aerodynamics into lateral motion model. It was represented by the following set of nonlinear systems equations

$$\begin{cases} \dot{v}_x = \frac{1}{m}[T + mv_y r - mfg + c_f \frac{v_y + l_f r}{v_x}\delta_f + v_x^2(fk_1 - k_2)] \\ \dot{v}_y = \frac{1}{m}[(c_f + T)\delta_f - (c_f + c_r)\frac{v_y}{v_x} - (l_f c_f - l_r c_r + mv_x^2)\frac{r}{v_x}] \\ \dot{r} = \frac{1}{I_z}[(l_f c_f + T)\delta_f - (l_f c_f - l_r c_r)\frac{v_y}{v_x} - (l_r^2 c_r + l_f^2 c_f)\frac{r}{v_x}] \end{cases} \tag{2.11}$$

where v_x and v_y are vehicle's longitudinal velocity and lateral velocity in vehicle coordinate respectively. T is the traction and/or braking force. f is the rotation coefficients. k_1 and k_2 are lift and drag parameters from aerodynamics respectively.

Besides, the following mapping function (12) describes the relationship between vehicle velocities denoted in orthogonal coordinates and that denoted in world coordinates

$$\begin{cases} \dot{x} = v_x \cos(\psi) - v_y \sin(\psi) \\ \dot{y} = v_x \sin(\psi) + v_y \cos(\psi) \\ \dot{\psi} = r \end{cases} \tag{2.12}$$

where (x, y) denote vehicle center gravity's position in world coordinates. The displacement driving requirements were brought in terms of (x, y) straightforward.

There has been considerable theoretical and experimental research on developing vehicle models of different levels of complexity. Thorough discussions requirement a dedicated publication and are not discussed in this chapter.

2.3.3 Lateral Motion Estimation

In many recent approaches, not all the vehicle characteristics are directly measured due to high cost or some other reasons. Instead, several special observers are used to reconstruct the needed information. In literals, these observers were also called virtual sensors.

For example, knowledge of sideslip angle, yaw rate and lateral velocity is essential in vehicle control, but is difficult to obtain directly. In 1997 and 1999, Kiencke etc. proposed a linear observer and a nonlinear observer using reduced order bicycle model in [81] and [82]. Soon after that, Venhovens and Naab used a Kalman filter in [83] for a linear vehicle model in 1999. In [84], Huh et. al. constructed the monitoring system based on KFMEC (Scaled Kalman Filter with Model Error Compensator) technique to improve the robustness of ordinary Kalman filters. In [85], Zhang, Xu and Rachid showed the feasibility of the sliding mode observer for vehicle lateral motion. Similar conclusions were reached by Perruquetti and Barbot in [86].

To filter out the unexpected effect of disturbances from the observer output, different robust design methods had been introduced in Luenberger observer construction. In [87]-[89], [92], H_∞ filer theory was employed to design the optimal observers to resist disturbance for reduced order bicycle model. In [90], H_∞ loop shaping was used for observer design of the linearized lateral motion model of a single-unit HDV (tractor-semitrailer type vehicle). In [91], H_∞ LMI design method was applied in Luenberger observer and fault detection filter design.

Most above observers utilized the accurate dynamic model using nominal values including tire concerning stiffness, vehicle mass and moment of inertia and distances between center of mass and tires. Thus, these observers depend on an accurate knowledge of these parameters, and are affected by variations in them. For instance, Stephant, Charara and Meizel pointed out that the speed of center of gravity is not an indispensable variable. One method to solve this problem is to choose the estimation method without utilizing the vehicle dynamic model, i.e. the observers proposed in [93] and [94]. However, the non model-based observers are naturally hard to be applied along with the steering control system. A more reasonable method is to design robust observer that is not sensitive to system parameter changes, or adaptive observer that can change itself according to parameter change. In [95], a robust observer was developed by including an extra term and adopting the Lyapunov stability theorem. It maintains the good disturbance rejection property that derived form [87]-[92], while provides tolerance to model variance as the observer too.

Recently, Stephant, Charara and Meizel carefully compared four observers including linear Luenberger observer and three nonlinear observers: extended Luenberger observer, extended Kalman filter and sliding-mode observer in [89]. Based on simulation results and practical experiments, they showed that all four observers can yield acceptable estimation results if the observer’s parameters are appropriately assigned.

2.4 Vehicle Lateral Motion Control

As early as 1969, Kasselmann and Keranen [71] developed an active steering system based on feedback from a yaw rate sensor. With continuous efforts, people gradually realized that the difficulties of steering control mainly lie in the following five aspects:

1) how to avoid skidding during steering which is one frequently encountered hazardous situation for drivers;
2) how to reject the disturbance caused by wind or some other reasons;
3) how to deal with vehicle dynamics uncertainty and variation;
4) how to handle actuator rate limits during steering;
5) how to handle time delay exists in feedback block during steering.

To answer these five questions, numerous designed methods had been proposed in the last two decades. In this paper, we will address robust controller, sliding model controller, fuzzy controller and adaptive controller. Some other controllers are briefly mentioned, too.

2.4.1 Frequency Domain Robust Steering Controller

Originated in the later 80s, frequency domain robust design techniques soon became and remained as one of the most important techniques in field of vehicle

lateral motion control. It had been proven to be a practical and efficient approach by lots of literature [73]-[75], [96]-[100].

One direct idea to avoid skidding is to remove the influence of r on the lateral acceleration. The lateral and yaw motions of a car with active steering is decoupled by Ackermann in [73]. It was proved that for an ideal longitudinal mass distribution, the decoupling by yaw rate feedback is robust with respect to uncertain nonlinear tire side force characteristic, velocity and vehicle mass. But Ackermann later showed that this was not a simple and cheap control system since it requires measuring longitudinal velocity of vehicle $v_x \approx v \sin\beta$, yaw rate r and its derivative, slip angle β simultaneously. Thus a practical controller was proposed in [75], in which only v_x needs to be measured. This simplified controller was proved to have similar steady-state behavior to a car.

In [92], it was further shown that additional feedback of the yaw rate r leads to a significant reduction of the deviation from the guideline in nearly all driving maneuvers compared to earlier controller designs which used solely feedback of the deviation y_f. Therefore, a feedback controller with respect to both r and y_f were proposed. It is written as

$$\dot{\delta}_f = u_f - k_r \cdot r \tag{2.13}$$

where u_f was a determined as

$$\frac{u_f(s)}{y_f(s)} = \omega_c^2 \frac{k_{DD}s^2 + k_D s + k_P}{s^2 + 2D\omega_c s + \omega_c^2} \tag{2.14}$$

where inside the bandwidth ω_c, k_P denotes a proportional part, k_D denotes a

differential part and k_{DD} denotes the double differential part.

As what revealed in [97] and [98], using careful poles and zeros assignment, the system can be well stabilized. Besides it, the redundancy of the design parameters can be used to count off the variance of vehicle dynamics. For instance, the Γ-stability boundaries was analyzed for parameters (k_D, k_{DD}) in [99]. Moreover, a generic control law for robust decoupling of lateral and yaw motion by yaw-rate feedback to front-wheel steering was derived in [108]. It showed that ideal steering dynamics were able to be achieved by velocity scheduled lateral acceleration feedback to front-wheel steering. For robust yaw stabilization a velocity-scheduled yaw-rate feedback to rear-wheel steering is given, by which the linearized system gets velocity-independent yaw eigenvalues. In [99], it was further proven that decoupling by yaw rate feedback is robust with respect to uncertain nonlinear tire side force characteristic, velocity and vehicle mass, if we assumed an ideal longitudinal mass distribution.

In the last 90's, H_∞ robust analysis method was introduced into steering controller design field to reduce the unexpected effect of wind disturbance. H_∞ theory is constructed to handle the deterministic disturbance model consisting of bounded energy (square-integrable) L_2 signals and allows controller design for narrow-band disturbance rejection, see Francis 1987 [100] and Zames 1981 [101]. In [102], Guvenc, Bunte and Odenthal etc. designed a disturbance observer, whose model regulation capability allows the specification and achievement of desired yaw

dynamics. The proposed integrated control model is shown in Fig.2.4, where G_{ref} was the transfer function from disturbance torque ρ_{ref} to yaw rate r. $\tilde{G}_u$ is the nominal system model and G_u is the un-modeled dynamics.

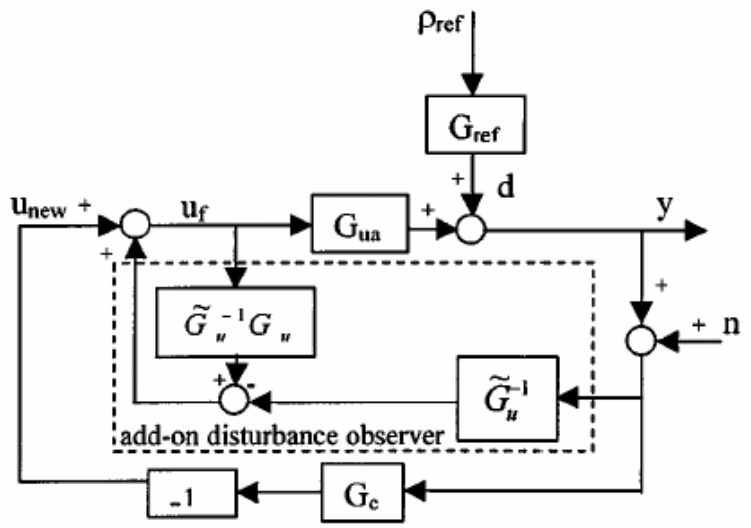

Figure 2.4 Diagram of system architecture with add-on disturbance observer [102].

It was shown that the model regulation and disturbance rejection property of this proposed observer can be considered as a special H_∞ loop shaping for path following. The filtering effect is chosen to satisfy the classical loop shaping constraint

$$|W_s S| + |W_T T| < 1, \text{ for } \forall \omega \tag{2.15}$$

where W_s and W_T are the sensitivity function weight and the complementary sensitivity function weight respectively. S and T denote the sensitivity function and transfer function, respectively.

Equivalently, Mammar etc. developed several two degree of freedom (2DOF)

steering controller in [103]-[105] using the H_∞ loop shaping technique, see Fig.2.5. The design task is directly assigned as finding a robust feedback control $\tilde{K}$ to guarantee the stabilizing of system and minimize energy bound of the transfer function from ρ_{ref} to pre-selected measurement output z_1, z_2 and z_3. Based on works of Kuzuya and Shin that was reported in [106], these robust 2DOF steering controller can be easily digital implemented.

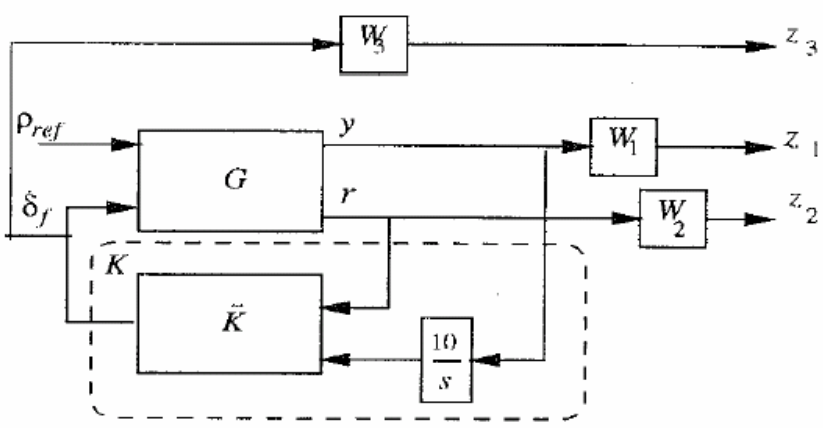

Figure 2.5 Diagram of system architecture with add-on disturbance observer [102].

In [109] and [107], the saturation properties of the steering actuator were studied. The actual feedback control architecture considering steering actuator rate limits are shown in Fig.2.6. Simulations and experiments pointed out that the steering angle rate actuator saturation forms a major limitation of performance. In [107], the undesirable limit cycles caused by saturations were analyzed by a describing function approach in combination with the representation of limit-cycle-free regions in a parameter plane

of velocity and road/tire friction coefficient. The results were formulated in terms of required actuator bandwidth that achieves robustness in the entire operating range. It turned out that the use of a fading integrator can reduce the required actuator bandwidth. Based on similar ideas, a compensator with high order was investigated in [99] to achieve better performance.

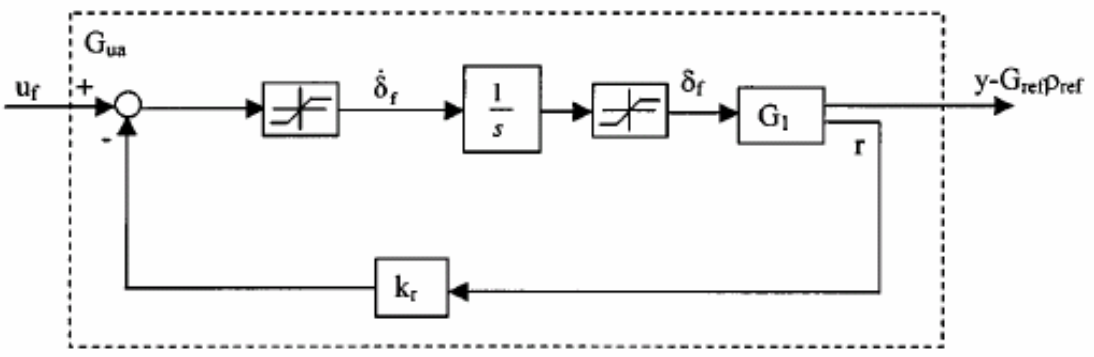

Figure 2.6 Feedback control architecture considering actuator saturation [99].

Some other approaches based on H_∞ theory can be found in [110]-[116]. Most of them were mainly devoted to find an optimal compromise point between steering performance and wind disturbance rejection. Specially, Brennan and Alleyne analyzed the effect of time delay in [116]. Constrained by the length, we will not discuss them here.

2.4.2 Sliding Mode Steering Controller

Sliding mode steering controller is another frequently used steering controller. Generally speaking, the basic idea of sliding mode control is to restrict the state space

trajectories of the dynamic system to a manifold called “sliding manifold” which is usually denoted by $S = 0$. This is achieved by directing the system trajectories towards this manifold “from both sides”.

In [97], the sliding manifold was chosen as

$$S = c\Delta r + \Delta \dot{r} \tag{2.16}$$

where $c > 0$ is a constant gain that determines system behavior once the motion of system (7) or (8) has been restricted to the neighborhood of the manifold $S = 0$.

The structure of the proposed controller was shown in Fig.2.7, in which the system ideal feedback control strategy is written as

$$r_d = -\frac{1}{l_s}\left[v(\beta + \psi) + Ky\right] \tag{2.17}$$

where $K > 0$ determines the desired rate of decay of y.

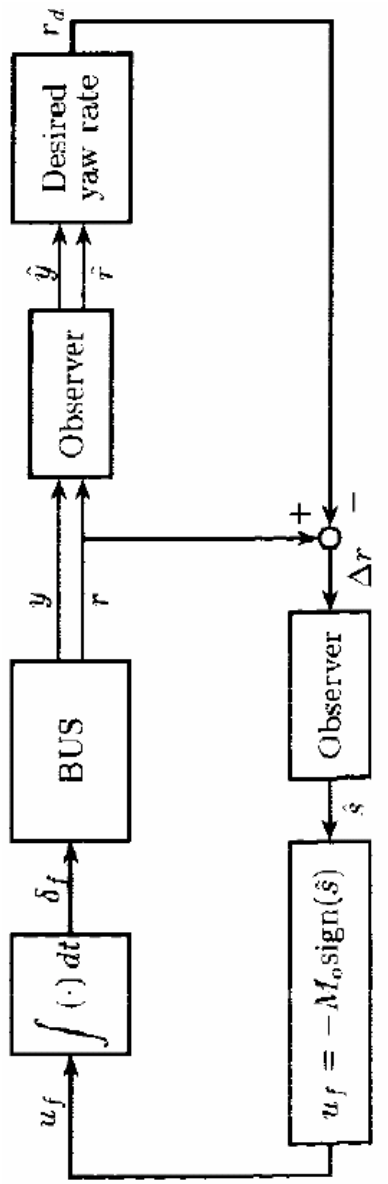

Figure 2.7 Diagram of a typical sliding mode steering controller [97].

Notice both the states β and ψ are unknown, the following observer (18) and (19) was introduced for estimating these two state variables

$$\dot{\hat{y}} = \hat{q} + l_s r + l_1 \bar{y}, \quad l_1 > 0 \tag{2.18}$$

$$\dot{\hat{q}} = l_2 \bar{y}, \quad l_2 > 0 \tag{2.19}$$

Thus the actual feedback control was obtained as

$$r_d = -\frac{1}{l_s}[\hat{q} + K\hat{y}] \tag{2.20}$$

and the feedback control was chosen as

$$u_f = -M_u \text{sign}(S) \tag{2.21}$$

where M_u is the available steering angle rate.

To further improve passenger comfort, it was proved to be advantageous to replace linear term $K\hat{y}$ in (20) by a saturation function

$$r_d = -\frac{1}{l_s}\left[\hat{q} + \lambda \frac{\hat{y}}{\sqrt{\hat{y}^2 + \varepsilon}}\right], \quad \lambda > 0, \quad \varepsilon > 0 \tag{2.22}$$

and the feedback control can be substituted by a continuous approximation as

$$u_f = -M_u \frac{S}{\sqrt{S^2 + 0.0001}} \tag{2.23}$$

It was proven in [97] that this sliding mode controller yields smaller deviations from the guideline and it has a more oscillatory behavior that shows up particularly in the lateral acceleration and in the steering angle rate, but not in the derivations from the guideline. Regarding settling times, there are no significant differences between the two controllers.

There were several other sliding mode steering controllers which chose different sliding manifold [117]-[122]. [117] studied the lateral and longitudinal control of vehicle using a PID typed sliding surfaces, whose stability was proven using Lyapunov theory. In [118], a velocity related sliding mode controller was proposed to deal the input couple problem. Another special sliding mode integral action controller

and the corresponding sliding mode observer are used to enhance vehicle stability in a split-μ maneuver in [112]. In [120], it was shown that the sliding mode controller can also be used to deal with the nonlinear front steering model considering track force control. Moreover, sliding mode steering controller is an important approach in tractor-trailer vehicles lateral motion control [121].

2.4.3 Adaptive Steering Controller

Because of its capability of handling model uncertainty and parameter variation, adaptive steering controllers achieve continuous interest in the last twenty years. Generally, there are two different approaches: model concentrated approaches and non-model concentrated approaches.

In [123], Brennan and Alleyne proposed a steering controller based on model reference control (MRC) with a modification based on rejection of known disturbance dynamics. Model reference control was initialed by Astrom and Wittenmark in 1997 [124]. It was proven in [123] that this method was effective for steering control systems consist of dynamic uncertainty and disturbance. In [125], a special adaptive observer was proposed to deal with system parameters variations. In [126], an adaptive rule was proposed to make the controller flexible with velocity change. In [144], a self-tuning regulator was proposed, which was claimed to have really nice performance. However, the authors also admitted that that adaptive steering controller is relatively complicated to be implemented in real life. Generally, the compromise for

a adaptive steering controller between precision and facility of implementation needs to be clarified in real applications.

In [127]-[129], the concepts of Selected Adaptive Critic (AC) and Dual Heuristic Programming (DHP) were used to design steering controller. Selected adaptive critic methods are known to be capable of designing (approximately) optimal control policies for non-linear plants (in the sense of approximating Bellman Dynamic Programming). The present research focuses on an AC method known as dual heuristic programming. There were lots of issues related to the pragmatics of successfully applying the AC methods.

In [127], a straight forward utility function to capture these requirements would take the following form:

$$\delta_f = -Ay_{f_{error}}^2 - B\dot{y}_{f_{error}}^2 - Cv_{y_{error}}^2 - D\dot{v}_{y_{error}}^2 \tag{2.24}$$

where A, B, C and D were determined from programming to indicate the human designer's judgement about the relative importance of each term, according to desired plant response characteristics (e.g., the derivative terms encourage more "damped" responses). Slightly different from [127], the control coefficients are achieved through self-learning using neural networks in [128]. In [129], it was further shown that DHP can be employed to optimize fuzzy steering controllers.

2.4.4 Fuzzy Steering Controller

Fuzzy set theory and Fuzzy inference was first presented by Zadeh in 1965.

Recently, some new approaches take advantage of Fuzzy inference to avoid addressing complex vehicle dynamics. Moreover, these approaches were proven to able to incorporate and utilize human steering skills to improve the automatic driving performance [130]-[138].

For example, a direct Fuzzy control strategy was proposed by Brown and Hung 1994 for the above 4WS car model. The corresponding Fuzzy control rule is something as

"

IF

Yaw_Rate_Error is Negative_Large (NL) AND

Front_Slip is Negative_Large (NL)

THEN

Command_Front_Steering_Angke is Positive_Large (PL)

"

The front steering command and the rear steering command were designed to cooperate appropriately to avoid skipping in [130]. Assigning appropriate fuzzy membership function and rule table, Brown and Hung claimed that the 4WS car using this Fuzzy controller was quite robust to wind guests and road perturbations.

There were several other directly fuzzy controllers reported in [131]-[135]. However, it should be remarked that, in spite of the well functioning of these fuzzy controllers, they were still heuristic controllers. Since no stability proof had was

presented, and then they were less reliable.

In some recent literals, the proposed fuzzy controllers were constructed as follows. First, an optimal steering controller was constructed for each local model, which indeed constructed a part of the fuzzy model. Then, local controllers were combined using fuzzy rules to form a fuzzy logic controller. Therefore, the performance of the fuzzy controller can be analyzed using linear matrix inequalities (LMI) or algebra Riccati equation (ARE). In [136]-[138], these methods were shown to be effective with both theoretical analysis and simulations.

2.4.5 Other Steering Controller

Recently, time domain robust design technique was used in vehicle lateral control too [139]-[140]. Although time domain robust design is intrinsically equivalent to frequency domain robust design, the obtained controllers differ in many aspects. A detailed discussion in this research direction is presented in our coming paper [141].

There were also some special nonlinear steering controllers proposed in [142]-[143]. Usually their stability was guaranteed by Lyapunov theory. However, most such approaches did not carefully consider robustness and actuator saturation.

In [144], a simple proportional controller was compared with H_∞ robust controllers, fuzzy controller and adaptive controller. This proportional feedback was found to yield the largest offset with respect to other controller, although it was only slightly affected by the wind force. On the other hand, the self-tuning regulator

presents the smallest errors. The responses of H_∞ and fuzzy controllers are comparable in most tests regarding to self-tuning regulator. Although these conclusions were made for special controllers, they were widely accepted to take valid in general situations.

2.5 Remarks

Some important contents leave untouched in this chapter due to length limits and their premature. For instance, we do not mention the following studies here.

1) the relationship between vehicle longitudinal and lateral motion should be further analyzed, although it was proven that these two motions can be roughly decoupled [146]-[147];

2) the effect of sensor installment and measurement error needs further discussions besides [148];

3) how to make intelligent steering controller cooperate appropriately with driver command needs to be carefully studied. Some previous works [149]-[152] had shown that this problem is quite complex, in which both drivers' characteristics, feelings, and driving status needs to be monitored and analyzed;

4) rollover avoidance using special steering control is gaining more attentions. Some promising results had been reported in [161]-[166].

5) Moreover, fault tolerant steering control and corresponding fault detection are obtaining more and more considerations recently [153]-[161]. With rapidly increasing demands on driving safety, a boom in this research field is expected in the near future.

CHAPTER 3 A ROBUST OBSERVER DESIGNED FOR VEHICLE LATERAL MOTION ESTIMATION

Lateral control of vehicles on automated highways often requires estimation of sideslip angle, yaw rate and lateral velocity, which are difficult to measure directly. Thus, several observers (virtual sensors) were developed in the last decade. To solve the unhandled estimation problem caused by dynamic model uncertainty, a robust observer using H_∞ design method is proposed in this chapter. It maintains the good disturbance rejection property that derived form previous research, and simultaneously provides acceptable tolerance to model variance. Specially, effects of displacements of sensory, dynamics variance caused by mass/velocity/tire-road frictions change or nonlinear characteristic are studied. Simulations demonstrate the usefulness of the proposed observer, [167]-[176].

3.1 Introduction

Since a vehicle is a highly complex system that constitutes of varied mechanical, electronic and electromechanical elements, numerous sensors were designed and applied to measure the movement information. But not all vehicle characteristics are measured directly due to high cost or other reasons. Instead, several special observers are used to reconstruct the needed information. In literals, these observers were also

called virtual sensors [176].

For example, knowledge of sideslip angle, yaw rate and lateral velocity is essential in vehicle control, but is difficult to obtain directly. In 1997 and 1999, Kiencke etc. proposed a linear observer and a nonlinear observer using reduced order bicycle model in [170] and [171]. Soon after that, Venhovens and Naab used a Kalman filter in [172] for a linear vehicle model in 1999. In [173], Huh et. al. constructed the monitoring system based on KFMEC (Scaled Kalman Filter with Model Error Compensator) technique to improve the robustness of ordinary Kalman filters. In [174], Zhang, Xu and Rachid showed the feasibility of the sliding mode observer for vehicle lateral motion. Another sliding mode observer was designed by Perruquetti and Barbot in [175]. Recently, Stephant, Charara and Meizel carefully compared four observers including linear Luenberger observer and three nonlinear observers: extended Luenberger observer, extended Kalman filter and sliding-mode observer in [176]. Based on simulation results and practical experiments, they showed that all four observers can yield acceptable estimation results if the observer's parameters are appropriately assigned.

To filter out the unexpected effect of disturbances from the observer output, different robust design methods had been introduced in Luenberger observer construction. In [177]-[179], [182], H_∞ filer theory was employed to design the optimal observers so as to resist disturbance. In [180], H_∞ loop shaping was used for observer design of the linearized lateral motion model of a single-unit HDV

(tractor-semitrailer type vehicle). In [181], H_∞ LMI design method was applied in Luenberger observer and fault detection filter design.

However, almost all above observers utilized the accurate dynamic model using nominal values including tire concerning stiffness, vehicle mass and moment of inertia and distances between center of mass and tires. Thus, these observers depend on an accurate knowledge of these parameters, and are affected by variations in them. For instance, Stephant, Charara and Meizel pointed out that the speed of center of gravity is not an indispensable variable. One method to solve this problem is to choose the estimation method without utilizing the vehicle dynamic model, i.e. the observer proposed in [179]. However, the non model-based observers are naturally hard to cooperate with the advanced control systems. A more reasonable method is to design a robust observer that is not sensitive to system parameter changes, or adopt an adaptive observer that can change itself according to dynamic change.

The robustness analysis for uncertain systems has been the focus of much research in recent years [192], [194]-[196]. In [192], a robust observer was developed by including an extra term. Combing the skills in [181]-[182], [194]-[196], a novel robust observer is designed in this chapter. It maintains the good disturbance rejection property that derived form [177]-[182], while provides tolerance to model variance as the observer in [194]-[196], too.

3.2 Sensor Sets and System Observability

The linear dynamic models (2.7) and (2.8) can be written into canonical form as

$$\dot{x} = Ax + Bu + Ew \tag{3.1}$$

where $x = [\beta \quad r \quad \psi \quad y_f \quad y_r]^T$ is the state variable, $u = [\delta_f \quad \delta_r]^T$ is the control input, and $w = [\rho_{ref} \quad f_w]^T$ is the disturbance. A, B and E are the corresponding system matrices.

The measurement output y is usually formulated as

$$y = Cx + Du \tag{3.2}$$

Here the structure of measurement matrices C and D are determined by the sensors applied. For example, by using the laser sensors proposed in [188], displacements y_f and y_s can be accurately obtained. It was also proven in [189] and [190] that Global Position Systems (GPS) can also be applied to approximately get heading angle ψ and displacements y_f and y_s simultaneously. With the Fiber Optic Gyroscopes (FOP) described in [191], heading angle ψ and yaw rate r are precisely measured. However, it requires considerable install and maintain cost.

Since the linear dynamic model (2.7) and (2.8) highly depend on system velocity, the system dynamics should be modified as below considering velocity variance and nonlinear properties

$$\dot{x} = (A + \Delta A)x + Bu + Ew \tag{3.3}$$

where ΔA denotes the variance matrix that is determined by variance of mass,

velocity, tire-road friction coefficients and nonlinear characteristics.

In this chapter, the norm of ΔA is bounded as

$$\|\Delta A\|_2 \le \varepsilon \tag{3.4}$$

Simulation reveals that ε mainly dependent on estimation error of velocity v and road adhesion factor μ.

It can be easily proven that the system is observable if either displacements y_f or y_r is measured. The system is unobservable if only ψ is measured. These conclusions take valid for both front steering vehicle and full steering vehicle.

Simulation also shows that to measure both y_f and y_r may increase the robustness of the observer. But many vehicles only equip front sensor because of cost consideration.

3.3 Robust Observer Design

In this chapter, the proposed robust observer for the systems (3.3)-(3.4) is chosen as

$$\begin{cases} \dot{\hat{x}} = A\hat{x} + Bu - L(y - \hat{y}) + \tau\alpha \\ \hat{y} = C\hat{x} + Du \\ \alpha = \dfrac{\varepsilon^2 \hat{x}^T \hat{x}}{(y - \hat{y})^T (y - \hat{y})} P^{-1} C^T (y - \hat{y}) \end{cases} \tag{3.5}$$

where $\hat{x}$ denotes observer state, $\hat{y}$ denotes observer output. L is the observer matrix. τ is a positive real scalar that needs to be determined.

Based on (3.3)-(3.5), we have the dynamics of observer error $e = x - \hat{x}$ as

$$\dot{e} = (A + LC)e + \Delta Ax + Ew - \alpha = (A + \Delta A + LC)e + \Delta A\hat{x} + Ew - \tau\alpha \tag{3.6}$$

Obviously, the design task here is to find the optimal matrix L to filter w from e. One frequently used performance index is chosen as:

Minimize the H_∞ norm of the transfer function matrix from w to e.

This naturally leads to the well-known H_∞ design problem, which was solved using a linear matrix inequality (LMI) problem by Boyd, Ghaoui, and E. Feron et. al in [192], or equivalently solved using a set of Algebraic Riccati Equations (ARE) shown by Nagpal and Khargonekar in [193].

In this chapter, we choose the energy constraint of the observer error as the design objective. It is written as:

Choose the smallest $\gamma > 0$ such that

$$\int_0^{+\infty} e^T e dt \le \gamma^2 \int_0^{+\infty} w^T w dt \tag{3.7}$$

Therefore, we can reach the main result as follows.

Theorem: H_∞ constraints (3.7) will be held if there exist a symmetry positive matrix P and two positive real numbers τ and λ that satisfy

$$\begin{bmatrix} P[A+LC]+(1+\lambda\varepsilon^2)I+[A+LC]^T P+(1/\lambda+1/\tau)2P^2 & | & PE \\ ---------- & + & --- \\ E^T P & | & -\gamma^2 \end{bmatrix} < 0 \tag{3.8}$$

Proof: Let's define a Lyapunov like function $V(t) = e^T Pe$, where P is a symmetry positive matrix. We have the time derivative of $V(t)$ along the trajectories of (3.6) as

$$\begin{aligned} \dot{V} &= e^T P[A+\Delta A+LC]e + e^T Ew + e^T \Delta A\hat{x} + e^T [A+\Delta A+LC]^T Pe \\ &+ w^T E^T e + \hat{x}^T \Delta A^T e - \tau e^T P\alpha - \tau\alpha^T Pe \end{aligned} \tag{3.9}$$

Thus, the design objective can be transformed as finding the smallest γ^2 that satisfies:

$$T = \dot{V} + e^T e - \gamma^2 w^T w \le 0 \tag{3.10}$$

Substituting (3.9) into (3.10) yields

$$\begin{aligned} T &= \begin{bmatrix} e \\ w \end{bmatrix}^T \begin{bmatrix} P[A+LC]+I+[A+LC]^T P & | & PE \\ ---------- & + & --- \\ E^T P & | & -\gamma^2 \end{bmatrix} \begin{bmatrix} e \\ w \end{bmatrix} \\ &+ 2e^T P\Delta Ae + 2e^T P\Delta A\hat{x} - 2\tau e^T P\alpha \le 0 \end{aligned} \tag{3.11}$$

Note that

$$e^T P\Delta Ae \le \frac{1}{\lambda} e^T P^2 e + \lambda e^T \varepsilon^2 e \tag{3.12}$$

$$e^T P\Delta A\hat{x} \le \frac{1}{\tau} e^T P^2 e + \tau\hat{x}^T \varepsilon^2 \hat{x} \tag{3.13}$$

$$\hat{x}^T \varepsilon^2 \hat{x} \le e^T P\alpha \tag{3.14}$$

we have (3.8) is a sufficient condition for (3.11). □

Based on this Theorem, the robust observer design problem can be formulated as

below:

Design Task 3.I

Min γ

with $\gamma > 0$, $\lambda > 0$ and moderate $\tau > 0$ such that

$$\begin{bmatrix} PA + A^T P + XC + C^T X^T + (1+\lambda\varepsilon^2)I + (1/\lambda + 1/\tau)2P^2 & | & PE \\ ---------- & + & --- \\ E^T P & | & -\gamma^2 \end{bmatrix} < 0 \quad (3.15)$$

and the observer matrix is

$$L = P^{-1}X \quad (3.16)$$

From the discussions in [194]-[196], (3.6) should be a forced, nonautonomous, dynamic system, and contains an unknown, perturbation term. Fortunately, we find that this condition can be naturally met. Besides, τ should not be too large due to the constraints on implementation of the observer. In the practice, τ should be determined by compromising all the requirements together. But simulations prove that constraints on τ will directly limit the range of γ at the same time, too.

3.4 Simulation Results

To demonstrate the feasibility of the proposed observer, its tracking performance is compared with a linear Luenberger observer that is only optimized using H_∞ method to reject disturbance.

Using similar transformation, the linear Luenberger observer is formulated as

$$\begin{cases} \dot{\hat{x}} = A\hat{x} + Bu - L'(y - \hat{y}) \\ \hat{y} = C\hat{x} + Du \end{cases} \tag{3.17}$$

Its performance index is also chosen as

Minimize the H_∞ norm of the transfer function matrix from w to e.

Thus its design task should be

Design Task 3.II

Min γ

with $\gamma > 0$, $\mu > 0$ and moderate $\tau > 0$ such that

$$\begin{bmatrix} P[A + L'C] + [A + L'C]^T P + I & | & PE \\ - - - - - - - - - - - - - - - - - - & + & - - - \\ E^T P & | & -\gamma^2 \end{bmatrix} < 0 \tag{3.18}$$

or equivalently

$$\begin{bmatrix} PA + A^T P + X'C + C^T X'^T + I & | & PE \\ - - - - - - - - - - - - - - - - - - & + & - - - \\ E^T P & | & -\gamma^2 \end{bmatrix} < 0 \tag{3.19}$$

with the observer matrix

$$L' = P^{-1} X' \tag{3.20}$$

Suppose the vehicle is front steering and only the front sensor is applied. Thus

$$C = [0 \quad 0 \quad 0 \quad 1], \; D = [0 \quad 0 \quad 0 \quad 0] \tag{3.21}$$

The parameters are assigned as:

$\tilde{m}$ = 1500 kg, $\tilde{I}_z$ =2500 kg.m.m, l_f = 1.2 m, l_r =1.5 m, l_{fs} = 5 m, l_w = 0.5 m, c_f = c_r = 80000kN/rad.

Here τ is chosen 10. The variance bound of velocity is Δv = 1 m/s, $\Delta\tilde{m}$ = 100 kg, $\Delta\mu$ = 0.1. We can choose

$$\varepsilon = \sqrt{5}$$

Suppose v is incorrectly estimated as 16m/s when it equals to 15m/s and μ is misestimated as 0.7 instead of 0.8 during the simulation.

The Luenberger observer matrix is

$$L' = [0.2869 \quad -3.6024 \quad -0.1984 \quad -0.0019]^T \times 10^4$$

The robust observer matrix is

$$L = [0.3687 \quad -5.4516 \quad -0.2345 \quad -0.0025]^T \times 10^4$$

and symmetry matrix P is chosen as

$$P = \begin{bmatrix} 3.1771 & 0.3082 & -2.1728 & 0.4347 \\ 0.3082 & 0.0443 & -0.5471 & 0.1093 \\ -2.1728 & -0.5471 & 9.3211 & -1.8620 \\ 0.4347 & 0.1093 & -1.8620 & 0.3823 \end{bmatrix} \times 10^{10}$$

The gain τ is chosen as

$$\tau = 10$$

Fig.3.1 shows the tracking result of slideslip angle β using the linear Luenberger observer optimized by solving Design Task 3.II. Fig.3.2 shows the direct tracking output of β using the proposed observer optimized by solving Design Task

3.I. Fig.3.3 shows the smoothed tracking result of β using a 10 points average filter.

Here, the red lines represent the actual value while the blue lines denote the estimation results. The maximum estimation error of the linear Luenberger observer is around 12%, while the estimation error of the proposed robust observer is around 2%. It is apparent that the proposed observer will yield better tracking performance.

Simulation also reveals that there is not a global optimal observer matrix that can deal with all the velocity settings. Thus, the observer matrix L and nonlinear term $\tau\alpha$ should change with velocity v to maintain good tracking result. Fortunately, drivers will not change the vehicle's speed too much when he/she is steering. Thus the change of feedback matrix will not violate the observer system's stability.

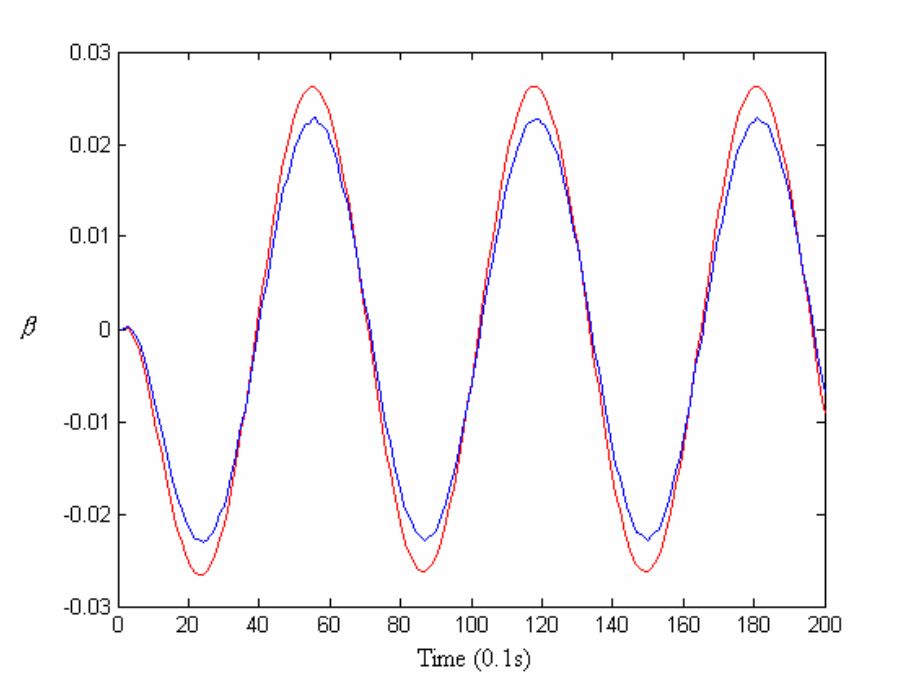

Figure 3.1 Tracking result using the linear Luenberger observer.

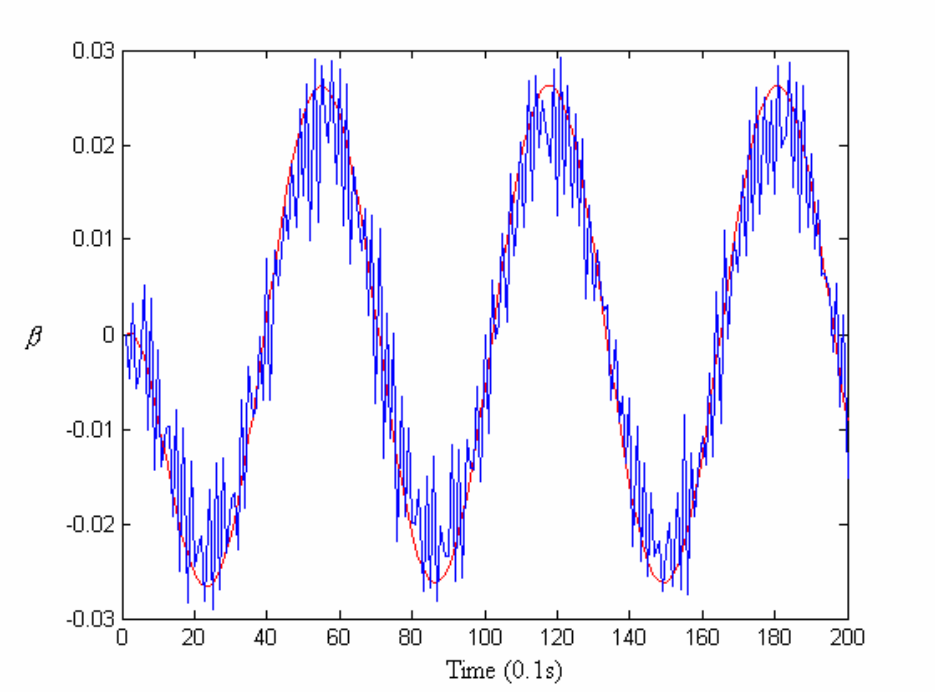

Figure 3.2 Tracking result using the proposed robust observer.

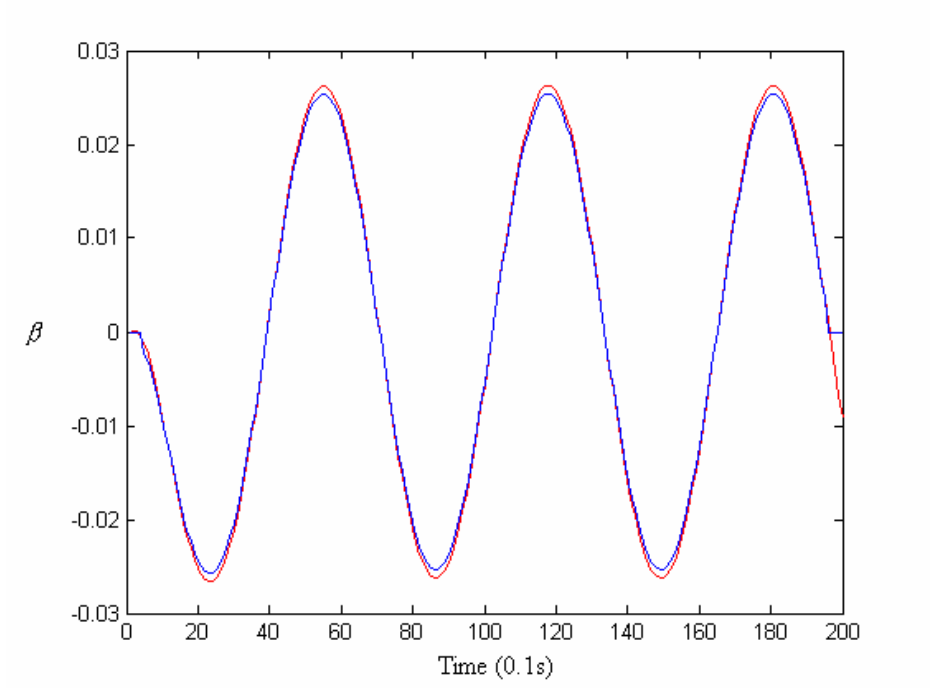

Figure 3.3 Smoothed tracking result using the proposed robust observer.

CHAPTER 4 AN LMI APPROACH TO ROBUST VEHICLE STEERING CONTROLLER DESIGN

Being parallel to frequency domain robust steering controller designs, time domain robust steering controller designs attract continuous interest in the last decade. Based on previous research results, a systematic time design framework is proposed in this chapter. The design task is constructed as a multi-objective optimization problem which simultaneously considers system stabilization, disturbance rejection, actuator saturation and time delay. A mixed L_1 / H_∞ robust controller is finally obtained by solving a set of linear matrix equalities (LMI) that guarantee the performance requirements regarding these mentioned factors. Simulations show the effectiveness of the proposed design method.

4.1 Introduction

Advanced vehicle control systems help drivers by taking control of the steering, brakes and/or throttle to maneuver the vehicle in a safe sate. Thus, it is also called driver aid systems and intelligent (autonomous) driving systems in some literals. The related technologies include smart cruise control, collision avoidance systems, and vehicle platooning, etc. By focusing on motion control aspects, corresponding research can be divided into three directions: lateral control, longitudinal control and

their combinations.

The main task of longitudinal control is vehicle following/ tracking. It requires that an appropriate headway should be maintained between the lead vehicle and the controlled vehicle to avoid collision. The lateral control usually refers to vehicle steering control. Its prime task is path (road) following, or plainly, to keep the vehicle on the road. Based on previous research [197]-[211], the difficulties of steering control mainly lie in the following five aspects:

1) how to avoid skidding during steering;
2) how to reject the disturbance caused by wind or some other reasons;
3) how to deal with vehicle dynamics uncertainty;
4) how to handle actuator rate limits during steering;
5) what is the vehicle's maximum speed limit for a certain curve with given curvature.

To answer these five questions, numerous designed methods had been proposed in the last two decades.

Originated in the later 80s, classic frequency domain design techniques remained as the most important technique in field of vehicle steering control. It had been proven to be a practical and efficient approach in a great number of literals [197]-[211]. To avoid skidding, one direct idea of it is to remove the influence of yaw on lateral

acceleration. In [200]-[203], Ackermann etc. decoupled the lateral and yaw motions of a car with active steering. Moreover, they proved that for an ideal longitudinal mass distribution, the decoupling by yaw rate feedback is robust with respect to uncertain nonlinear tire side force characteristic, velocity and vehicle mass. In [204], Ackermann showed that a simplified controller that has acceptable steady-state behavior. In [205], it was further revealed that additional feedback of the yaw rate can lead to a significant reduction of the deviation from the guideline in nearly all driving maneuvers compared to earlier controller designs which used solely feedback of the deviation. Besides, the redundancy of the design parameters can be used to count off the variance of vehicle dynamics. For example, the Γ-stability boundaries for mass and velocity variance were analyzed by Ackermann and Sienel in [206].

In the last 90's, H_∞ robust analysis method was introduced into steering controller design field. H_∞ theory is constructed to handle the deterministic disturbance model consisting of bounded energy (square-integrable) L_2 signals and allows controller design for narrow-band disturbance rejection, see Francis 1987 [207] and Zames 1981 [208]. In [209], Guvenc, Bunte and Odenthal etc. designed a disturbance observer, whose model regulation capability allows the specification and achievement of desired yaw dynamics. Actually, the model regulation and disturbance rejection property of this proposed observer could be considered as a special H_∞ loop shaping for path following. Similarly in [210], Mammar, Baghdassarian and Nouveliere presented another robust two degree of freedom controllers (2DOF)

controller using the H_∞ loop shaping technique described in [211]. Kuzuya and Shin further discussed implementation of a robust 2DOF steering controller in [212].

In [209] and [213], the saturation properties of the steering actuator were studied. Simulations and experiments pointed out that the steering angle rate actuator saturation forms a major limitation of performance. In [213], the undesirable limit cycles caused by saturations were analyzed by a describing function approach in combination with the representation of limit-cycle- free regions in a parameter plane of velocity and road/tire friction coefficient. The results were formulated in terms of required actuator bandwidth that achieves robustness in the entire operating range. It turned out that the use of a fading integrator can reduce the required actuator bandwidth. Based on similar ideas, a compensator with high order was designed using H_∞ loop shaping in [209] to achieve better performance.

There are several other vehicle steering controllers including varied sliding mode steering controllers presented in [202] and [214]-[216]; some fuzzy controllers descried in [217]-[219]; and several adaptive controllers proposed in [220]-[221]. In [221], four special controllers, H_∞, adaptive, fuzzy and PID controllers, were compared by simulations over a test track circuit. It is remarked clearly that the simple proportional controller is the one that makes the largest errors, while the self-tuning regulator yields the best response. H_∞ and fuzzy controllers have equivalent responses regarding adaptive controller.

However, most previous research did not study the vehicle's worst displacement

from guideline. This leads to two important problems. The first is that some controllers may temporally drive the vehicle off the lane although the final offsets are zero. The second is what the maximum speed limit is not clearly pointed out for a certain curve with given curvature. To answer these two problems, this chapter addresses point-wise-in-time error bound of vehicle offset, using L_1 theory originated by Vidyasagar in 1986 [222]. L_1 theory was developed to capture worst-case peak amplitude response due to bounded amplitude persistent L_∞ disturbances, which more precisely fits road curvature disturbance. Further analysis in this chapter shows that actuator saturation can be alternatively handled by control the upper input-output bound of steering angle and road curvature.

Therefore, a synthesized design framework is proposed for steering controller in this chapter. It formulates the design task into a multi-objective optimization problem which considers both system quadratic stabilization and disturbance rejection with constraints on actuator saturation. All the constraints are transformed into a set of linear matrix equalities (LMI) which can be easily solved by recently developed toolbox [237]-[238]. A mixed L_1 / H_∞ robust controller is finally generated by solving the optimization problem.

4.2 System Controllability and Observability

The design specifications are primarily given in terms of maximal displacement from the guideline and maximal steering angle and steering angle rate. Here, we

assume

$$\left\|\delta_f\right\| \le \delta_{\max},\ \left\|\dot{\delta}_f\right\| \le \dot{\delta}_{\max},\ \left\|\delta_r\right\| \le \delta_{\max},\ \left\|\dot{\delta}_r\right\| \le \dot{\delta}_{\max} \tag{4.1}$$

$$\left\|y_f\right\| \le y_{\max},\ \left\|y_r\right\| \le y_{\max} \tag{4.2}$$

In the rest of this chapter, we will consider front steering model with front vision sensor only, and all the conclusions below can be directly applied to other situations.

Considering the control input, we can rewrite system as

$$\begin{bmatrix} \dot{\beta} \\ \dot{r} \\ \dot{\psi} \\ \dot{y}_f \\ \dot{\delta}_f \end{bmatrix} = \begin{bmatrix} a_{11} & a_{12} & 0 & 0 & b_{11} \\ a_{21} & a_{22} & 0 & 0 & b_{21} \\ 0 & 1 & 0 & 0 & 0 \\ v & l_{fs} & v & 0 & 0 \\ 0 & 0 & 0 & 0 & 0 \end{bmatrix} \begin{bmatrix} \beta \\ r \\ \psi \\ y_f \\ \delta_f \end{bmatrix} + \begin{bmatrix} 0 \\ 0 \\ 0 \\ 0 \\ 1 \end{bmatrix} u_f + \begin{bmatrix} 0 & d_1 \\ 0 & d_2 \\ -v & 0 \\ -vl_{fs} & 0 \\ 0 & 0 \end{bmatrix} \begin{bmatrix} \rho_{ref} \\ f_w \end{bmatrix} \tag{4.3}$$

which can be further written into canonical form as

$$\dot{x} = Ax + Bu + Ew \tag{4.4}$$

where $x = \begin{bmatrix} \beta & r & \psi & y_f & \delta_f \end{bmatrix}^T$ is state variable, $u = u_f$ is control input, and $w = \begin{bmatrix} \rho_{ref} & f_w \end{bmatrix}^T$ is taken as disturbance. A, B and E are the corresponding system matrices chosen as

$$A = \begin{bmatrix} a_{11} & a_{12} & 0 & 0 & b_{11} \\ a_{21} & a_{22} & 0 & 0 & b_{21} \\ 0 & 1 & 0 & 0 & 0 \\ v & l_{fs} & v & 0 & 0 \\ 0 & 0 & 0 & 0 & 0 \end{bmatrix},\ B = \begin{bmatrix} 0 \\ 0 \\ 0 \\ 0 \\ 1 \end{bmatrix},\ w = \begin{bmatrix} \rho_{ref} \\ f_w \end{bmatrix},\ E = \begin{bmatrix} 0 & \tilde{d}_1 \\ 0 & \tilde{d}_2 \\ -v & 0 \\ -vl_{fs} & 0 \\ 0 & 0 \end{bmatrix}$$

Here the wind disturbance is normalized to the same amplitude level to road curvature with

$$\tilde{d}_1 = \sigma d_1,\ \tilde{d}_2 = \sigma d_2$$

where $\tau > 0$ is a scale number which is determined by

$$\sigma = \left\| \rho_{ref} \right\|_{\max} / \left\| f_w \right\|_{\max}$$

It is easily to check that (A, B) is controllable pair for most vehicle parameter setting. In the rest of this chapter, we assume the system is controllable even under model uncertainty.

The measurement output y is normally chosen as

$$y = Cx \tag{4.5}$$

where the structure of measurement matrix C is determined by the sensors applied.

For example, displacements y_f and y_s can be accurately obtained by using the laser sensors proposed in [224]. With the Fiber Optic Gyroscopes (FOP) described in [225], heading angle ψ and yaw rate r could be precisely measured, although it requires considerable cost. It was also shown in [226] and [227] that Global Position Systems (GPS) can also be applied to approximately estimate heading angle ψ and displacements y_f and y_s simultaneously.

There were several approaches of vehicle sideslip angle and lateral forces that had been reported in the last decade. In 1997 and 1999, Kiencke etc. proposed a linear observer and a nonlinear observer using reduced order bicycle model in [228] and [229]. Soon after that, Venhovens and Naab used a Kalman filter in [230] for a linear vehicle model in 1999. In [231], Huh et. al. constructed the monitoring system based on KFMEC (Scaled Kalman Filter with Model Error Compensator) technique to improve the robustness of ordinary Kalman filters. Besides Kalman filter, sliding

mode observer were designed, too. In [232], Zhang, Xu and Rachid showed the feasibility of the sliding mode observer for vehicle lateral motion. Similar conclusions were reached by Perruquetti and Barbot in [233]. Recently, Stephant, Charara and Meizel carefully compared four observers including linear Luenberger observer and three nonlinear observers: extended Luenberger observer, extended Kalman filter and sliding-mode observer in [234]. Based on simulation results and practical experiments, they showed that all four observers can yield acceptable estimation results if the observer's parameters are appropriately assigned.

It can be easily proven that the system is observable if either displacements y_f or y_r is measured. This conclusion takes valid for both front steering vehicle and full steering vehicle.

In the rest of this chapter, we assume displacement y_f and yaw rate r are measured, which is similar to the situation considered in [200]-[206]. Obviously, (A, C) yields an observable pair for almost all vehicle parameter settings.

4.3 Robust Steering Controller Design

4.3.1 Feedback Controller

In general, the system with disturbance $w \in C^{n_w}$, saturation control input and bounded state can be written as:

$$\begin{cases} \dot{x} = Ax + Bu' + Ew \\ z_\infty = C_\infty x \\ z_1 = C_1 x \\ z_u = u' = sat(Kx) \end{cases} \tag{4.6}$$

where $z_\infty \in C^{n_{z_\infty}}$ is the H_∞-performance output, $z_1 \in C^{n_{z_1}}$ is the L_1 -performance output, $z_u \in C^{n_u}$ is the auxiliary performance output for bounded control input. C_∞ and C_1 are measurement matrices. Here, we set $C_1 = \begin{bmatrix} 0 & 0 & 0 & 1 & 0 \\ 0 & 0 & 0 & 0 & 1 \end{bmatrix}$ and $C_\infty = I$.

The design objective is to design a feedback control

$$u' = sat(Kx) = \begin{cases} Kx, & |Kx| \le u_{\lim} \\ sign(Kx) * u_{\lim}, & |Kx| > u_{\lim} \end{cases} \tag{4.7}$$

to achieve the following three objectives:

Design Objective 4.I

4.I.1) guarantee the quadratic stability of system (6);

4.I.2) minimize the H_∞ norm of the transfer function matrix from w to z_∞ so as to reject disturbance;

4.I.3) keep z_1 bounded to satisfy the offset constraints.

The first two objectives naturally leads to the famous H_∞ design problem, which was solved using a linear matrix inequality (LMI) problem by Boyd, Ghaoui, and E. Feron et. al in [223], or equivalently solved using a set of Algebraic Riccati Equations (ARE).

In [233], Abedor, Nagpal and Poolla addressed the actuator saturation by the

star-norm approach proposed in [234], which estimates the upper bound of the induced L_1-norm by over bounding the reachable set with an ellipsoid. In [235]-[236], Nguyen and Jabbari further showed that the saturation limits could be explicitly taken into account by constraining the linear feedback within the upper bound. This new method has the following main properties: 1) controllers are designed so that actuators are used at or near capacities and 2) the guaranteed performance bound is a function of the actuator capacity. This method is similar to the H_∞ loop shaping proposed in [209], since both of them tried to keep the linear feedback within saturation limits. However, L_1-norm is more suitable than H_∞-norm to describe the time-domain point-wise-in-time bound of actuator saturation and peek offset.

Extending the conclusions in [235]-[236], we further add the L_1-norm constraints on system state and formulate a mixed L_1/H_∞ robust controller as follows. The system dynamics is rewritten as:

$$\begin{cases} \dot{x} = Ax + Bu + Ew \\ z_\infty = C_\infty x \\ z_1 = C_1 x \\ z_u' = u = Kx \end{cases} \tag{4.8}$$

and the design objective is to design a feedback control $u = Kx$ to achieve the following four objectives

Design Objective 4.II

4.II.1)-3) same as 4.I.1)-4.I.3);

4.II.4) keep z_u' bounded to guarantee the inputs to remain less than or

equal to the saturation limits.

Before we enter the main part of this chapter, let's introduce two lemmas in which only one disturbance input is considered.

Lemma 4.1 [223]: Consider system $\begin{cases} \dot{\chi} = A_\chi \chi + E_\chi \omega \\ z_\chi = C_\chi \chi \end{cases}$ with A_χ stable. If there exists a constant symmetry matrix $Q_\chi > 0$, for some scalar $\alpha > 0$, such that the

$$A_\chi Q_\chi + Q_\chi^T A_\chi + \alpha Q_\chi + \alpha^{-1} E_\chi E_\chi^T \le 0 \tag{4.9}$$

then the reachable set X is contained inside the ellipsoid $\left\{\chi : \chi^T Q_\chi^{-1} \chi \le \omega_{\max}^2\right\}$, and $\max_{t\ge 0} |z_\chi| \le \left\| C_\chi^T Q_\chi^{-1} C_\chi \right\|^{1/2}$.

Lemma 4.2 [223]: Consider system (10) with $z_{ui} = u_i$ for $i = 1,..., n_u$. Given some desired level of performance $\gamma_\infty > 0$ and $\gamma_{u,i} > 0$ associated with each input, a observer-based state feedback controller

$$\begin{cases} \dot{\hat{x}} = A\hat{x} + Bu + LC(y - C\hat{x}) \\ u_i = -\dfrac{\lambda}{2} B_i^T Q^{-1} \hat{x} \end{cases} \tag{4.10}$$

guarantees the quadratic stability of (8) with L_2-gain γ_∞ from w to z_∞ and bounded control input if there exist a symmetry constant matrix $Q > 0$ and a scalar $\lambda > 0$ for some $\alpha > 0$ such that the following LMIs are feasible

$$\begin{bmatrix} AQ + QA^T - \lambda BB^T & E & QC_\infty^T \\ E & -\gamma_\infty^2 & 0 \\ C_\infty Q & 0 & -I \end{bmatrix} < 0 \tag{4.11}$$

$$\begin{bmatrix} AQ + QA^T + \alpha Q - \lambda BB^T & E \\ E^T & -\alpha \end{bmatrix} \le 0 \tag{4.12}$$

$$\begin{bmatrix} 4Q & \lambda B_i \\ \lambda B_i^T & \gamma_{u,i}^2 \end{bmatrix} > 0 \tag{4.13}$$

where B_i is the ith column of the input matrix B. Moreover, the control input is in the ellipsoid $\xi_F = \{x : x^T Q^{-1} x \le w_{\max}^2\}$, or equivalently $\|u_i\|_\infty \le \gamma_{u,i} w_{\max}$. Here L is an appropriately chosen observer matrix. The design of L can be found in [228], [232], [234]-[236]. Here, we chose $w_{\max} = \|\rho_{ref}\|_{\max}$.

Extending the conclusions in Lemma 2, multiple disturbance inputs can be treated as follows. First determining the largest disturbance amplitude $w_{\max} = \max_{k \in n_w} \{w_k\}$, then assuming all the disturbance inputs to have the same peak amplitude $w_{\max}$. Since the L_1-norm of w is defined to be the supremum over all time of the two-norm of w at each time instant, the multiple disturbance inputs case can then be considered by simply over bounding w in Lemma 2 with $w \le \sqrt{n_w} w_{\max}$.

Based on these two lemmas, we can reach the main result as follows.

Theorem 4.1: Consider system (4.8) with $z_{ui} = u_i$ for $i = 1,..., n_u$ and $j = 1,..., n_{z_1}$. Given some desired level of performance $\gamma_\infty > 0$, $\gamma_{u,i} > 0$ and $\gamma_{1,j} > 0$ associated with each input, the state feedback controller (4.10) guarantees the quadratic stability of (4.8) with L_2-gain γ_∞ from w to z_∞ and bounded control input if there exist a symmetry constant matrix $Q > 0$ and a scalar $\lambda > 0$ for some $\alpha > 0$ such that the LMIs (4.11)-(4.13) are feasible

$$\begin{bmatrix} Q & QC_{1,j}^T \\ C_{1,j} Q & \gamma_{1,j}^2 \end{bmatrix} > 0 \tag{4.14}$$

where $C_{1,j}$ is the jth row of matrix C_1. Moreover, we can have $\|u_i\|_\infty \le \sqrt{n_w} \gamma_{u,i} w_{\max}$

and $\left\| z_{1,j} \right\|_\infty \le \sqrt{n_w}\gamma_{1,j} w_{\max}$.

Proof: Indeed, the controller given in (4.10) is the simplest controller that can be obtained from (4.8), see [223]. Consider a more generic control feedback matrix will lead to a bilinear matrix inequality design problem that has not been thoroughly solved yet.

LMI (4.11) is necessary and sufficient for the existence of a state feedback controller for system (4.8) which guarantees quadratic stability with $\int_0^{+\infty} z^T z dt \le \gamma_\infty^2 \int_0^{+\infty} w^T w dt$.

Inequalities in (4.12) and (4.13) are the necessary and sufficient conditions for $\left\| u_i \right\|_\infty \le \sqrt{n_w}\gamma_{u,i} w_{\max}$. Similarly to the proof for Lemma 2, the sufficiency of (4.13) for $\left\| z_j \right\|_\infty \le \sqrt{n_w}\gamma_{1,j} w_{\max}$ can be directly obtained from (4.12) and Lemma 1. □

Based on Theorem 1, the robust controller design problem is formulated as below:

Design Task 4.III

Min γ_∞

with pre-selected $\alpha > 0$, $\gamma_{u,i} > 0$ and $\gamma_{1,j} > 0$ for $i = 1,..., n_u$ and $j = 1,..., n_{z_1}$ such that LMIs (4.11)-(4.14) holds for system (4.8), which satisfies limits (4.1)-(4.2) as

$$\|u_1\|_\infty \le \gamma_{u,1} w_{\max} \le \dot{\delta}_{f\max} \tag{4.15}$$

$$\|z_{1,1}\|_\infty \le \sqrt{2}\gamma_{1,1} w_{\max} \le \delta_{f\max} \tag{4.16}$$

$$\|z_{1,2}\|_\infty \le \sqrt{2}\gamma_{1,2} w_{\max} \le y_{f\max} \tag{4.17}$$

Grid search can be used to find global optimal parameter α, $\gamma_{u,i}$ and $\gamma_{1,j}$. However, it was found that variation of α does not significantly change the performance γ_∞. $\gamma_{u,i}$ and $\gamma_{1,j}$ are usually chosen to be smaller that maximum allowable values to counterbalance uncertainty.

4.3.2 Robustness Analysis Considering Model Uncertainty

The system uncertainties are mainly caused by vehicle mass, velocity and tire-road-friction variation. Simulations show that this variation is highly structured. Thus, some frequently used robust analysis techniques cannot be applied since they are too conservative in this situation.

In this chapter, the robustness of the proposed controller is directly studied by checking the roots function (21) for the closed-loop system (10)-(12) in terms of m, v and μ.

$$\begin{aligned} h(m,v,\mu) &= \det\left[sI - A(m,v,\mu) + \frac{\lambda}{2} B(m,v,\mu) B_{\text{nominal}}^T Q^{-1} \right] \\ &= s^n + c_{n-1}(m,v,\mu) s^{n-1} + \ldots + c_0(m,v,\mu) = 0 \end{aligned} \tag{4.18}$$

Using Routh-Hurwitz criteria, the stability bound of m, v and μ can be determined. Simulations reveal that the obtained feedback controller can guarantee system's quadratic stability in most cases with variation limits as

$$|\Delta m| \le 200\,kg\ ,\ \ |\Delta v| \le 5m/s\ ,\ \ |\Delta \mu| \le 0.1 \tag{4.19}$$

Simulation reveals that bound of actuator input and offset may be violated in some situations. So the feedback controller should change with vehicle velocity to maintain good steering performance. Fortunately, drivers will not change the vehicle's speed too much when he/she is steering, and changing feedback matrix will not violate system's stability, if drivers do not steer.

4.3.3 Higher Order Controller Design

Comparing to frequency domain approaches, one common shortcoming of time domain robust controller design is that it fits for fixed order controller design only. Although feedback controllers using information of $x = [\beta \quad r \quad \psi \quad y_f \quad \delta_f]^T$ can satisfy safety requirements for many vehicles, a higher order controller is still required.

In [202], [206], the feedback control rule was formulated by

$$\delta_f = 0.89 \cdot r - \omega_c^2 \frac{k_{DD}s^2 + k_D s + k_P}{s^2 + 2D\omega_c s + \omega_c^2} y_f \tag{4.20}$$

where inside the bandwidth ω_c, k_P denotes a proportional part, k_D denotes a differential part and k_{DD} denotes the double differential part. It showed in [202], [206] that this filtering feedback of y_f can be sued to improve driving performance.

From the viewpoint of H_∞ filtering, Eq.(4.20) can be viewed as a special higher feedback. By introducing an intermediate state ζ and an auxiliary control u_{aux}, we can extend the original feedback mode (4.10) into a high order controller, which is

approximately equivalent to what was proposed in [202], [216].

Discarding the contribution of ρ_{ref} to y_f, we can have

$$\dot{y}_f \approx v \cdot \beta + l_{fs} \cdot r + v \cdot \psi \tag{4.21}$$

Thus, the kth derivative of $y_f^{(k)}$ should only be determined by β, r, δ_f and its second order derivatives as

$$y_f^{(k)} \approx g_{k,1} \cdot \beta + g_{k,2} \cdot r + g_{k,3} \cdot \delta_f + g_{k,4} \cdot \dot{\delta}_f \tag{4.22}$$

where those higher order derivatives of δ_f are discarded since they are small. Here, $g_{k,i}$ are recursively derived from Eq.(4.8) and (4.22). For example, we have $g_{2,1} = v \cdot a_{11} + l_{fs} \cdot a_{21}$ and $g_{3,1} = g_{2,1} \cdot a_{11} + g_{2,2} \cdot a_{21}$.

Thus, a higher order controller can be formulated as

$$\begin{bmatrix} \dot{\beta} \\ \dot{r} \\ \dot{\psi} \\ \dot{y}_f \\ \dots \\ y_f^{(n_f)} \\ \dot{\delta}_f \\ \dot{\zeta} \\ \dots \\ \zeta^{(n_s)} \end{bmatrix} = \begin{bmatrix} a_{11} & a_{12} & 0 & 0 & \dots & 0 & b_{11} & 0 & \dots & 0 \\ a_{21} & a_{22} & 0 & 0 & \dots & 0 & b_{21} & 0 & \dots & 0 \\ 0 & 1 & 0 & 0 & \dots & 0 & 0 & 0 & \dots & 0 \\ v & l_{fs} & v & 0 & \dots & 0 & 0 & 0 & \dots & 0 \\ \dots & \dots & \dots & \dots & \dots & \dots & \dots & \dots & \dots & \dots \\ g_{n_s,1} & g_{n_s,2} & 0 & 0 & \dots & 0 & g_{n_s,3} & 0 & \dots & 0 \\ 0 & 0 & 0 & 0 & \dots & 0 & 0 & 0 & \dots & 0 \\ 0 & 0 & 0 & 0 & \dots & 0 & 0 & 0 & \dots & 0 \\ \dots & \dots & \dots & \dots & \dots & \dots & \dots & \dots & \dots & \dots \\ 0 & 0 & 0 & 0 & \dots & 0 & 0 & 0 & \dots & 0 \end{bmatrix} \begin{bmatrix} \beta \\ r \\ \psi \\ y_f \\ \dots \\ y_f^{(n_f-1)} \\ \delta_f \\ \zeta \\ \dots \\ \zeta^{(n_s-1)} \end{bmatrix}$$
$$+ \begin{bmatrix} 0 & 0 \\ 0 & 0 \\ 0 & 0 \\ 0 & 0 \\ \dots & \dots \\ g_{n_f,4} & 0 \\ 1 & 0 \\ 0 & 0 \\ \dots & \dots \\ 0 & 1 \end{bmatrix} \begin{bmatrix} u_f \\ u_{aux} \end{bmatrix} + \begin{bmatrix} 0 & d_1 \\ 0 & d_2 \\ -v & 0 \\ -vl_{fs} & 0 \\ \dots & \dots \\ 0 & 0 \\ 0 & 0 \\ 0 & 0 \\ \dots & \dots \\ 0 & 0 \end{bmatrix} \begin{bmatrix} \rho_{ref} \\ f_w \end{bmatrix} \tag{4.23}$$

where n_f and n_s denotes the maximum derivative order of displacement y_f and

intermediate state ζ. Normally, we keep $n_f < n_s$.

The special filter is constructed by determining a proper auxiliary control

$$\zeta^{(n_f)} = F\tilde{x} \tag{4.24}$$

where $\tilde{x}$ is the state vector appeared in (4.23), and F is the auxiliary feedback matrix. It is obvious that the feedback rule (4.23) can be approximately realized with an appropriately chosen F.

Theorem 4.1 still holds for extended system (4.23). Simulations prove that higher order controller can yields better performance especially smaller displacement and better robustness to model uncertainty. However, additional implementation cost should also be considered when a practical control device is designed.

4.3.4 Robustness Analysis Considering Time Delay

Considering time delay exists in the observer, the feedback control should consists of two parts: r, y_f and δ_f which can be instantly measured, β and ψ which need to be estimated from observer. Taking time delay during estimation, the actual feedback can be rewritten as

$$u(t) = K \cdot \left(\begin{bmatrix} 0 \\ r(t) \\ 0 \\ y_f(t) \\ \delta_f(t) \end{bmatrix} + \begin{bmatrix} \beta(t-\tau) \\ 0 \\ \psi(t) \\ 0 \\ 0 \end{bmatrix} \right) = K_1 x(t) + K_2 x(t-\tau) \tag{4.25}$$

where τ denotes the delay cause by observer estimation. It is a constant determined by the applied observation algorithm and implementation method. Usually, we can

assume

$$\tau \le 0.1\,\mathrm{s} \tag{4.26}$$

The robustness of the proposed controller can be checked using the following theorem based on [239]-[240].

Theorem 4.2: if there exits three symmetry positive matrix P_1, P_2 and P_3 such that

$$H = \begin{pmatrix} [A+BK]^T P_1 + P_1[A+BK] + \tau[P_2+P_3] & * & * \\ \tau[A+BK_1]^T[BK_2]^T P_1 & -P_2 & 0 \\ \tau[BK_2]^T[BK_2]^T P_1 & 0 & -P_3 \end{pmatrix} < 0 \tag{4.27}$$

then the system is asymptotically stable for delay $\tau > 0$.

Proof: Define Lyapunov function

$$V(x(t)) = x^T(t)P_1x(t) + \int_0^{\tau}\int_{t-s}^{t} x^T(z)P_2x(z)dzds$$

we can easily check that

$$\dot{V}(x(t)) \le x^T(t)Hx(t) < 0$$

thus, it comes the conclusion. □

It should be pointed out that bound limit on displacement and actuator saturation may be violated under this situation even LMIs (4.12) holds. It simply leads to a bilinear matrix inequality design problem if we try to consider time delay controller (4.25) simultaneously. However, simulations show that bound limit on y_f is naturally satisfied with controller (4.10) in many cases if we appropriately choose $\gamma_{u,i}$ and $\gamma_{1,j}$.

4.3.5 Simulation Results

To demonstrate the feasibility of the proposed controller, its performance is compared with a robust controller that is only optimized to reject disturbance. Its design task is written as

Design Task 4.IV

Min γ

with $\gamma_\infty > 0$ such that LMIs (4.11) holds for system (4.8).

Suppose the vehicle is front steering and only the front sensor is applied. The parameters are assigned as:

$\tilde{m}$ = 1500 kg, $\tilde{I}_z$ =2500 kg.m.m, l_f = 1.2 m, l_r =1.5 m,

l_{fs} = 5 m, l_w = 0.5 m, c_f = c_r = 80000kN/rad.

$\delta_{\max}$ = 0.7 rad, $\dot{\delta}_{\max}$ = 0.4 rad/s, $w_{\max}$ = 0.02.

The variance bound of velocity is Δv = 1 m/s, $\Delta\tilde{m}$ = 100 kg, $\Delta\mu$ = 0.1. Suppose v is incorrectly estimated as 16m/s when it equals to 15m/s and μ is misestimated as 0.7 instead of 0.8 during the simulation.

The feedback matrices are chosen as

$$K = \begin{bmatrix} -48.4976 \\ -40.4636 \\ -60.4330 \\ -7.8951 \\ -92.6678 \end{bmatrix} \quad \text{and} \quad K' = \begin{bmatrix} -9.3907 \\ -0.1934 \\ -16.9858 \\ -1.7986 \end{bmatrix}$$

which are obtained in Task I and II respectively. Checking LMIs (26), we have the system is still stable for $\tau \le 0.2$ s .

Calculation shows that the maximum offset can be kept less than 0.2. The read line in Fig.4.1 denotes the control output of y_f using K', while the blue line denotes the control output of y_f using K. It is clear that the proposed controller yields better performance.

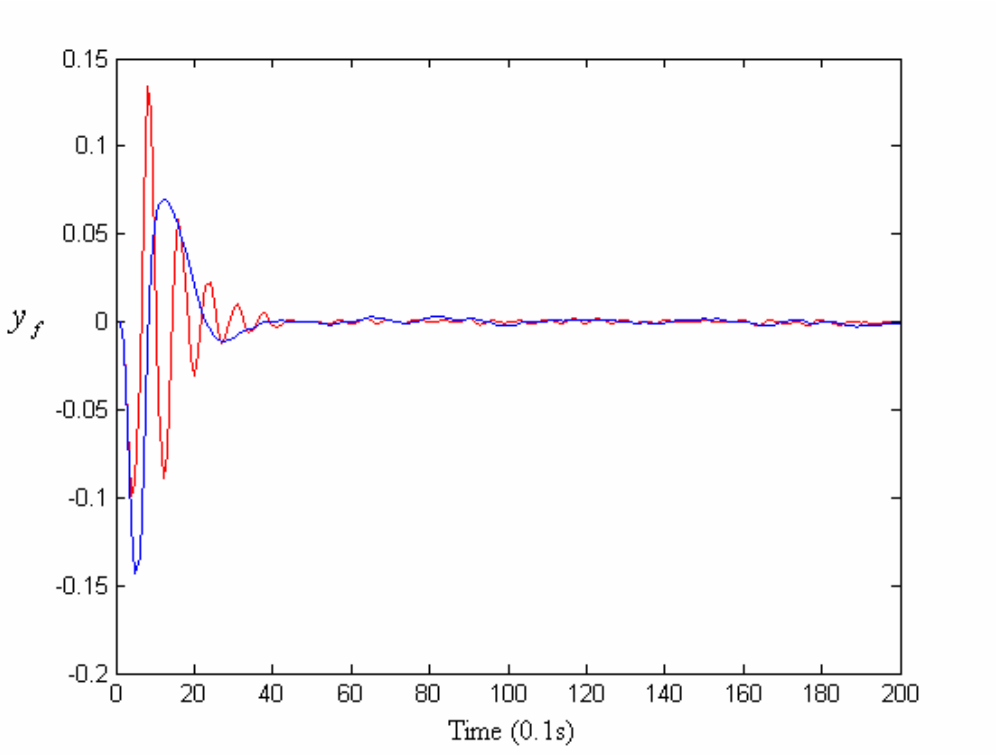

Figure 4.1 Control outputs of y_f using different controllers.

4.4 Speed Limit Estimation and Guideline Planning

4.4.1 Speed Limit Estimation for Steering and Lane Change

Obviously, we can pick up appropriate Q to satisfy the actuator saturation as

$$\left\| u_f \right\|_{\max} \le \sqrt{2}\gamma_{uf} w_{\max} \le \dot{\delta}_{f\lim}, \quad \left\| \delta_f \right\|_{\max} \le \sqrt{2}\gamma_{1,1} w_{\max} \le \delta_{f\lim} \tag{4.28}$$

Simultaneously, the maximum offset can be determined by

$$\left\| y_f \right\|_{\max} \le \sqrt{2}\gamma_{1,2} w_{\max} \tag{4.29}$$

Therefore, considering (6), we can have the safe constraints for a steering guideline with $\left\| \rho_{ref} \right\|_{\max}$ as

$$h_{\min}(x) \le -\sqrt{2}\gamma_{1,4} w_{\max} + g(x) \le -\left\| y_f \right\|_{\max} + g(x) \le y,$$

$$y \le \left\| y_f \right\|_{\max} + g(x) \le \sqrt{2}\gamma_{1,4} w_{\max} + g(x) \le h_{\max}(x) \tag{4.30}$$

where $h_{\min}(x)$ and $h_{\max}(x)$ represent the road boundary respectively. As shown in Fig.4.2, the real steering trajectory will be restricted within two envelope curves determined by the guideline and maximum offset $\left\| y_f \right\|_{\max}$. If the two envelope curves do not interfere with the road boundaries, then the controller can guarantee the safety of the steering process.

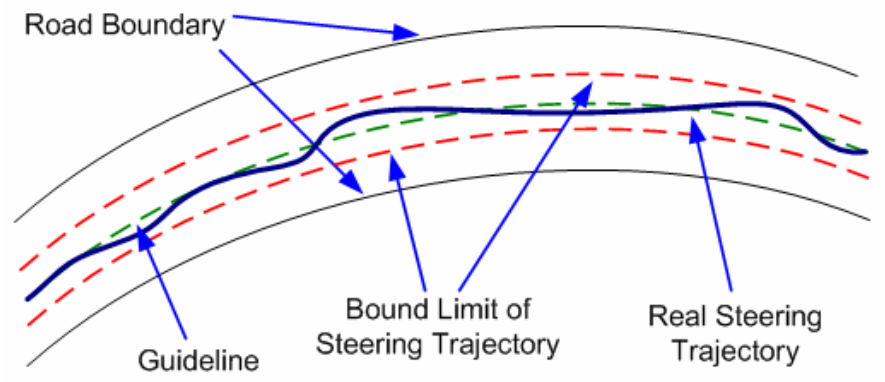

Figure 4.2 Bounds of real steering trajectory. The green dash line is the guideline. The two red dash lines are bounds (envelope) curves. The blue curve denotes the real trajectory.

Thus, we can have a rough estimation of the safe speed limit regarding curvature, if we simply choose the middle curve of a road curve as the guideline. The estimation can be formulated as follow:

Planning Task 4.V

Max v

under given bound $w_{\max} = \left\| \rho_{ref} \right\|_{\max}$ and road width D;

with certain $Q > 0$, $\lambda > 0$ and $\alpha > 0$ such that (13)-(17) holds as well as

$$\left\| y_f \right\|_{\max} \le \sqrt{2}\gamma_{1,2} w_{\max} \le D/2 \tag{4.31}$$

Normally, we will use grid search technique to check the existence of a feasible controller over the solution space of v. Fig.4.3 shows that the speed space is divided into two parts. The area above represents the estimated unsafe driving scenarios. Normally, the estimated speed limit is smaller than the actual maximum allowable speed.

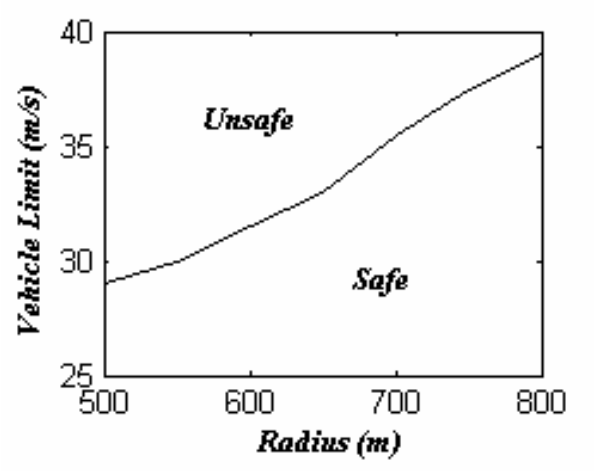

Figure 4.3 Relation between vehicle velocity limit and road curvature (denoted by radius).

The speed limit for frequency domain steering controller (2.13)-(2.14) can be obtained by frequency L_1 design theory as

$$\|y_f\|_{\max} \le \left\| \frac{y_f(s)}{\rho_{ref}(s)} \right\|_1 w_{\max} \tag{4.32}$$

Moreover, there were several other steering controllers such as sliding mode controllers, fuzzy controllers and etc.. In [221] Chaib, Netto and Mammar compared the performances of a linear robust controller, a fuzzy controller and an adaptive controller. They showed that a linear steering controller is usually outperformed by other nonlinear steering controllers in several aspects including maximum offset value. Thus, the safe speed limit obtained here can also be viewed as an acceptable yet not very accurate estimation for the other nonlinear steering controllers.

For the lane changing trajectory planning problem, similar method can also be applied except the steering guideline is substituted by lane changing path. Since the

vehicle speed is often considered to be varied during the whole process, we just choose the largest speed to solve LMI (4.11)-(4.13) as the in estimation process for simplicity.

4.4.2 Optimal Guideline/Trajectory Planning

In the above analysis, we just simply chose the middle curve of the road as the guideline. However, further analysis shows that we can pick up other guidelines to improve ride safety, comfort, and some other demands of the driver/passengers.

Consider the two different guidelines and corresponding steering behaviors given in Fig.4.4. The red guideline leads the driver to start steering at point A; while the blue guideline starts at point O. Since point A lags point O, the peek value of the desired curvature for the red guideline is higher than that of the blue guideline. Therefore, the steering process using the blue guideline yield smaller offset. Moreover, it allows faster speed to pass this curve. However, since the curvature of the blue guideline is relatively flatter, it is closer to the road boundary too. This may be dangerous although the maximum offset is small. So we cannot make the guideline as flat as possible since the vehicle may bump off the road.

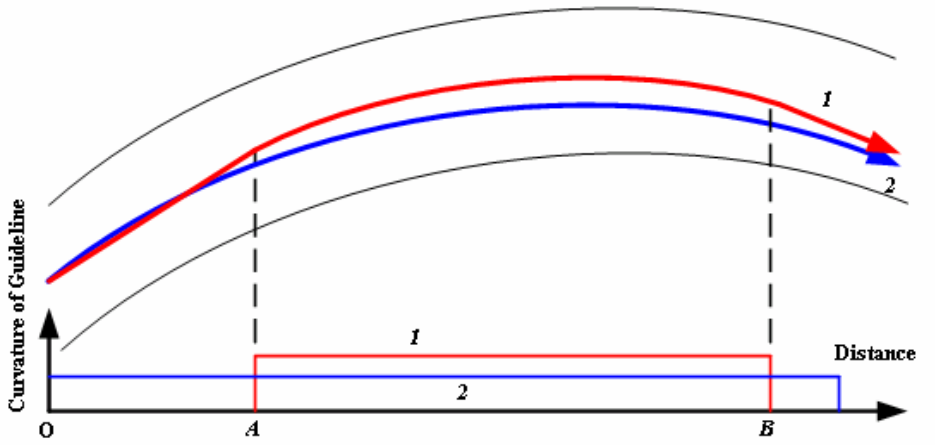

Figure 4.4 Comparison of two different guidelines and corresponding steering behaviors.

Besides the safety consideration, the driver/passengers' feelings and characteristic demands should not be neglected. As pointed out in [214]-[216], some drivers want to drive as fast as possible on the highway to save time, while some drivers want to make the acceleration/deceleration of the vehicle as small as possible to make the long trip comfortable. Thus, some optimal performance indices should be introduced associated with the trajectory generation problem.

Based on our previous discussions [214]-[16], we just consider two objectives there: least time consuming and least jerk during steering.

The time T used for steering can be approximately written as:

$$T \approx \frac{\text{length of the guideline}}{v} \tag{4.33}$$

The maximum jerk during steering can be roughly estimated as:

$$\begin{aligned} J &\approx \left\| \ddot{y}_f \right\|_{\max} \approx \left\| v \cdot \dot{\beta} + v \cdot \dot{r} + v \cdot \dot{\psi} \right\|_{\max} \\ &\approx \left\| v \cdot (a_{11}\beta + a_{12} r + b_{11}\delta_f) + l_s \cdot (a_{21}\beta + a_{22} r + b_{21}\delta_f) + v \cdot r \right\|_{\max} \end{aligned} \tag{4.34}$$

Thus, we can introduce an auxiliary L_1 -performance output, by setting the measurement matrix as

$$C_1' = \begin{bmatrix} 0 & 0 & 0 & 1 & 0 \\ 0 & 0 & 0 & 0 & 1 \\ v \cdot a_{11} + l_s \cdot a_{21} & v \cdot a_{12} + l_s \cdot a_{21} + v & 0 & 0 & b_{11} + b_{21} \end{bmatrix}$$

and get the bound of jerk as

$$\|J\|_{\max} \le \sqrt{2}\gamma_{1,3} w_{\max} \tag{4.35}$$

Thus, the optimal steering guideline planning problem can be formulated as

Planning Task II:

Min $H = q(T, \|J\|_{\max})$

with certain steering guideline to satisfy safety requirement. Here $q(T, \|J\|_{\max})$ is a certain evaluation function that takes compromising between time and comfort considerations.

Normally, we can express the steering guideline with a five point Bezier curve and search optimal the optimal Bezier I interpolation points. Constrained by the length of this chapter, we will not discuss the details here.

4.4.3 Graphical User Interface Design

The graphical user interface for driver guidance received constant consideration recently. In steering, an appropriate aid system should notify the driver about the

desired steer angle and the actual steer angle.

For instance, a graphical user interface device is shown in Fig.4.5 below. The blue curves indicate the road boundaries. The green arrow in the right top corner indicates the optimal front steering angle, and the red arrow shows the actual front steering angle. Thus, the driver will try to adapt the right steering police by making the red arrow overlap the green arrow. This process is quite straightforward and drivers can easily get accustomed with it.

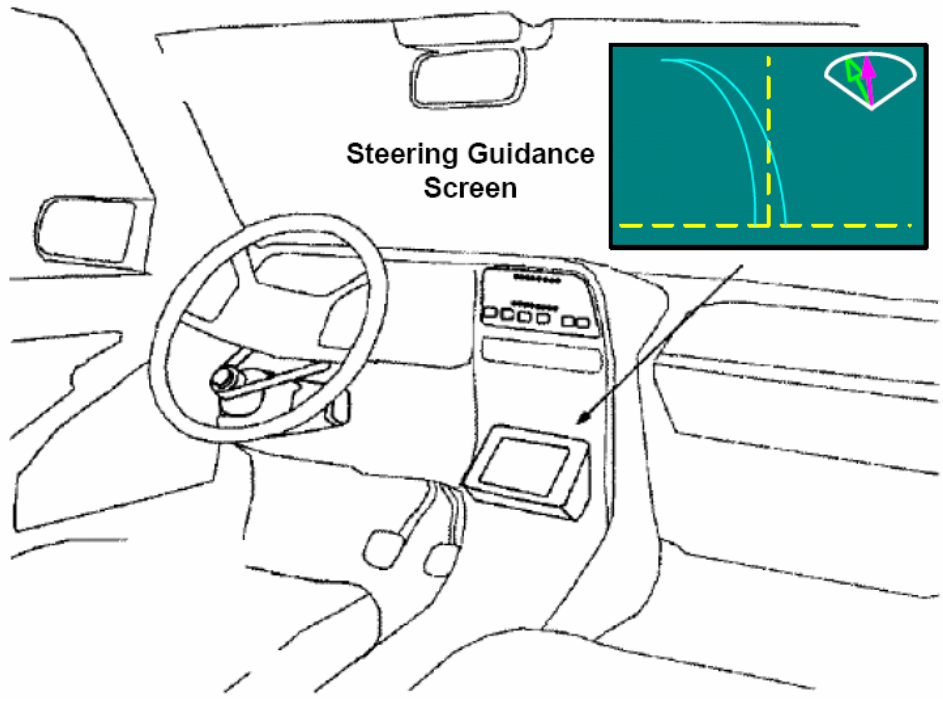

Figure 4.5 A graphical user interface device for steering guidance.

CHAPTER 5 COOPERATIVE DRIVING AT BLIND CROSSINGS USING INTER-VEHICLE COMMUNICATIONS

Cooperative driving technology with inter-vehicle communication attracts increasing intentions recently. It aims to improve driving safety and efficiency using appropriate motion scheduling of all the encountered vehicles. Under cooperative driving control, the motion of individual vehicles can be conducted in a safe, deterministic and smooth manner. This is particularly useful to heavy duty vehicles, since their acceleration/deceleration capacity is relatively low. Specifically in this chapter, cooperative driving at blind crossings (crossings without traffic lights) is studied. A concept of safety driving patterns is proposed to represent the collision free movements of vehicles at crossings. The solution space of all allowable movement schedules is described by a spanning tree in terms of safety driving patterns; four trajectory planning algorithms are formulated to determine the driving plans with least execution times using schedule trees. The corresponding group communication strategy for inter- vehicle networks is also analyzed. Finally, simulation studies have been conducted and results demonstrate the potentiality and usefulness of the proposed algorithms for cooperative driving at blind crossings.

5.1 Introduction

A variety of techniques had been introduced to increase the capacity and safety of the existing highway systems. Among these techniques, the technology of cooperative driving with inter-vehicle communications is now considered as a potential solution to alleviate traffic jam and reduce collisions.

The concept of cooperative driving was first presented by JSK (Association of Electronic Technology for Automobile Traffic and Driving) in Japan in the early 1990s [244]. It was originally used as flexible platooning of automated vehicles with a short inter-vehicle distance over a couple of lanes. At that time, it was known as super smart vehicle systems (SSVS) [244]-[246]. Using appropriate inter-vehicle communications to link vehicles, cooperative driving enables vehicles to perform safe and efficient lane changing and merging, and thus improve the traffic control performance. Since then, the feasibility and benefits of cooperative driving have been further discussed and examined world-widely, i.e. in California PATH project in USA [247][248], Chauffeur project in EU [249], and Demo 2000 Cooperative Driving System in Japan [250].

Generally, all these approaches focus on two questions: how to exchange the information among vehicles and how to guide vehicles using the obtained information. The answer to the former question is inter-vehicle communications [247]-[254]. It enables the vehicles to share information about their driving status and goals, which greatly extend the horizon of drivers or intelligent driving systems. The latter question

is answered by using cooperative trajectory planning [247]-[254], [255]-[258].

The conventional implementation of inter-vehicle communication links vehicles through a remote service station (i.e. the communication tower mentioned in [251] and [252]). The driving information of a vehicle will be first transformed to service station and then broadcasted to other related vehicles. Or, the vehicles inquiry service station to locate other vehicles. These approaches increase considerably the cost for building and maintaining remote service stations.

Different from the methods above, many new designs use the peer-to-peer ad-hoc network to achieve vehicular information sharing. As shown in [253], peer-to-peer ad-hoc communication networks integrate four valuable features: ad-hoc connectivity, local peer-to-peer networking, short-range and inter-personal communication. Currently, inter-vehicle communication networks are still under discussions due to varied driving behaviors and high mobility [254].

From the control systems perspective, cooperative driving can be used to enhance the ride safety and quality. Cooperative trajectory planning is one frequently used control method in this field. It designs time varying velocity profiles for the encountered vehicles to perform a designed maneuver. Using these methods, the motion of individual vehicles can be performed in a safe, smooth and deterministic manner. This is particularly useful to heavy duty vehicles, because their acceleration/deceleration capacity is quite low [255]-[258].

In this chapter, we use the idea of the cooperative driving to study vehicle

collision avoidance at road junctions, which is more complex than longitudinal control of vehicle platoons. In [259], a simple case of two vehicles had been analyzed using game theory. The differential game approaches assume that all the encountered vehicles cannot know each others' decision [259]-[260]. Therefore, a cooperative driving method should naturally outperform it, especially when simultaneously dealing with multi-vehicles.

The difficulties of cooperative driving at junctions lie in two aspects. The first one is to quickly determine whether a special driving plan is safe. In longitudinal platoon control, all vehicles are moving in the same direction, so it is much more complex to guarantee the ride safety for crossing at junctions, because vehicles may steer to totally different directions. The second one is to pick up the one with the least time cost from hundreds of possible schedules for alleviating congestions, an objective not considered in platoon control.

5.2 Problem Description

5.2.1 Driving at Blind Crossings

One basic method towards collision free and fast movement of vehicles is to install traffic light systems. However, because of cost and some reasons such as in construction sites and military zones, many road junctions have no traffic lights. We will focus on vehicle driving scenarios at such blind crossings.

Usually, vehicle flows are assumed to arrive continuously at a junction area.

However, at a particular time, we only need to consider a few vehicles which are moving in the vicinity of the crossing. Under this consideration, the continuous traffic flow can be truncated intro small segments, which simplifies the problem greatly.

The simple grouping algorithm used here is to label the vehicles by the times they enter the virtual circle centered at the junction point. As shown in Fig.5.1, the four shadow vehicles inside the cycle will be considered as a group to take part in cooperative driving; while the other three vehicles will not be considered temperately. The radius of this virtual circle should be determined appropriately by inter-vehicle communication protocol that has been selected for this application.

It should be pointed out that normally the blind crossings are not busy. Simulation shows that this grouping algorithm does well for such kind of crossings.

Moreover, it is also assumed that all vehicles have relatively low speeds when approaching the junction and they will not change lanes after entering the virtual circle since we consider it is too close to safely change lanes within the virtual circle. Slowing down makes the vehicles have more time to negotiate with each others and prepare for suddenly emerged pedestrians.

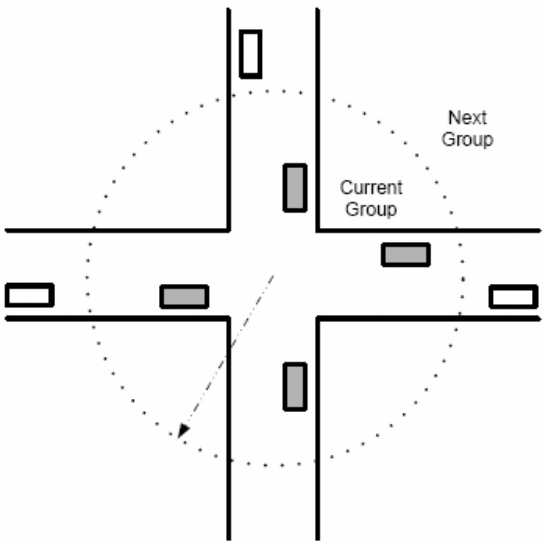

Figure 5.1 Vehicle grouping at crossings.

5.2.2 Inter-Vehicle Communication

The inter-vehicle communications plays an important role in cooperative driving, since the necessary driving information of other vehicles has to be transmitted to the vehicle that makes the final driving decision.

There were many discussions on designing, implementing and testing of the inter-vehicle communications, i.e. COCAIN (Cooperative Optimized Channel Access for INter-vehicle communication) proposed by Kaltwasser and Kassubek in [261], TELCO (Telecommunication Network for Cooperative Driving) proposed by Verdone in [262], DOLPHIN (Dedicated Omni-purpose inter-vehicle communication Linkage Protocol for HIghway automatioN) proposed by Tokuda, Akiyama and Fujii in [263].

In blind crossing driving scenario, the encountered vehicles need to share the

following information among each other:

(a) the desired moving lane number of each vehicle before the cooperative driving plan is made;

(b) the driving plan of each vehicle after the cooperative driving plan is made;

(c) the real-time position (represented as lane number and distance from the crossings) and speed of each vehicle;

(d) the emergency signal if needed.

In order to efficiently exchange information, we propose a new model based on the hierarchical group message-deliver models discussed in [263]-[268].

When approaching the crossing areas, the original vehicle platoon splits into several independent groups. The maximum allowable size of such a group is set as three in this chapter. The initial groups are constructed by randomly assigning several temporary dominant vehicles and letting them pick up its neighbor vehicles into its group. The groups contain more than three vehicles will reject the tail vehicles to meet the limits. The rejected vehicles will try to merge into other groups or formulate a new group.

In this mode, the vehicles are supposed to be self-organized into several small groups as shown in Fig.5.2, before they enter the virtual circle.

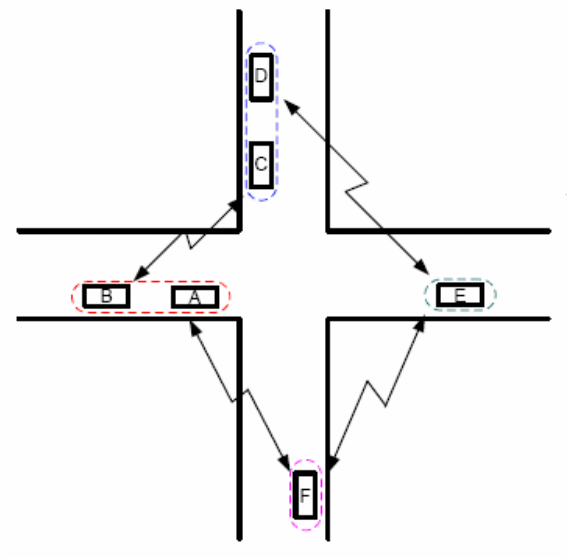

Figure 5.2 Vehicle groups and group inter-vehicle communication.

A vehicle is assumed to store the real-time positions, speeds and desired driving lane information of all vehicles in the same group. It communicates with each other periodically to update position and speed information. Simulations presented in Section 5 show that three is an appropriate size for an independent group for blind crossing scenarios.

When vehicle A and B in two different groups communicate with each other, vehicle A will transfer the driving information of all vehicles in the same group to B. The received driving information from B will be soon delivered to other vehicles in the group of vehicle A. So does vehicle B to A.

It is also assumed that all vehicles have constant speed before the cooperative driving plan being set. Thus, one vehicle can predicate the movements of other

vehicles in the near future based on received driving information.

Although the data transmission rate is constrained by several factors including media and communication protocol, we assume that the vehicles within the virtual cycle can properly acquire timely the necessary driving information of each other. Based on the experiment results in [268]-[270], such assumptions are valid for most blind crossings, because the radius of the virtual circle and the number of encountered vehicles are both limited in those driving scenarios.

The inter-vehicle communication network will use tags to label the groups/vehicles encountered. If all the vehicles' moving information has been collected by one vehicle, it will proceed the trajectory planning. It will simultaneously send messages to block off other vehicles for taking this job.

After the cooperative driving plan is made, the schedule will be properly delivered. Constrained by the communication rate, the driving plan should be represented concisely. A detailed description of the representation method will be presented in Section 4.

When one vehicle leaves the virtual circle, it will leave the current communication group and join a new platoon.

Emergency signals will be broadcasted to all vehicles with the highest priority.

5.3 Cooperative Driving Schedule

5.3.1 Collision Free Driving Represented by Safe Patterns

In order to guarantee the safety of driving, the concept of safe driving patterns is introduced first.

Generally, the collision may occur when

(i) two vehicles move along the same lane, and the lag one runs into the lead one;

(ii) two vehicles moves on different lane but pass the same point simultaneously.

The most frequently used control strategy for blind crossings is the zone blocking strategy. It divides the crossing zone into server sub zones and only one vehicle is allowed to enter a zone at any time to avoid collisions.

Based on a similar idea, a simplified strategy is proposed here, which only allows safe driving patterns (vehicle pairs) to pass the junctions at one particular time. It is similar to the concept of phase of traffic flows in traffic lights control.

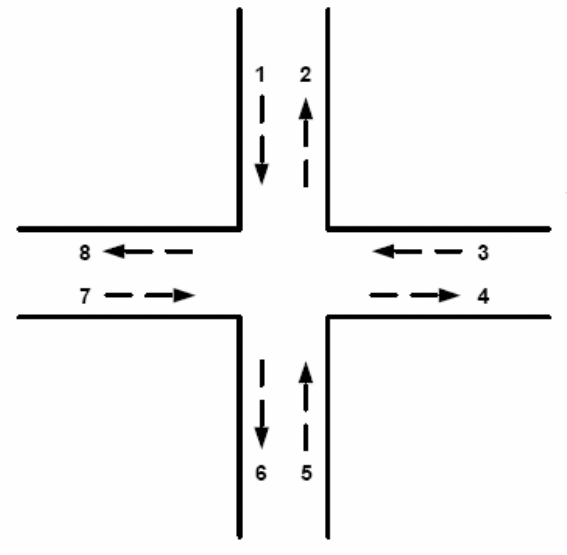

Figure 5.3 Diagram of two-lane junctions.

For instance, consider the two-lane road junctions shown in Fig.5.3. Taking symmetry into account, there only exist three driving patterns that allow two vehicles cross junction area safely and simultaneously:

(a) one vehicle drives from lane 1 to lane 8 while the other vehicle drives from lane 5 to lane 2;

(b) one vehicle drives from lane 1 to lane 8 while the other vehicle drives from lane 5 to lane 4;

(c) one vehicle drives from lane 1 to lane 6 while the other vehicle drives from lane 5 to lane 2.

In terms of safe driving patterns, we can represent a driving schedule as an

ordered series of safe patterns. To illustrate this idea, consider a typical driving scenario shown in Fig.5.4, in which vehicle A needs to move from lane 7 to lane 4, vehicle B from lane 7 to lane 6, vehicle C from lane 1 to lane 8, vehicle D from lane 1 to lane 4.

One possible driving schedule for this scenario is to let vehicle A pass the junction first; then let vehicle B and C pass the junction at the same time; and finally let vehicle D pass. Apparently, we can represent this schedule as the following sequence

$$A \mid B, C \mid D \tag{5.1}$$

where "|" is a separator symbol that divides the sequence into three subsets: A, B and C, D. B and C are in one subset indicating they will pass the junctions at the same time.

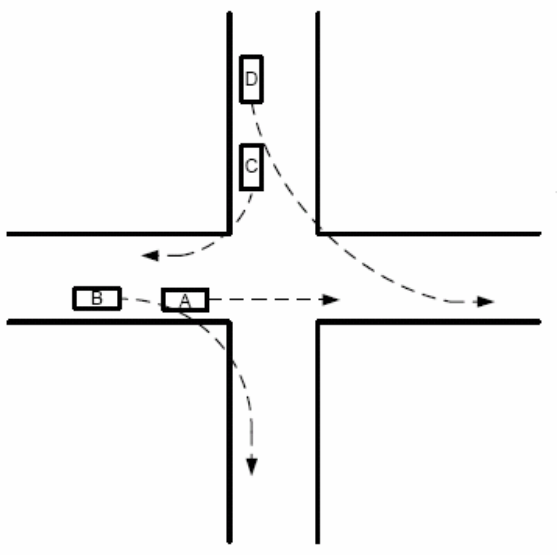

Figure 5.4 A four-vehicle driving scenario for a two-lane junction.

Generally, consider N vehicles $i_1, i_2, \dots, i_N$ moving towards the junction. Their order of passing the junction area, i.e. the cooperative driving schedule is specified as

$$i_1, i_5, \dots, | i_2, i_4, \dots, | i_3, \dots, i_N \tag{5.2}$$

When one particular driving schedule is determined, the corresponding trajectory planning process for each vehicle will then be carried out. Notice that different driving schedules lead to different passing times. An optimal cooperative driving plan needs to find the schedule that completes the total driving process with the least time. In the rest of this section, we will discuss how to generate all allowable driving schedules. The optimal schedule search process will be described in Section 5.4.

5.3.2 Solution Tree Generation and Labeling

In general, searching the allowable driving schedule will yield a tree in which each node represents a particular driving plan (sequence) except for the root node. One basic algorithm to generate such a tree is as follows:

Basic Solution Tree Generation Algorithm.

Suppose there are N vehicles under consideration.

1. Generate the root node of the tree;
2. Generate N children for the root node which represent all the possible

permutation orders of the vehicle sequence without any separator symbols. It is apparently that all these orders can be enumerated through basic permutation algorithm.

3. For each node in the second level of the tree, generate $N-1$ children by inserting only one separator into the driving sequence that is represented by it, since there are only $N-1$ positions that a separator can be inserted.

4. For each node in the third level of the tree, generate $N-2$ children by inserting only one separator into the driving sequence that is represented by it, since there are only $N-2$ positions that a separator can be inserted.

…

N. For each node in the $N-1$ level of the tree, generate one child by inserting only one separator into the driving sequence that is represented by it, since there is only one position that a separator can be inserted.

However, a great number of nodes in this tree can be discarded since they represent invalid driving schedules, for which no trajectory planning is needed.

One apparent fact is that lead vehicles will always pass the junction areas earlier than lag vehicles in the platoon, because we assume that the lag vehicle will not change lanes. For instance, in the driving scenario shown in Fig.5.4, vehicle A should

always pass the crossing earlier than vehicle B. Thus the node B A C D and all its children should be invalid.

Based on this fact, we can modify the above algorithm as

Modified Solution Tree Generation Algorithm.

Suppose there are N vehicles under consideration.

1. Generate the root node of the tree;
2. Generate N children for the root node which represent all the possible permutation orders of the vehicle sequence without considering separator symbols. Then, prune all the obtained nodes that represent invalid order of driving.

3.-N. Same as Basic Solution Tree Generation Algorithm.

To guarantee a collision free movement, the safety of the simultaneously moving subnets in a driving sequence has to be checked. It is apparent that each subset in a valid driving schedule should constitute of a safe driving pattern.

Note that M vehicles can safely cross the junctions at the same time if and only if every pair of these vehicles is a safety pattern. Therefore, the labeling algorithm is given by:

Safety Pair Labeling Algorithm.

If there are M ($M \geq 2$) vehicle j_1, j_2, …, j_M pass the crossing the junctions simultaneously, check the $M(M-1)/2$ distinct vehicle combinations (j_1, j_2), (j_1, j_3), …, (j_{M-1}, j_M) to see whether they are all safety patterns. If not, label the corresponding node as an unsafe node.

Using these two considerations, most unsafe driving schedules can be pruned from the solution tree. For examples, the driving plan tree stemmed from scenarios in Fig.5.4 only has a few valid nodes after pruning and labeling, i.e. there are only two valid driving schedules for the ordered sequence A, B, C, D, see Fig.5.5. The first schedule is specified by Eq. (1) and the second is simply let vehicle A, B, C, D pass the junction area sequentially.

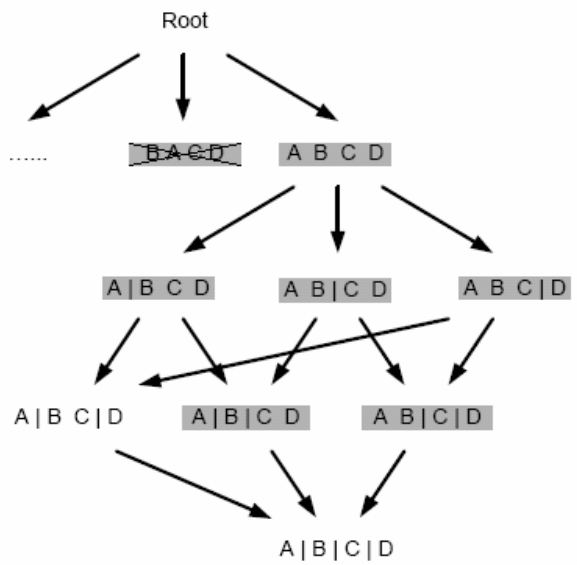

Figure 5.5 A schedule tree stemmed from the driving scenario shown in Fig.5.4. The shadow nodes represent invalid driving schedule.

After labeling, trajectory planning will be executed for every valid node with respect to its driving schedule. Some driving plans will be discarded since they are implicitly forbidden by the vehicle dynamics constraints.

5.4 Cooperative Trajectory Planning

5.4.1 Trajectory Planning

In general, a vehicle's trajectory crossing the junctions can be divided into three sequential stages:

(a) approach the junction. It should avoid collision between the lead vehicle and itself. Moreover, it should also avoid collision between itself and the last vehicle that had passed the junctions before it but does not form a safety pair with it;

(b) cross the junction, which is considered as a decelerate- accelerate process;

(c) leave the junction. It should avoid collision between the new lead vehicle and itself.

In order to solve these trajectory planning problems, the virtual vehicle mapping technique was proposed and employed by Uno, Sakaguchi and Tsugawa in [271] and [272]. The concept of a virtual vehicle is to map a vehicle on a lane onto an object

lane; then the interested vehicle can be controlled with respect to the virtual vehicle to guarantee safety.

Considering the risk of failure, an algorithm similar to what proposed in [271] and [272] is applied here. The only difference is that the lead vehicle is not mapped onto the symmetry position of the desired lane. Actually, it will be mapped into a position that lags off the mirror point to compensate the communication delay.

For example, as shown in Fig.5.6, vehicle A moves form lane 7 to lane 6 first; then vehicle B moves from lane 1 to lane 6. Since vehicle B passes the junction area right after vehicle A, it must make enough headway to avoid collision. Therefore, it generates a virtual vehicle A' by mapping vehicle A into its own lane using the data transmitted via the inter-vehicle communication. Classical longitudinal control will then be performed between virtual vehicle A' and vehicle B.

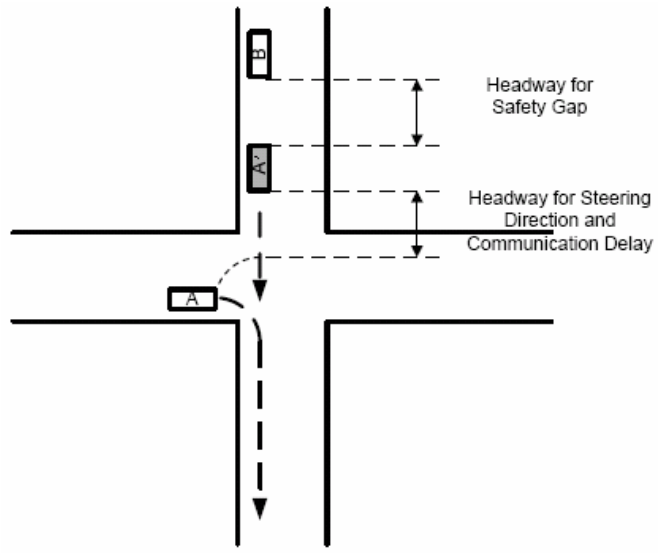

Figure 5.6 Trajectory generation considering one virtual vehicle.

The lengths of the two headways should be determined by the dynamic properties of encountered vehicles and the applied inter-communication protocols.

The trajectory profile of each vehicle in the driving schedule will be generated one by one with respect to the corresponding driving order passing the junction. Every vehicle can ‘know’ the trajectories of the other related vehicles that need to map onto its lane.

Since we need to improve traffic efficiency, the driving plan should keep the headway between the potential lead/virtual vehicle and itself to the minimum safe distance.

Generally, we can classify various driving scenarios into the following four cases.

Case A) there is neither a lead vehicle moving in the same lane nor a virtual vehicle that needs to map before the planning vehicle enters the junction area;

Case B) there is a lead vehicle moving in the same lane but no virtual vehicles that need to be mapped before the planning vehicle enters the junction areas. Indeed, it equivalently means that the planning vehicle will pass the junction area right after the lead vehicle;

Case C) there is not a lead vehicle moving in the same lane but a virtual vehicle that needs to be mapped before the planning vehicle enters the junction area;

Case D) there is a lead vehicle moving in the same lane, and there is also a virtual vehicle that needs to be mapped before the planning vehicle enters the junction area. Actually, it means that the planning vehicle will first follow the lead vehicle and then follow the virtual vehicle before it enters the junction.

Suppose the position of the planning vehicle is denoted by x_p and u is the control input to the vehicle. Their dynamics are constrained by

$$u_{\min} \le u \le u_{\max} \tag{5.3}$$

$$0 \le \dot{x}_p \le v_{\max} \tag{5.4}$$

where $u_{\min}$ and $u_{\max}$ are the bounds of control input u. $v_{\max}$ is the maximum allowable safe speed.

If the planning vehicle need to steer directions, there is an additional constraint

$$\dot{x}_p(t_3) \le v_{s\max} \tag{5.5}$$

where $v_{s\max}$ is the maximum allowable speed for steering, and t_3 is the time when the planning vehicle enters the junction area.

The corresponding trajectory planning algorithms can be formulated as follows.

Algorithm 5.I. Trajectory Planning for Case A.

5.I.1. Solve the time optimal trajectory planning problem before the planning vehicle enters the junction areas.

Obviously, the objective is

$$\min_{u} t_3 \tag{5.6}$$

constrained by the given boundary conditions

$$x_p(t_0) = x_{p0}, \quad x_p(t_3) = x_{ps} \tag{5.7}$$

where x_{p0} is the start position and x_{p2} is the final position beside junction areas; t_0 is the time that planning starts.

5.I.2. There is no planning at this stage. We simply assume that the time consumed during crossing and the vehicle speed leaves the junction areas only depend on vehicles speed.

The time that the planning vehicle leaves the junction areas should be

$$t_4 = t_s + f_1(\dot{x}_p(t_3)) \tag{5.8}$$

and the speed should be

$$\dot{x}_p(t_4) = f_2(\dot{x}_p(t_3)) \tag{5.9}$$

where t_4 is the time that the planning vehicle leaves junction areas.

5.I.3. Solve the tracking problem for the new lead vehicle before the virtual vehicle leaves the junction area.

Suppose the trajectory of the new lead vehicle is given as

$$\ddot{x}_n = f_3(t) \tag{5.10}$$

where x_n is the position of the new lead vehicle and $f_3(t)$ is its

movement descriptive function in terms of time.

Thus, the error e_{np} in headway from the pre-selected safe distance L_3 can be written as

$$e_{np} = x_n - x_p - L_3 \tag{5.11}$$

Obviously, the objective is

$$\min_u \int_{t=t_4}^{t_4+T} |e_{lp}| dt \tag{5.12}$$

constrained by (5.6), (5.7) and boundary condition (5.10). Here T is a predetermined time span that is long enough to appropriately describe the planning vehicle's movement after it leaves the junction areas.

Algorithm II. Trajectory Planning for Case B.

5.II.1. Solve the lead vehicle tracking problem before the lead vehicle leaves the junction area.

Suppose the trajectory of the lead vehicle is given by

$$\ddot{x}_l = f_4(t) \tag{5.13}$$

where x_l is the position of the lead vehicle and $f_4(t)$ is its movement descriptive function in terms of time.

Thus, the error e_{lp} in headway from the pre-selected safe distance L_1 can be written as

$$e_{lp} = x_l - x_p - L_1 \tag{5.14}$$

Obviously, the objective is

$$\min_u \int_{t=t_0}^{t_1} |e_{lp}| dt \tag{5.15}$$

constrained by the given initial conditions

$$x_p(t_0) = x_{p0} \tag{5.16}$$

(5.6), (5.7) and boundary condition (5.10), where t_1 is the time that the lead vehicle enters the junction areas.

5.II.2. same as Algorithm 5.I.1 expect the initial condition is given by

$$x_p(t_1) = x_{p1} \tag{5.17}$$

where x_{p1} is the planning vehicle's position at time t_1.

5.II.3. same as Algorithm 5.I.2.

5.II.4. same as Algorithm 5.I.3.

Algorithm III. Trajectory Planning for Case C.

5.III.1. Solve the virtual vehicle tracking problem before the virtual vehicle leaves the junction area.

Assume the trajectory of the virtual vehicle be

$$\ddot{x}_v = f_5(t) \tag{5.18}$$

where x_v is the position of the virtual vehicle and $f_5(t)$ is its movement descriptive function in terms of time.

Thus, the error e_{vp} in headway from the pre-selected safe distance L_2 can be written as

$$e_{vp} = x_v - x_p - L_2 \tag{5.19}$$

Obviously, the objective is

$$\min_u \int_{t=t_0}^{t_2} |e_{lp}| dt \tag{5.20}$$

constrained by the given initial conditions (5.17), and dynamic constraints (5.6) and (5.7), where t_2 is the time that the virtual vehicle leaves the junction areas.

5.III.2. same as Algorithm 5.I.1 expect the initial condition is given as

$$x_p(t_2) = x_{p2} \tag{5.22}$$

where x_{p2} is the planning vehicle's position at time t_2.

5.III.3. same as Algorithm I.2.

5.III.4. same as Algorithm I.3.

Algorithm IV. Trajectory Planning for Case D.

5.IV.1. same as Algorithm II.1.

5.IV.2. same as Algorithm III.1 expect the initial condition is given as (5.18) and t_1 is the time that the lead vehicle enters the junction areas.

5.IV.3. same as Algorithm I.1 expect the initial condition is given as (5.22) and t_2 is the time that the virtual vehicle leaves the junction areas.

5.IV.4. same as Algorithm I.2.

5.IV.5. same as Algorithm I.3.

It should be pointed out that the choice of vehicle dynamic models and/or longitudinal driving controllers will not vary the feasibility of the proposed planning framework. Furthermore, some other driving performance index such as ride comfortableness can be formulated and applied here. Some related discussion on objective choice of vehicle trajectory planning can be found in our previous works [273]-[276].

However, there is still one important issue left. Limited by the communication rate, the cooperative driving plan should not be too complicated. Otherwise, the cooperative driving plan cannot be correctly delivered to all the encountered vehicles.

Here, we further constrain the trajectory of one vehicle constitutes of at most five steady acceleration/deceleration process. Thus, one vehicle's trajectory will be determined by at most seven dataset as follows:

<star time t_0, velocity $\dot{x}_p(t_0)$>, <velocity change time t_1, velocity $\dot{x}_p(t_0)$>, ……,
<end time t_6, velocity $\dot{x}_p(t_6)$>

(5.22)

The velocity between time t_i and t_{i+1} can be written as

$$\dot{x}_p(t) = \dot{x}_p(t_i) + [\dot{x}_p(t_{i+1}) - \dot{x}_p(t_i)] \cdot \frac{t - t_i}{t_{i+1} - t_i} \tag{5.23}$$

This method greatly reduces the computation costs of the above trajectory planning problems without losing too much generality. Moreover, this technique also relieves the burden of the inter-vehicle communication network, since there are only twelve variables in (23) need to be encoded and delivered to the involved vehicle. The vehicle will resolve the control inputs from this simplified velocity profile based on its own dynamic equation.

5.4.2 Best Driving Plan Search

The total time cost of trajectory is countered from the time when the cooperative driving process begins to the time when the last vehicle leaves the junction area. All the un-discarded driving plans will be compared, and the one with least time cost will be chosen as the actual driving plan.

The diagram of this cooperative driving planning framework is shown in Fig.5.7. To summarize, the safety of the framework is guaranteed by selecting safe driving patterns; and the efficiency is achieved by adopting the time optimal driving plan.

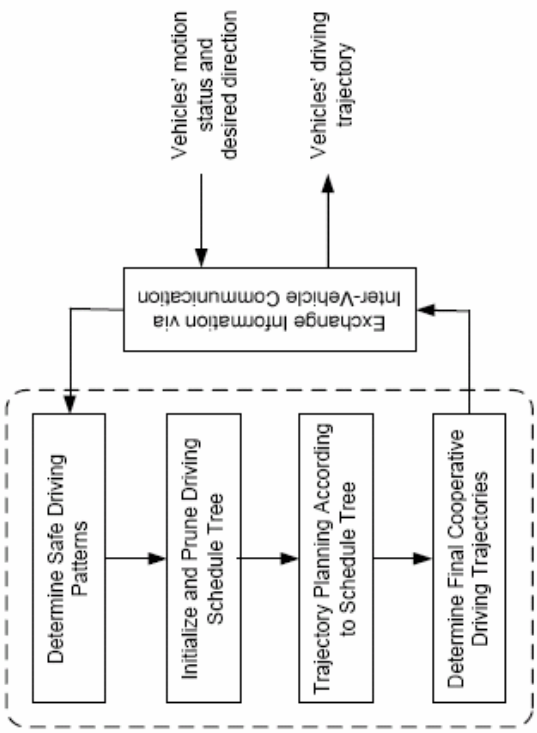

Figure 5.7 The cooperative driving planning framework.

In the searching process of optimal driving plan, the upper level nodes in the schedule tree will be examined earlier with respect to the lower level plans. If one plan is proven to be valid, then all its children nodes will be omitted, because a valid node always represents the plan that uses less time than that of its children plans. For example, if solution A | B C | D in Fig.5.5 is a valid plan, then its child node A | B | C | D need no analysis.

5.5 Simulation Results

5.5.1 Simulation Results for Trajectory Planning

A demonstration simulation case shown in Fig.5.8 is studied here. In this scenario,

vehicle A moves from lane 7 to lane 6, vehicle B from lane 3 to lane 6, vehicles C and D from lane 1 to lane 6.

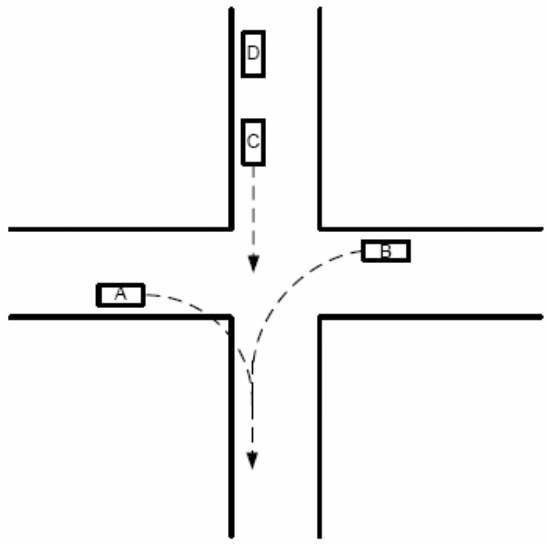

Figure 5.8 A three-vehicle driving scenario for a two-lane junction.

The speeds of the four vehicles are all 10m/s at the beginning time. The current distances between vehicle A, B, C, D and the junction areas is 20m, 10m, 15m and 30m respectively.

Suppose the four vehicles have identical dynamic properties. The maximum navigation speeds for them are all 10m/s before they enter the junction and 20m/s after they leave. The maximum steering speeds are all 5m/s.

The maximum control input is constrained by

$$-10\,m/s^2 \le u \le 10\,m/s^2 \tag{5.24}$$

The length of each vehicle is assumed as 4m. The safety headway L_1 defined in

(15) is chosen as 5m, while the safety headway L_2 defined in (20) is 7m.

Apparently, there exist several allowable driving plans. Let's take the trajectory planning process for the driving plan B | C | D | A as an example. It lets vehicle B, C, D and A pass the junction sequentially. The trajectory planning will be carried out for vehicle B, C, D and A sequentially.

1) the trajectory planning that vehicle B should adopt is Algorithm I.

   First, it will carry out a time optimal trajectory until it enters the junction areas. Obviously, this trajectory should begin at $t = 0$ s and end at $t = 1.125$ s. In the first 0.625s, vehicle B keeps speed at 10m/s, and then slows down with $u = -10 m/s^2$ in the next 0.5 s.

Suppose that vehicle B passes the junction areas within 1.5 s, and its speed becomes 4m/s when it leaves the junction areas. Then, it accelerates to 20m/s with $u = 10 m/s^2$ in the next 1.6 s. It will keep this speed in the rest of the planning. Thus, its speed profile should be what shown in Fig.5.9(a).

2) vehicle C will pass the junction areas right after vehicle B. Apparently, it should use planning Algorithm III.

Here, we divide its trajectory into three parts:

2.1) from $t = 0$ s to $t = 2.625$ s, it carries out a decelerate process to enlarge the headway between the virtual vehicle and itself;

2.2) it passes the junction areas after vehicle B;

2.3) it tracks the new head vehicle B.

The initial distance between vehicle C and virtual vehicle B is -2m. Mapping vehicle B into the lane of vehicle C, we can have the virtual vehicle's speed trajectory as shown in Fig.5.9(b).

To accurately solve the minimum tracking error problem (21) is difficult and unnecessary. Here, we adopt the following simple driving trajectory: first, it continuously decelerates with $u = -8m/s^2$ from $t = 0$ s to $t = 0.8$ s. Then, it keeps constant speed at 2m/s from $t = 0.8$ s to $t = 2.625$ s.

It should be pointed out that this speed profile is clear and easy to adopt for human drivers. Moreover, it is approximately optimal too.

Suppose vehicle C pass the junction areas in 1s with speed keeping at 2m/s. It accelerates to 20m/s with $u = 10m/s^2$ in the next 1.8 s and keeps this speed in the rest of our planning. Thus, the whole speed profile for vehicle C can be shown as Fig.5.9(c).

3) the trajectory of vehicle D follows Algorithm II.

It can be depicted as

3.1) decelerate with $u = -8m/s^2$ from $t = 0$ s to $t = 0.8$ s;

3.2) keeps speed at 2m/s from $t = 0.8$ s to $t = 4.625$ s;

3.3) after crossing the junction areas, it accelerates to 20m/s with $u = 10m/s^2$ in the next 1.8 s and keeps this speed in the rest of our planning. Fig.5.9(d) shows the speed profile for it.

4) finally, let's apply Algorithm III for vehicle A.

Similarly, we can get a simple speed profile as

4.1) decelerate to 0m/s with $u = -2.5m/s^2$ from $t = 0$ s to $t = 4$ s and stop in the next 0.625 s;

4.2) cross the junction in 1s and simultaneously accelerate to 2m/s.

4.3) accelerates to 20m/s with $u = 10m/s^2$ in the next 1.8 s and keeps this speed in the rest of our planning. The entire process is shown in Fig.5.9(e).

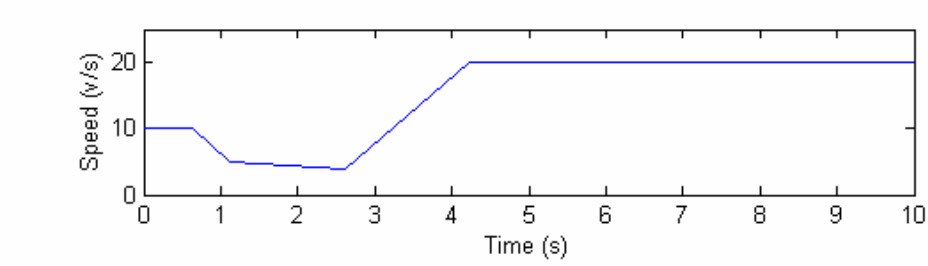

(a)

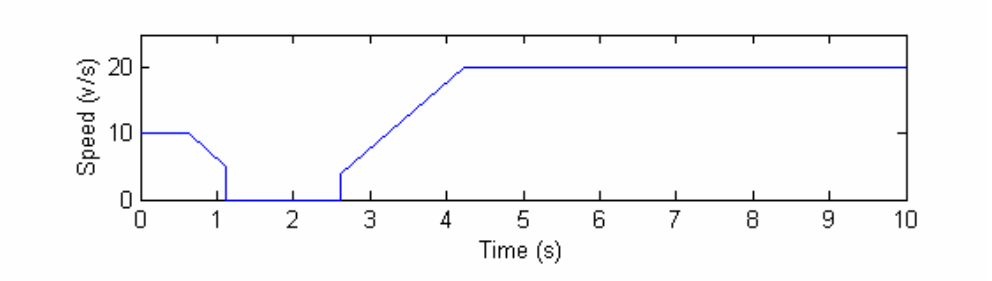
Speed (v/s)
20
10
0
0 1 2 3 4 5 6 7 8 9 10
Time (s)

(b)

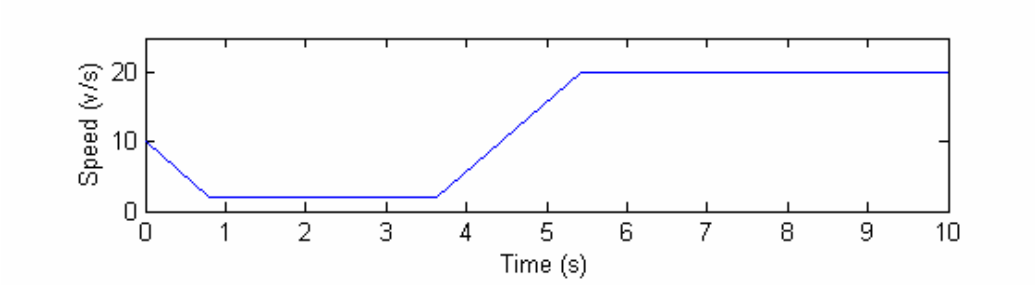
Speed (v/s)
20
10
0
0 1 2 3 4 5 6 7 8 9 10
Time (s)

(c)

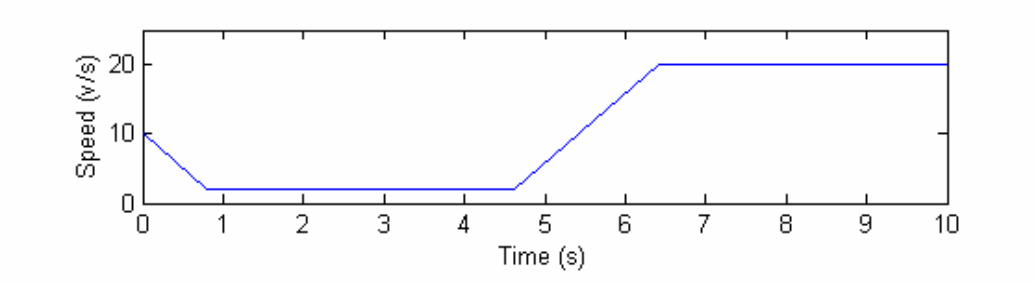
Speed (v/s)
20
10
0
0 1 2 3 4 5 6 7 8 9 10
Time (s)

(d)

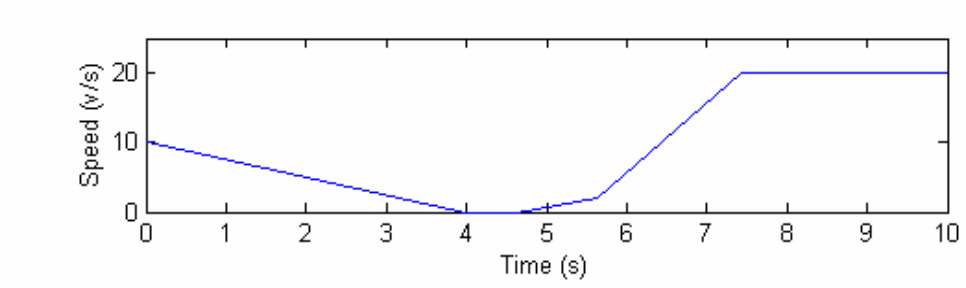

(e)

Figure 5.9 Speed profiles for vehicle B (a), virtual vehicle B (b), vehicle C (c), vehicle D (d) and vehicle A (e).

Thus, the total time consumed for driving plan B | C | D | A is 5.625 s. The time costs for other driving plans are also listed in Table.5.I. It is clear that the optimal driving plan may significantly save time for the entire traffic flow. In this case, the final optimal driving schedule is B | C | D | A.

Table 5.1 Comparison for Different Driving Plans

Driving Plan	Time Consumed
B | D | C | A	5.63s
B | A | D | C	6.55s
A | B | D | C	6.72s
A | D | C | B	6.83s
B | D | A | C	7.55s
……	……

5.5.2 Simulation Results for Inter-Vehicle Communication

To test our task managing strategy for communications in multi-car at blind crossings, a simple time division event-driven multi-agents communication model is set up and simulated.

There are four parameters in this model:

1. the communication group size;
2. the total number of vehicle;
3. the contacting rate. It is a probability that is used to describe how easy one “free” vehicle can get connected with another “free” vehicle. Here, “free” means that vehicles are not engaged in a conversation. The higher the contacting rate, the easier one free vehicle sets up a conversation with another free vehicle. This parameter is determined by the media, protocol and burden of the inter-vehicle communication networks. Apparently, a high burden will lead to a low contacting rate.
4. the forbidding time length. It is a number to describe how long one free vehicle should wait before it communicates again with the same vehicle that it has “talked” before. Notice that one vehicle prefers to receive new information other than obtain old information again and again from the same vehicle.

It is assumed that the data information will be transferred in a constant speed. When one free vehicle carries out conversation with another free vehicle, they will become occupied and do not response to other request.

By choosing different values of these parameters, we compare the effect of communication group size and forbidding time length. Fig.5.10 shows the average communication time with respect to different group sizes while the forbidding time length is chosen to be 1. Obviously, three is an appropriate size for an independent group in this case. Similar conclusions were reached for different forbidding time lengths.

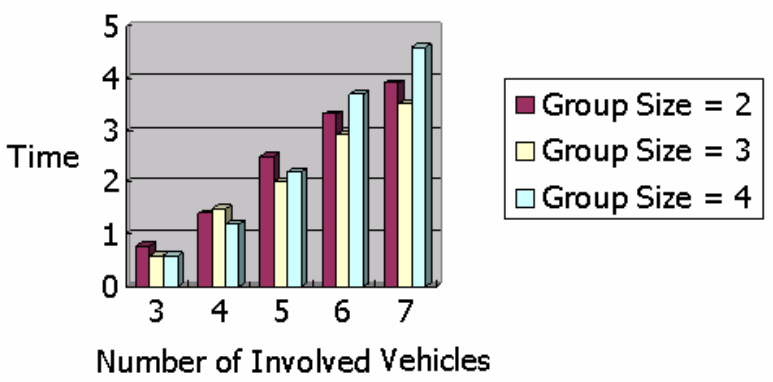

Figure 5.10 Average communication time with respect to different group sizes (forbidding time length = 1).

Fig.5.11 shows the average communication time with respect to different forbidding time length while group size is chosen as 3. It reveals that the forbidding time length should be mediate. However, there is not a simple rule to choose an

appropriate the forbidding time length for different group sizes and the total number of vehicles.

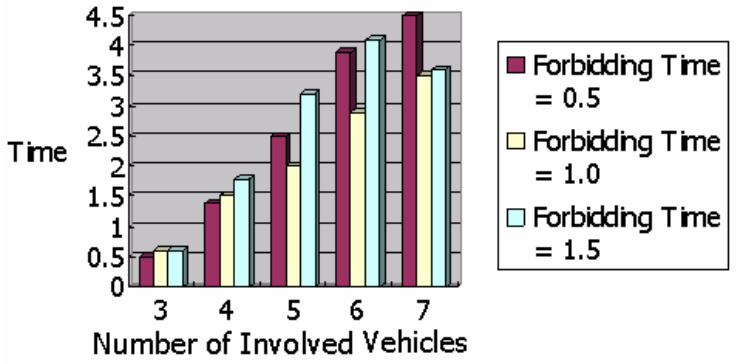

Figure 5.11 Average communication time with respect to different forbidding time lengths (group size = 3).

5.6 Discussions

Although our algorithms work well in many scenarios of driving at junctions in simulation, there are still several problems that need to be further addressed:

1) The complexity of this cooperative driving planning will increase quickly with the number of vehicles. How to generate the solution space more efficiently has to be further analyzed before the proposed algorithm applied in real applications. Besides, our simulations reveals that a periodic-turned traffic light system is really a simple yet effective solution for busy road crossings, i.e. if there are more than ten vehicles move toward the junction area simultaneously.

2) The actual driving scenario at junctions might be more complex than what we discussed here. One important case is how to deal with

emergencies, especially the sudden appearance of pedestrians. One potential answer is to share each vehicle's sensor information through the inter-vehicle communication as what has been discussed in [248]. If an emergence happens, the first 'known' vehicle will soon stop all the related vehicles synchronically. For example, as shown in Fig.5.12, an emergent halt signal sent out from vehicle A quickly stops vehicle B that intends to move to the blocked lane, when it suddenly 'sees' a bicycle on that lane. The cooperative driving plan will be regenerated when the detected obstacles moved away.

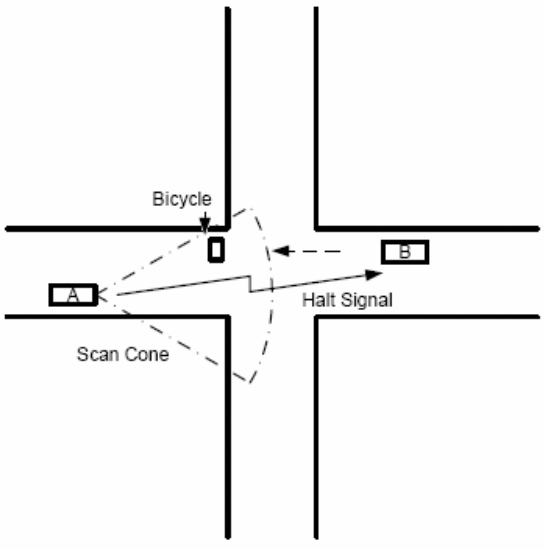

Figure 5.12 Handling an emergency case.

3) In this chapter, the speed and position of all the vehicles are assumed to be accurately measured. In case of colliding with the lead vehicle, the

headway for the steering direction and communication delay is often enlarged to counterbalance the measurement error. However, if the sensors on vehicle fail and send out wrong data, it may still cause severe accidents. Our framework does not provide a mechanism to detect such faults yet. One possible way to solve this problem is to introduce vehicle-to-road communication and let a road monitor system to check the potential faults.

4) The geometry constraints of vehicles and junction areas have not been well discussed in this chapter. However, they should not be neglected in real conditions. For instance, if a van truck steers from lane 1 to lane 8 as depicted in Fig.5.3, it may block off lane 2 at the same time. This problem can be solved by judging whether two vehicles form a safe driving pattern or not by considering both their moving directions and geometry characteristics.

CHAPTER 6 TIRE FAULT OBSERVER BASED ON ESTIMATION OF TIRE/ROAD FRICTION CONDITIONS

Many tire fault monitors are designed nowadays because tire failure is proved to be one of the main causes of traffic accidences. However, most of them are high in manufacturing cost and unreliable. This chapter is devoted to solve this problem and a new practical tire fault observer is proposed. Based on the new introduced dynamic tire/road friction model that considers external disturbances, the observer estimate and track the changes of tire/road friction conditions using only vehicle track forces and wheel angular velocity information. Tire fault diagnosis is carried out as follows. Since the wheel speed sensor is one basic component of normal anti-lock brake system (ABS), the observer proposed could be easily realized in low cost within an anti-lock brake system.

6.1 Introduction

Nowadays, people find out that many traffic accidences, extremely some really bad ones, are caused by tire failure. Therefore, to measure and monitor the tire and to determine the road surface friction in a cruising state well within the safe limit is quite important. In the last decade, there are numerous literatures on it. One basics way to solve this problem is to model tire/road friction and to estimate the related parameters online so as to monitor the state of the tire indirectly. The most often used description

of the tire/road model is a set of curves of the wheel slip with which the normalized friction force is defined. And based on it, the tire/road friction condition could be analyzed [277][278].

In this field, the two analytical models presented by Bakker et al. [279] are often used by researchers. In these two models, $\mu = F / F_n$ (where F denotes the Friction force and F_n denotes the normalize force) is mainly determined by the wheel slip s with regard to some other parameters such as speed. Here s is defined as

$$s = \begin{cases} 1 - \dfrac{r\omega}{v}, if\ v > r\omega, v \neq 0, braking \\ 1 - \dfrac{v}{r\omega}, if\ v < r\omega, \omega \neq 0, driving \end{cases}$$

in which r is the radius of the wheel, ω is the angular velocity, v is the longitudinal velocity.

The two curves shown in the following Fig.6.1, which is obtained by Harned et al. [280], demonstrates the typical relation between μ and s under different road conditions. However, this model lacks a physical interpretation and it's difficult to put into use for too many underdetermined parameters.

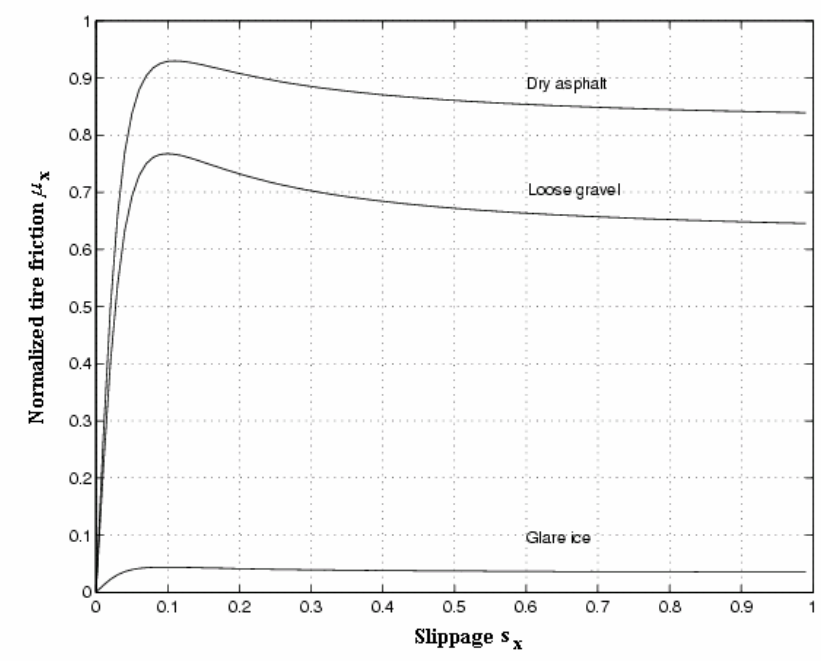

(a)

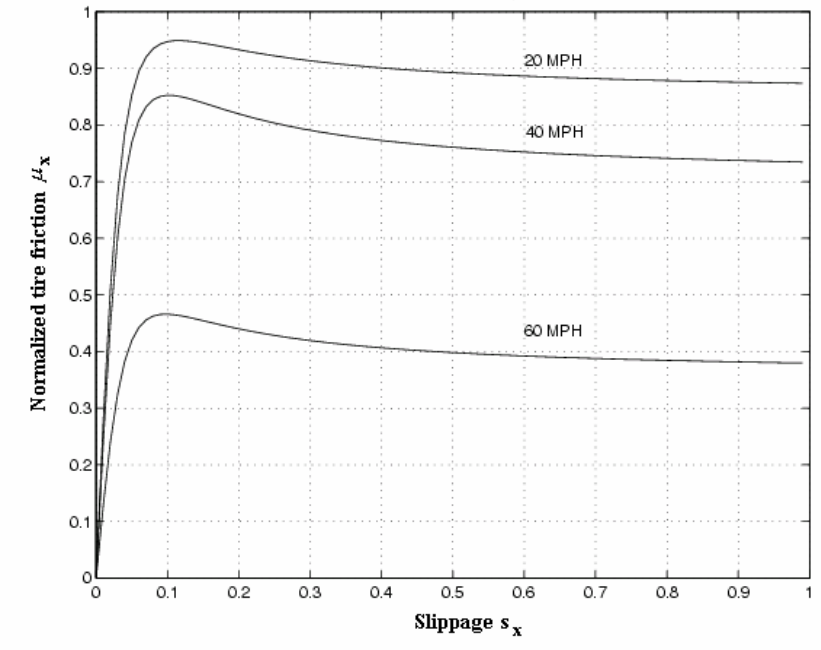

(b)

Figure 6.1 Typical tire/road friction profiles for: (a) vehicle running on different road surface conditions with velocity 20m/h, (b) vehicle running on dry asphalt road with different vehicle velocities [280].

Recently, dynamic friction models, such as the one presented by Candudas de Wit et al. in [281], have been proposed successfully to identify and compensate the friction in mechanical systems. In [282] Candudas de Wit et al. use the so called LuGre model to estimate a parameter in the model that reflects changes in the tire/road characteristics for the first time. In this chapter, both the angular and longitudinal velocity is assumed to be measurable. Since in some applications, the longitudinal velocity cannot be obtained, it's necessary to design an observer to estimate the slip ratio using the angular information only. In [283] and [284], Candudas de Wit, Jingang Yi and et al. formulate the model together with a new nonlinear observer to solve this problem.

This chapter is devoted to extend the approach of [285] and [286] in two ways. First, the inevitable disturbance of the model parameter is considered in the model since the actual road condition parameter should be varied within a certain range for a certain time. Second, a proper fault detection rule should be set associated with the system when it's used as a fault observer. In order to achieve these two goals, a modified model is proposed and a novel fault observer for the tire/road contact friction is constructed as following in this chapter based on strong practical stable theory.

6.2 Problem Formulation

A potential advantage of such models is their ability to describe closely some of

the physical phenomena found in road/tire friction (i.e. hysteresis loops, pre-sliding displacement, etc), and to depend on a parameter directly related with the phenomena to be observed, like for instance the change on the road characteristics (i.e. dry or wet). Dynamic models can be formulated as a lumped or distributed ones.

The lumped friction model proposed in Canudas-de-Wit and Tsiotras [282] is based on a similar dynamic friction model for contact-point friction problems developed previously, which is called LuGre model. The model given below has been proved to be a good approximation of distributed tire/road friction models that are able to represent the typical characteristics as the ones displayed by Fig.6.1.

$$\dot{z} = -v_r - \theta \frac{\sigma_0 |v_r|}{g(v_r)} z \tag{6.1}$$

$$F = (\sigma_0 z + \sigma_1 \dot{z} - \sigma_2 v_r) F_n \tag{6.2}$$

with $g(v_r) = \mu_c + (\mu_s - \mu_c) e^{-|v_r / v_s|^{1/2}}$.

Here σ_0 is the rubber longitudinal stiffness, σ_1 is the rubber longitudinal damping, σ_2 is the viscous relative damping, μ_s is the normalized static friction coefficient, and μ_c is the normalized Coulomb friction. v_s is the Stribeck relative velocity, F_n is the normal force, and $v_r = v - r\omega$ is the relative velocity. z is an introduced parameter denotes the internal friction state. Surfaces are very irregular at the microscopic level and two surfaces therefore make contact at a number of asperities. It could be viewed as two rigid bodies that make contact though elastic bristles. z could be viewed as the average deflection of those bristles.

And θ is an undetermined parameter of the tire/road condition on which we focus in this chapter. It will change with the variation of the road condition if the tire condition doesn't change. Under normal tire pressure, some typical data of it is: for dray asphalt conditions, $\theta = 1$; for wet asphalt conditions, $\theta = 2.5$ and for snow conditions, $\theta = 4$. The abnormal tire pressure will lead to significant variation of θ.

In most of the previous works, no disturbance is considered in the modeling process. However, the road condition could not be ideal and should be varied within a certain range. In this chatper, we model all the disturbance of into the variation of θ as following

$$\dot{\theta} = \varepsilon \tag{6.3}$$

where ε represent the certain stable stochastic disturbance process. Since the highway road condition doesn't vary abruptly, without lose any generality, we could assume this disturbance satisfies:

1) ε is bounded as $|\varepsilon| \le \tau$, $\tau > 0$;

2) θ is bounded, i.e. $|\theta - \bar{\theta}| = \left|\theta_0 + \int_0^t \varepsilon d\tau - \bar{\theta}\right| \le \Delta\theta_{\max}$, where θ_0 denotes the initial value of θ and $\bar{\theta}$ denotes the expectation of θ.

The value of τ and $\Delta\theta_{\max}$ should be determined by the actual environment. From the practical tests, we could see that these values are normally small. So

estimating and monitoring the value of θ, we could detect a fault if the value of θ becomes especially abnormal. In the following parts, we will see how to design a fault observer for θ and how to get a fault detection rule. Before further discussion, let's review some basic properties of this model.

Remark 6.1: the model has the following important properties:

(i) $1 \geq \mu_s \geq g(v_r) \geq \mu_c \geq 0, \ \forall v_r \in R;$

(ii) $f(v_r) = \dfrac{|v_r|}{g(v_r)}$ is positive and bounded and $f'(v_r)$ is also bounded, i.e.

$0 \leq f(v_r) \leq \rho_1, \qquad 0 \leq |f'(v_r)| \leq \rho_2, \ \forall v_r \in R.$

Considering the lumped tire/road friction model together with velocity dynamics, the estimation model can be formulated as following

$$m\dot{v} = 4F - \sigma_v mgv \tag{6.4}$$

$$J\dot{\omega} = -rF - u_T \tag{6.5}$$

where J and m is the inertia and ¼ mass of the wheel. The term σ_v is the rolling resistance coefficient and g is the gravity constant.

Assume that only the variable ω is measurable, and the lumped friction parameters with $\theta = 1$ has been identified offline (see table 1 for sample data from Triangle Tire Corporation).

Table 6.I Sample data of the off-line identification for LuGre Model

Parameter	Value	Unit

σ_0	25	1/m
σ_1	5	s/m
σ_2	0.1	s/m
μ_c	0.5	-
μ_s	0.9	-
v_s	12.5	m/s

6.3 Observer Design

Let's introduce the same change of coordinates in [280]: $x_1 = \sigma_0 z$, $x_2 = v$, $x_3 = v_r = v - r\omega$. From which we can get:

$$\dot{x}_1 = \sigma_0 \dot{z} = -\sigma_0 x_3 - \sigma_0 \theta \frac{|x_3|}{g(x_3)} x_1 \tag{6.6}$$

$$\dot{x}_2 = g[x_1 + \sigma_1(-x_3 - \theta \frac{|x_3|}{g(x_3)} x_1) - \sigma_2 x_3] - g\sigma_v x_2 \tag{6.7}$$

$$\dot{x}_3 = \dot{v} - r\dot{\omega} = \alpha[x_1 + \sigma_1(-x_3 - \theta \frac{|x_3|}{g(x_3)} x_1) - \sigma_2 x_3] - g\sigma_v x_2 + u_T \tag{6.8}$$

where $\alpha = g(1 + \frac{mr^2}{4J})$.

Define x, y respectively as $x = [x_1 \quad x_2 \quad x_3]^T$, $y = \frac{1}{r}(x_2 - x_3) = \omega$, and introduce $\varphi(x) = \frac{|x_3|}{g(x_3)} x_1$, we could rewrite the system as

$$\dot{x} = Ax + B\theta\varphi(x) + Eu_T \tag{6.9}$$

$$y = Cx \tag{6.10}$$

where $A = \begin{bmatrix} 0 & 0 & -\sigma_0 \\ -g & -g\sigma_v & -g(\sigma_1 + \sigma_2) \\ \alpha & -g\sigma_v & -\alpha(\sigma_1 + \sigma_2) \end{bmatrix}$, $B = \begin{bmatrix} -\sigma_0 \\ -g\sigma_1 \\ -\alpha\sigma_1 \end{bmatrix}$, $C = \begin{bmatrix} 0 & \frac{1}{r} & -\frac{1}{r} \end{bmatrix}$,

$$E = \begin{bmatrix} 0 \\ 0 \\ 1 \end{bmatrix}.$$

Notice that (A, C) is a observer pair, we can introduce the observer feedback matrix L and obtain the following observer structure which are like the ones proposed in [282] and [284]:

$$\dot{\hat{x}} = A\hat{x} + B\hat{\theta}\varphi(\hat{x}) - L(y - \hat{y}) + kB\,\mathrm{sgn}(y - \hat{y}) + Eu_T \tag{6.11}$$

$$\dot{\hat{\theta}} = \gamma_1 \varphi(\hat{x})(y - \hat{y}) \tag{6.12}$$

$$\hat{y} = C\hat{x} \tag{6.13}$$

where $k = \max_x \{x : 2\theta_{\max} |\varphi(x)|\}$. From above, we have $k < \infty$. And γ_1 is a positive real number that is introduced to adjust the variation rate of $\hat{\theta}$.

From the above observer, we can get the dynamics of the estimated error as

$$\dot{x}_e = \dot{x} - \dot{\hat{x}} = [A + LC]x_e + B[\theta\varphi(x) - \hat{\theta}\varphi(\hat{x})] - kB\,\mathrm{sgn}(y_e) \tag{6.14}$$

$$\dot{\theta}_e = \dot{\theta} - \dot{\hat{\theta}} = \varepsilon - \gamma_1 \varphi(\hat{x}) y_e \tag{6.15}$$

$$y_e = y - \hat{y} = Cx_e \tag{6.16}$$

Before we reach the main results, let's introduce the definition of the strong practical stable and a useful lemma.

Definition：if the solution of the dynamic system $\begin{cases} \dot{x} = f(t, x) \\ x(t_0) = x_0 \end{cases}$ exits for any initial value $x(t_0) = x_0$ during (t_0, ∞)， and there exits a positive real number d and a time $t_d > 0$ such that the solution satisfies $\|x(t)\| \le d$, for any $t \ge t_d$, this system is said to be strong practical stable with respect to d. Here $\|x\|$ denotes

$ess.\sup.\{|x|\}$.

Lemma 1 (see [287][288]): The dynamic system described in definition 1 is strong practical stable with respect to $d_0 = (r_1^{-1} \cdot r_2)(c)$, if there exits a first-order derivable positive function $V(\bullet): R^n \times R \to R^+$, a continuous positive infinity function $r_i(\bullet): R^+ \to R^+$, $i = 1,2$, and a positive infinity function $r_3(\bullet): R^+ \to R^+$ satisfies: a) there exits a positive real number c such that $r_3(\|x\|) > 0$ for any $x > c$ and $r_3(\|c\|) = 0$; b) $r_1(\|x\|) \le V(x,t) \le r_2(\|x\|)$; c) $\frac{\partial V(x,t)}{\partial t} = \nabla_x V(x,t) \cdot f(x,t) \le -r_3(\|x\|)$.

With this representation we shall now verify the following Theorem under the assumed condition holds.

Theorem 1: The observer error state system designed above is strong practical stable with respect to $\bar{d} = \sqrt{\frac{\lambda_{\max}(P) \cdot 4|\theta_e|_{\max} \tau + 4|\theta_e|^2_{\max}}{\lambda_{\min}(P) \cdot \lambda_{\min}(Q)} \cdot \frac{\gamma_2}{\gamma_1}}$, when there exit positive symmetric matrix P and Q satisfy the following equations

$$-Q = [A + LC]^T P + P[A + LC] \tag{6.17}$$

$$PB = \gamma_2 C^T \tag{6.18}$$

where γ_2 is a positive weighted number.

Proof: Considering the Lyapunov function $V(t,x) = x_e^T P x_e + \frac{\gamma_2}{\gamma_1}\theta_e^2$, Since

$$\theta\varphi(x) - \hat{\theta}\varphi(\hat{x}) = [\theta\varphi(x) - \theta\varphi(\hat{x})] + [\theta\varphi(\hat{x}) - \hat{\theta}\varphi(\hat{x})] = \theta[\varphi(x) - \varphi(\hat{x})] + \theta_e\varphi(\hat{x})$$

We should have

$$\dot{V} = x_e^T \{[A+LC]^T P + P[A+LC]\} x_e - k x_e^T PB \operatorname{sgn}(y_e) - k[B\operatorname{sgn}(y_e)]^T P x_e$$
$$+ x_e^T PB[\theta\varphi(x) - \hat{\theta}\varphi(\hat{x})] + [\theta\varphi(x) - \hat{\theta}\varphi(\hat{x})]^T B^T P x_e + 2\frac{\gamma_2}{\gamma_1}\theta_e[\varepsilon - \gamma_1\varphi(\hat{x})y_e]$$
$$= x_e^T \{[A+LC]^T P + P[A+LC]\} x_e - 2k\gamma_2 y_e \operatorname{sgn}(y_e)$$
$$+ 2\gamma_2 y_e[\theta\varphi(x) - \hat{\theta}\varphi(\hat{x})] + 2\frac{\gamma_2}{\gamma_1}\theta_e[\varepsilon - \gamma_1\varphi(\hat{x})y_e]$$
$$= x_e^T \{[A+LC]^T P + P[A+LC]\} x_e + 2\gamma_2 y_e\{[\theta\varphi(x) - \hat{\theta}\varphi(\hat{x})] + \theta_e\varphi(\hat{x})\}$$
$$- 2k\gamma_2 y_e \operatorname{sgn}(y_e) - 2\gamma_2\theta_e\varphi(\hat{x})y_e + 2\frac{\gamma_2}{\gamma_1}\theta_e\varepsilon$$
$$= x_e^T \{[A+LC]^T P + P[A+LC]\} x_e + 2\gamma_2\theta[\varphi(x) - \varphi(\hat{x})]y_e$$
$$- 2k\gamma_2 y_e \operatorname{sgn}(y_e) + 2\frac{\gamma_2}{\gamma_1}\theta_e\varepsilon$$

Based on the assumption, we should have

$$\left|\theta[\varphi(x) - \varphi(\hat{x})]\right| \le \theta_{\max}[\left|\varphi(x)\right| + \left|\varphi(\hat{x})\right|] \le 2k ,$$

Thus

$$2\gamma_2\theta[\varphi(x) - \varphi(\hat{x})]y_e - 2k\gamma_2 y_e \operatorname{sgn}(y_e) \le 0$$

And since $\left|\varepsilon\right| \le \tau$, we can have

$$\dot{V} \le x_e^T \{[A+LC]^T P + P[A+LC]\} x_e + 4\frac{\gamma_2}{\gamma_1}\left|\theta_e\right|_{\max}\tau$$

Notice (20), we should have

$$\dot{V} \le -\lambda_{\min}(Q)\left\|x_e\right\|^2 + 4\frac{\gamma_2}{\gamma_1}\left|\theta_e\right|_{\max}\tau$$

If we choose

$$r_1(\left\|x_e\right\|) = \lambda_{\min}(P)\left\|x_e\right\|^2, \quad r_2(\left\|x_e\right\|) = \lambda_{\max}(P)\left\|x_e\right\|^2 + 4\frac{\gamma_2}{\gamma_1}\left|\theta_e\right|_{\max}^2,$$

$$r_3(\left\|x_e\right\|) = \lambda_{\min}(Q)\left\|x_e\right\|^2 - 4\frac{\gamma_2}{\gamma_1}\left|\theta_e\right|_{\max}\tau$$

Then based on lemma 2, the observer error state system is strong practical stable

with respect to

$$\bar{d} = \sqrt{\frac{\lambda_{\max}(P)\cdot 4\left|\theta_e\right|_{\max}\tau + 4\left|\theta_e\right|^2_{\max}}{\lambda_{\min}(P)\cdot\lambda_{\min}(Q)}\cdot\frac{\gamma_2}{\gamma_1}}$$

Based on this result, if the tire in the steady state, and the observer output error should be bounded as

$$\left|y-\hat{y}\right| = \left|\frac{1}{r}[(x_2-\hat{x}_2)-(x_3-\hat{x}_3)]\right| \le \frac{1}{r}(\left|x_2-\hat{x}_2\right|+\left|x_3-\hat{x}_3\right|) \le \frac{2}{r}\bar{d}$$

Thus two fault detection rules can be formulated as:

1) trigger the fault alarm should if $\left|y-\hat{y}\right| > \frac{2}{r}\bar{d}$;

2) trigger the fault alarm should if $\left|\hat{\theta}-\bar{\theta}\right| > \Delta\theta_{\max}$.

The estimated value of $\hat{\theta}$ will indicate the approximate tendency of θ from which we can judge what type of error occurs. Generally, $\hat{\theta}$ will be abnormally big expected if the tire pressure is too high; $\hat{\theta}$ will be abnormally small if the tire pressure is too low. In the practice, τ and $\Delta\theta_{\max}$ could be determined by measurement. And a helpful Matlab toolbox that could be used to solve this LMI problem could be found in [286].

6.4 Simulation Results

Using the data given in Table 6.I and assuming

$$r = 0.2\text{m},\ \ m = 5\text{kg},\ \ J = 0.25kgm^2\text{kg},\ \ F_n = 15Kgm^2/s^2$$

we should have

$$A=\begin{bmatrix} 0 & 0 & -20 \\ -9.8 & -4.9 & -50.96 \\ 12.86 & -4.9 & -66.88 \end{bmatrix},\ B=\begin{bmatrix} -20 \\ -49 \\ -64.21 \end{bmatrix},\ C=\begin{bmatrix} 0 & 4 & -4 \end{bmatrix}$$

Choose

$$P=\begin{bmatrix} 1.0 & 0.1 & -0.3872 \\ 0.1 & 1.0 & -0.8552 \\ -0.3872 & -0.8552 & 0.8342 \end{bmatrix},\ L=\begin{bmatrix} 5 \\ 0 \\ 5 \end{bmatrix},\ Q=\begin{bmatrix} -11.92 & -7.14 & 7.65 \\ -7.14 & -31.63 & 28.39 \\ 7.65 & 28.39 & -26.82 \end{bmatrix}$$

we can have

$$\lambda_{\max}(P)=1.9,\ \lambda_{\min}(P)=0.006,\ \lambda_{\min}(Q)=0.67$$

Assume

$$\left|\theta_e\right|_{\max}=0.2,\ \tau=0.1,\ \gamma_1=20000,\ \gamma_2=1$$

we will have

$$\bar{d}=0.062 \text{ and } \left|y-\hat{y}\right|=0.495.$$

In the simulation process, the value of θ changes from 1 to 3 at $t=5$. The following Fig.6.2 and Fig.6.3 show the value of $y-\hat{y}=\omega-\hat{\omega}$, θ and $\hat{\theta}$ respectively. From the Fig.6.2, we can find that $y-\hat{y}=\omega-\hat{\omega}$ exceeds the threshold 0.495 immediately after $t=5$. $\hat{\theta}$ reaches the new value 3 soon after $t=5$, and reaches 3 at $t=7$. We can also see that the statistic characteristics of the error output changes, too. It's obvious that the fault alarm will be trigger in time.

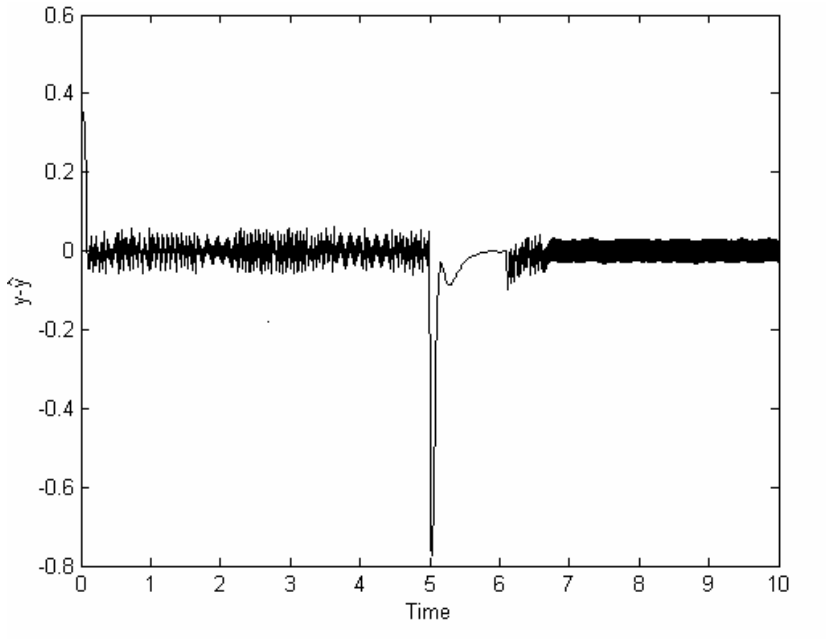

Figure 6.2 Variation of $y - \hat{y} = \omega - \hat{\omega}$ when the jump error occurs.

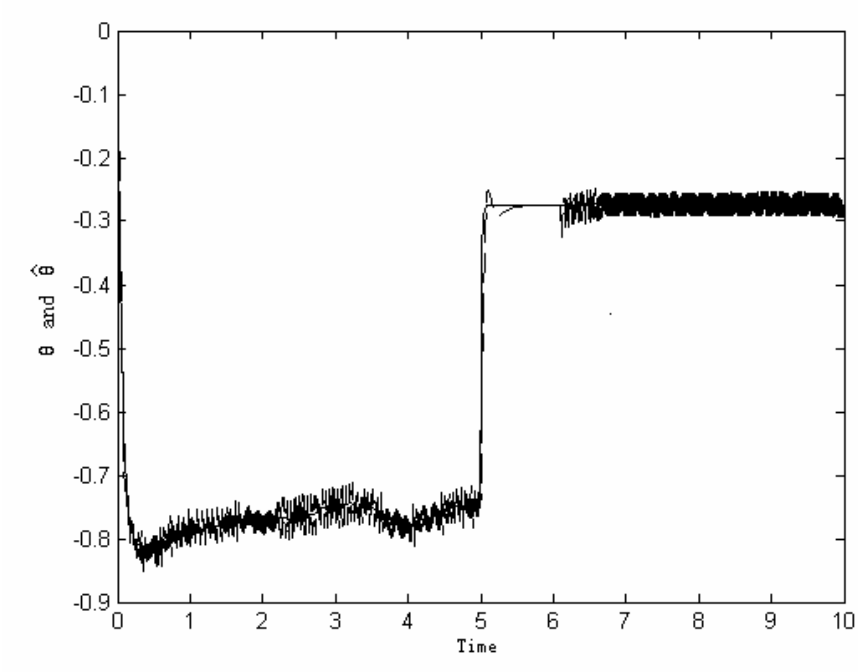

Figure 6.3 Variation of θ and $\hat{\theta}$ when the jump error occurs

Assume in the following simulation process, the value of θ shifts from 1 to 3 during $t = 5$ and $t = 10$. The following Fig.6.4 and Fig.6.5 show the value of $y - \hat{y} = \omega - \hat{\omega}$, θ and $\hat{\theta}$ respectively. From Fig.6.4 we can find that $y - \hat{y} = \omega - \hat{\omega}$ does not exceed the threshold 0.495. But $\hat{\theta}$ keeps following θ all the time. It's obvious that the fault alarm will be trigger in time, too.

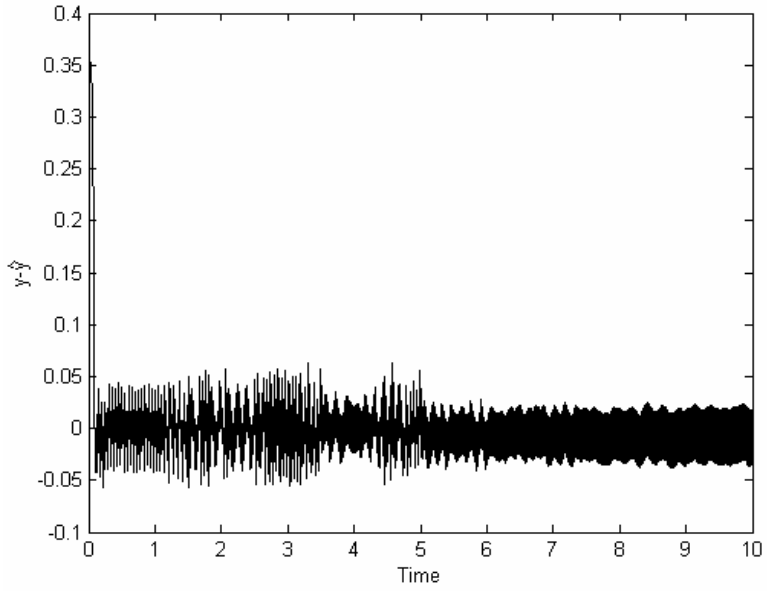

Figure 6.4 Variation of $y - \hat{y} = \omega - \hat{\omega}$ when the shift error occurs.

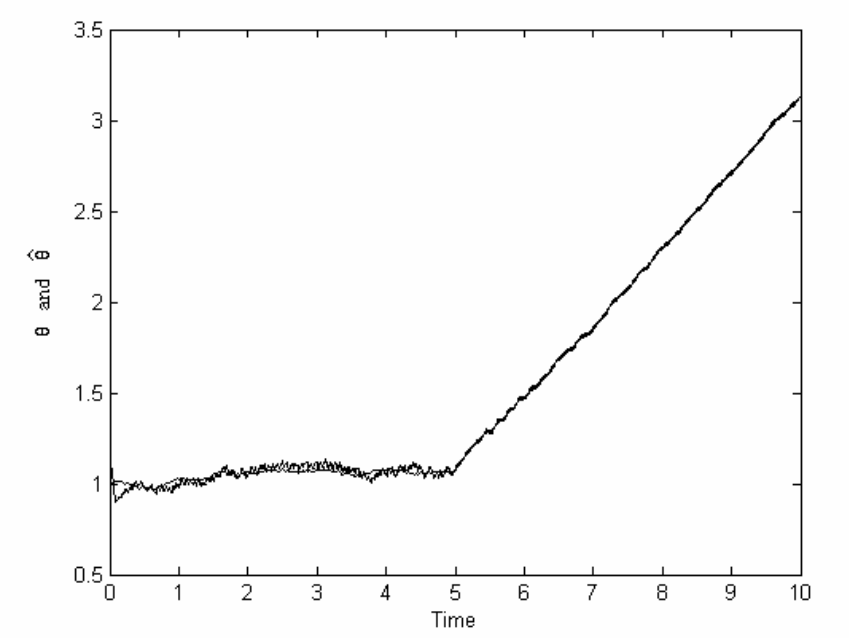

Figure 6.5 Variation of θ and $\hat{\theta}$ when the shift error occurs.

REFERENCES

[1] Ashley, S. (1998), Smart cars and automated highways, Mechanical Engineering Magazine.

[2] Bishop, R. (2000), A survey of intelligent vehicle applications worldwide, Proceedings of the IEEE Intelligent Vehicles Symposium, pp: 25-30.

[3] Broggi, A., Bertozzi, M., and Fascioli, A. (1999), ARGO and the MilleMiglia in Automatico Tour, IEEE Intelligent Systems, 14 (1), pp: 55-64.

[4] Broggi, A., Cellario, M., and Lombardi, P., et. al (2003), An evolutionary approach to visual sensing for vehicle navigation, IEEE Transactions on Industrial Electronics, 50 (1), pp: 18-29.

[5] Chowanietz, E. G. (1995a), Automobile electronics in the 1990s. Part 1: Powertrain electronics, Electronics & Communication Engineering Journal, 7 (1), pp: 23-36.

[6] Chowanietz, E. G. (1995b), Automobile electronics in the 1990s .Part 2: Chassis electronics, lectronics & Communication Engineering Journal, 7 (2), pp: 53-58.

[7] Claesson, V., Poledna, S. and Soderberg, J. (1998), The XBW model for dependable real-time systems, Proceedings of International Conference on Parallel and Distributed Systems, pp: 130-138.

[8] Darenberg, W. (1987), Automatische Spurfuhrung von Kraftfahrzeugen, Automobil-Industrie, pp: 155–159, (in German).

[9] Dravidam, U. and Tosunoglu, S. (1999), A survey on automobile collision avoidance system, Florida Conference on Recent Advances in Robotics, Gainesville, Florida.

[10] Eom, M. H., Han, E. Y., and Chang, H. S. (2001), Implementation of Internet-based land vehicle tracking system using Java, Proceedings of 2001 International Conferences on Info-tech and Info-net, 1, pp: 52–57.

[11] Fenton, R. E., Melocik, G. C. and Olson, K.W. (1976), On the steering of automated vehicles: Theory and experiment, IEEE Transactions on Automatic Control, 21, pp: 306–315.

[12] French, R., Noguchi, Y., and Sakamoto, K. (1994), International competitiveness in IVHS: Europe, Japan, and the United States," in Proceedings of 1994 Vehicle Navigation and Information Systems Conference, pp: 525–530.

[13] Fritz, H. (1995), Autonomous lateral road vehicle guidance using neural network controllers, Proceedings of Euroupean Control Conference, 3, pp: 285–290.

[14] Hatipoglu, C., Ozguner, U., and Redmill, K. A. (2003), Automated lane change controller design, IEEE Transactions on Intelligent Transportation Systems, 4 (1), pp: 13-22.

[15] Hayama, R., Nishizaki, K. and Nakano, S. et. al (2000), The vehicle stability control responsibility improvement using steer-by-wire, Proceedings of the IEEE Intelligent Vehicles Symposium, pp: 596-601.

[16] Hori, Y.; (2002), Future vehicle driven by electricity and control-research on four

wheel motored "UOT Electric March II", The 7th International Workshop on Advanced Motion Control, pp: 1-14.

[17] Huh, K., Seo, C. and Kim, J., et. al (1999), Active steering control based on the estimated tire forces, Proceedings of American Control Conference, 1, pp: 729-733.

[18] Jochem, T., Pomerleau, D., and Kumar, B., et. al (1995), PANS: a portable navigation platform, Proceedings of the Intelligent Vehicles '95 Symposium, pp: 107-112.

[19] Jones, W. D. (2002), Building safer cars, IEEE Spectrum, 39 (1), pp: 82-85.

[20] Kiencke, U. (2001), Future perspectives of automotive control, Proceedings of the 18th IEEE Instrumentation and Measurement Technology Conference, 3, pp: 1510-1518.

[21] Larsen, R. (1995), AVCS: an overview of current applications and technology, Proceedings of Intelligent Vehicles '95 Symposium, pp: 152-157.

[22] Li, L. and Wang, F.-Y. (2002), Vehicle trajectory generation for optimal driving guidance, Proceedings of the IEEE 5th International Conference on Intelligent Transportation Systems, pp: 231-235.

[23] Lygeros, J., Godbole, D. N., and Broucke, M. (2000), A fault tolerant control architecture for automated highway systems, IEEE Transactions on Control Systems Technology, 8 (2), pp: 205-219.

[24] Martin, A., Marini, H. and Tosunoglu, S. (1999a), Intelligent vehicle/highway system: a survey -Part 1, Florida Conference on Recent Advances in Robotics,

University of Florida, Gainesville, Florida.

[25] Martin, A., Marini, H. and Tosunoglu, S. (1999b), Intelligent vehicle/highway system: design of a blind spot detector using proximity sensors - Part 2, Florida Conference on Recent Advances in Robotics, University of Florida, Gainesville, Florida.

[26] Menig, P. and Coverdill, C. (1999), Transportation recorders on commercial vehicles, International Symposium on Transportation Recorders, Arlington, Virginia.

[27] Metz, D. and Williams, D. (1989), Near time-optimal control of racing vehicles, Automatica, Volume 25, Issue 6, Pages 841-857.

[28] Mirchandani, P. B. and Head, K. L. (2001), RHODES: A Real-Time Traffic Signal Control System: Architecture, Algorithms and Analysis, K. L. Transportation Research: Part B, pp: 415-432.

[29] National Automated Highway System Research Program: A Review, TRB Special Reports #253.

[30] Nobe, S. A. and Wang, F.-Y. (2001), An overview of recent developments in automated lateral and longitudinal vehicle controls, IEEE International Conference on Systems, Man, and Cybernetics, 5, pp: 3447-3452.

[31] Parsons, R. and Zhang, W. B. (1989), Program on advanced technology for the highway—Lateral guidance system requirements definition, in Proceedings of Interntional Conference on Application of Advanced Technology in Transportation Engineering, pp: 257–280.

[32] Patwardhan, S., Tan, H. S., and Guldner, J. (1997), A general framework for automatic steering control: System analysis, Proceedings of American Control Conference, pp. 1598–1602.

[33] Pohl, A., Steindl, R., and Reindl, L. (1999), The “intelligent tire” utilizing passive SAW sensors measurement of tire friction, IEEE Transactions on Instrumentation and Measurement, 48 (6), pp: 1041-1046.

[34] Puri, A. and Varaiya, P. (1995), Driving safely in smart cars, 1995 Proceedings of the American Control Conference, 5, pp: 3597-3599.

[35] Ribbens, W. (2002), Understanding Automotive Electronics, Newnes.

[36] Ronald K. Jurgen ed. (1999), Automotive Electronics Handbook, McGraw-Hill Professional.

[37] Schoner, H.-P. and Hille, P. (2000), Automotive power electronics. New challenges for power electronics, 2000 IEEE 31st Annual Power Electronics Specialists Conference, 1, pp: 6-11.

[38] Shladover, S. (1995), Review of the state of development of advanced vehicle control systems (AVCS), Vehicle System Dynamics, 24 (6-7), pp: 551-595.

[39] Simon, A. and Becker, J. C. (1999), Vehicle guidance for an autonomous vehicle, Proceedings of IEEE/IEEJ/JSAI International Conference on Intelligent Transportation Systems, pp: 429-434.

[40] Simon, A., Sohnitz, I., and Becker, J., et. al (2000), Navigation and control of an autonomous vehicle, The 9th IFAC Symposium on Control in Transportation Systems.

[41] Sohnitz, I. and Schwarze, K. (1999), Control of an autonomous vehicle: design and first practical results, Proceedings. 1999 IEEE/IEEJ/JSAI International Conference on Intelligent Transportation Systems, pp: 448-452.

[42] Tsugawa, S., Aoki, M., and Hosaka, A., et. al (1996), A survey of present IVHS activities in Japan, Proceedings of the 13th International Federation of Automatic Control World Congress, Q, pp: 147–152.

[43] Tsumura, T., (1994), AGV in Japan-recent trends of advanced research, development, and industrial applications, Proceedings of the IEEE/RSJ/GI International Conference on Intelligent Robots and Systems '94. 'Advanced Robotic Systems and the Real World', 3, pp: 1477-1484.

[44] Toy, C., Leung, K., and Alvarez, L., et. al (2002), Emergency vehicle maneuvers and control laws for automated highway systems, IEEE Transactions on Intelligent Transportation Systems, 3 (2), pp: 109-119.

[45] Vahidi, A. and Eskandarian, A. (2003), Research advances in intelligent collision avoidance and adaptive cruise control, IEEE Transactions on Intelligent Transportation Systems, 4 (3), pp: 143-153.

Varaiya, P. (1993), Smart cars on smart roads: problems of control, IEEE Transactions on Automatic Control, 38 (2), pp: 195-207.

[46] Wang, F.-Y., Shan, G., and Ding, Y., et. al. (2002), Research in intelligent tire and its key Technologies, Rubber Industry Sinica, 50 (12), pp: 713-719, (in Chinese).

[47] Wang, F.-Y., Tang, S., and Sui, Y., et. al (2003), Toward intelligent transportation

systems for the 2008 Olympics, IEEE Intelligent Systems, 18 (6), pp: 8-11.

[48] Wang, F.-Y., Wang, X., and Li, L., et. al (2003), Design and construction of a digital vehicle proving ground, IEEE Intelligent Systems, 18 (2), pp: 12-15.

[49] Weber, M. and Weisbrod, J. (2003), Requirements engineering in automotive development: experiences and challenges, IEEE Software, 20 (1), pp: 16-24.

[50] Yih, P., Ryu, J. and Gerdes, J. C. (2003), Modification of vehicle handling characteristics via steer-by-wire, Proceedings of American Control Conference, 3, pp: 2578-2583.

[51] Zhang, W., Shladover, S., and Hall, R., et. al (1994), A functional definition of automated highway systems, TRB Paper 940988.

[52] Zheng, N.-N., Tang. S., and Cheng, H., et. al (2004), Intelligent transportation systems - toward intelligent driver-assistance and safety warning systems, pp: 8-11.

[53] K. Chen and B. A. Galler, "An overview of intelligent vehicle-highway systems (IVHS) activities in North America", Proceedings of the 5th Jerusalem Conference on Information Technology, 'Next Decade in Information Technology', 1990. pp: 694-701.

[54]R. Larsen, "AVCS: an overview of current applications and technology", Proceedings of the Intelligent Vehicles Symposium, 1995, pp: 152-157.

[55]R. Bishop, "A survey of intelligent vehicle applications worldwide", Proceedings of the IEEE Intelligent Vehicles Symposium, 2000, pp: 25-30.

[56]V. Claesson, S. Poledna, and J. Soderberg, "The XBW model for dependable

real-time systems," Proceedings of International Conference on Parallel and Distributed Systems, 1998, pp: 130-138.

[57] K. Huh, C. Seo, and J. Kim, et. al, "Active steering control based on the estimated tire forces," Proceedings of American Control Conference, 1999, vol. 1, pp: 729-733.

[58] R. Hayama, K. Nishizaki, and S. Nakano, et. al, "The vehicle stability control responsibility improvement using steer-by-wire," Proceedings of the IEEE Intelligent Vehicles Symposium, 2000, pp: 596-601.

[59] P. Yih, J. Ryu, and J. C. Gerdes, "Modification of vehicle handling characteristics via steer-by-wire," Proceedings of American Control Conference, 2003, vol. 3, pp: 2578-2583.

[60] G. J. Morgan-Owen and G. T. Johnston, "Differential GPS positioning," Electronics & Communication Engineering Journal, 1995, vol. 7, no. 1, pp: 11-21.

[61] J. A. Farrel and M. Barth, The global positioning system & inertial navigation, McGraw-Hill, 1995.

[62] S. L. Miller, B. Youngberg, and A. Millie, et. al, "Calculating longitudinal wheel slip and tire parameters using GPS velocity," Proceedings of American Control Conference, 2001, vol. 3, pp: 1800-1805.

[63] D. M. Bevly, R. Sheridan, and J. C. Gerdes, "Integrating INS sensors with GPS velocity measurements for continuous estimation of vehicle sideslip and tire cornering stiffness," Proceedings of American Control Conference, 2001, vol. 1, pp: 25-30.

[64] F. X. Cao, D. K. Yang, and A. G. Xu, et. al, "Low cost SINS/GPS integration for

land vehicle navigation," Proceedings of The IEEE 5th International Conference on Intelligent Transportation Systems, 2002, pp: 910-913.

[65] F. Napolitano, T. Gaiffe, and Y. Cottreau, et. al., "PHINS: the first inertial navigation system based on fiber optic gyroscopes," Proceedings St Petersbourg International Conference on Navigation Systems, 2002.

[66] H. Edgar, Inertial measuring systems with fibreoptic gyroscopes, ATZ worldwide, 104, 2002.

[67] C.-Y. Chan, "Magnetic sensing as a position reference system for ground vehicle control," IEEE Transactions on Instrumentation and Measurement, 2002, 51 (1), pp: 43-52.

[68] J. I. Hernandez and C.-Y. Kuo, "Steering control of automated vehicles using absolute positioning GPS and magnetic markers," IEEE Transactions on Vehicular Technology, 2003, vol. 52, no. 1, pp: 150-161.

[69] S. M. Donecker, T. A. Lasky, and B. Ravani, "A mechatronic sensing system for vehicle guidance and control," IEEE/ASME Transactions on Mechatronics, 2003, vol. 8, no. 4, pp: 500-510.

[70] W. S. Wijesoma, K. R. S. Kodagoda, and A. P. Balasuriya, et. al, "Road edge and lane boundary detection using laser and vision," Proceedings of 2001 IEEE/RSJ International Conference on Intelligent Robots and Systems, 2001, vol. 3, pp: 1440-1445.

[71] M. Segel, "Theoretical prediction and experimental substantiation of the response

of the automobile to steering control," Proceedings of Automobile division of the institute of mechanical engineers, 1956, vol. 7, pp: 310–330.

[72]J. Kasselmann and T. Keranen, "Adaptive steering," Bendix Technical Journal, 1969, vol. 2, pp. 26-35.

[73]J. Ackermann, "Robust car steering by yaw rate control", Proceedings of the 29th IEEE Conference on Decision and Control, 1990, pp: 2033-2034.

[74]J. Ackermann and W. Dareberg, "Automatic track control of a city bus", IFAC Theory Report on Benchmark problems for Control systems design, 1990.

[75]J. Ackermann and W. Sienel, "Robust yaw damping of cars with front and rear wheel steering," IEEE Transactions on Control Systems Technology, 1993, vol. 1, no. 1, pp: 15-20.

[76]E. Bakker, H. B. Pacejka, and L. Lidner, "A new tire model with an application in vehicle dynamics studies," Proceedings of International Congress and Exposition, 1989, SAE paper 890087.

[77]H. B. Pacejka and R. S. Sharp, "Shear force development by pneumatic tires in steady state conditions: a review of modeling aspects," Vehicle Systems Dynamics, 1991, vol. 20, pp: 121-176.

[78]E. Ono, S. Hosoe, and D. Tuan, et. al, "Bifurcation in vehicle dynamics and robust front wheel steering control," IEEE Transactions on Control Systems Technology, 1998, vol. 6, no. 3, pp: 412-420.

[79]J. Stephant, A. Charara, and D. Meizel, "Virtual sensor: application to vehicle

sideslip angle and transversal forces, " IEEE Transactions on Industrial Electronics, 2004, vol. 51, no. 2, pp: 278-289.

[80] A. Alloum, "Modelisation et commande dynamique d'un vehicule pour la securite de conduite," Ph.D. thesis, U.T.C., Compiegne, France, 1994.

[81] U. Kiencke and A. Daiß, "Observation of lateral vehicle dynamics," Control Engineering Practice, 1997, vol. 5, no. 8, pp: 1145–1150.

[82] U. Kiencke and L. Nielsen, Automotive Control System, Berlin, Germany: Springer-Verlag, 2000.

[83] P. J. T. Venhovens and K. Naab, "Vehicle dynamics estimation using Kalman filters," Vehicle Systems Dynamics, 1999, vol. 32, pp. 171–184.

[84] K. Huh, J. Kim, and K. Yi, et. al, "Monitoring system design for estimating the lateral tire force", Proceedings of American Control Conference, 2002, vol. 2, pp: 875-880.

[85] J. R. Zhang, S. J. Xu, and A. Rachid, "Robust sliding mode observer for automatic steering of vehicles," Proceedings of IEEE Intelligent Transportation Systems, 2000, pp: 89-94.

[86] W. Perruquetti and J.-P. Barbot, Sliding Mode Control in Engineering, New York: Marcel Dekker, 2002.

[87] R. E. Fenton and I. Selim, "On the optimal design of an automotive lateral controller," IEEE Transactions on Vehicular Technology, 1988, vol. 37, no. 2, pp: 108-113.

[88] J. Farrelly and P. Wellstead, "Estimation of vehicle lateral velocity," Proceedings of the 1996 IEEE International Conference on Control Applications, 1996, pp: 552-557.

[89] J.-Y. Wang and M. Tomizuka, "Gain-scheduled H_∞ loop-shaping controller for automated guidance of tractor-semitrailer combination vehicles," Proceedings of American Control Conference, 2000, vol. 3, pp: 2033-2037.

[90] S. Ibaraki and M. Tomizuka, "Taming internal dynamics by mismatched and H_∞-optimized state observer," Proceedings of American Control Conference, 2000, vol. 1, no. 6, pp: 715-719.

[91] S. Ibaraki, S. Suryanarayanan, and M. Tomizuka, " H_∞ optimization of Luenberger state observers and its application to fault detection filter design," Proceedings of the 40th IEEE Conference on Decision and Control, 2001, vol. 2, pp: 1011-1016.

[92] Y. Aoki, T. Inoue, and Y. Hori, "Robust design of gain matrix of body slip angle observer for electric vehicles and its experimental demonstration", The 8th IEEE International Workshop on Advanced Motion Control, 2004, pp: 41-45.

[93] S. Saraf and M. Tomizuka, "Slip angle estimation for vehicles on automated highways," Proceedings of the American Control Conference, 1997, vol. 3, pp: 1588-1592.

[94] Y. U. Yim and S.-Y. Oh, "Modeling of vehicle dynamics from real vehicle measurements using a neural network with two-stage hybrid learning for accurate

long-term prediction," IEEE Transactions on Vehicular Technology, 2004, vol. 53, no. 4, pp: 1076-1084.

[95]L. Li, F.-Y. Wang and Q. Zhou, "A robust observer designed for vehicle lateral motion estimation," to be published soon.

[96]J. Ackermann and W. Sienel, "robust automatic steering of a bus," Proceedings of European Control Conference, 1993, pp: 1534-1539..

[97]J. Ackermann, J. Guldner, and W. Sienel, et. al, "Linear and nonlinear controller design for robust automatic steering", IEEE Transactions on Control Systems Technology, 1995, vol. 3, no. 1, pp:132-143.

[98]J. Ackermann, "Robust control prevents car skidding", IEEE Control Systems Magazine, 1997, vol. 17, no. 3, pp: 23-31.

[99]J. Guldner, W. Sienel, and H.-S. Tan, et. al, "Robust automatic steering control for look-down reference systems with front and rear sensors," IEEE Transactions on Control Systems Technology, 1999, vol. 7, no. 1, pp: 2-11.

[100] B. A. Francis, A course in H_∞ control theory, New York: Springer- Verlag, 1987.

[101] G. Zames, "Feedback and optimal sensitivity: Model reference transformations, multiplicative seminorms, and approximate inverses," IEEE Transactions on Automatic Control, 1981, vol. 26, pp: 301-320.

[102] B. A. Guvenc, T. Bunte, and D. Odenthal, et. al, "Robust two degree-of-freedom vehicle steering controller design," IEEE Transactions on Control

Systems Technology, 2004, vol. 12, no. 4, pp: 627-636.

[103] S. Mammar, "Lateral vehicle control using gain scheduled H_∞ controllers," Proceedings of IEEE Conference on Intelligent Transportation System, 1997, pp: 248-253.

[104] S. Mammar, V. B. Baghdassarian, and L. Nouveliere, "Speed scheduled vehicle lateral control", Proceedings of the 1999 IEEE/IEEJ/JSAI International Conference on Intelligent Transportation Systems, 1999, pp: 80-85.

[105] S. Mammar, D. Koenig, and L. Nouveliere, "Combination of feed-forward and feedback H_∞ control for speed scheduled vehicle automatic steering", Proceedings of American Control Conference, 2001, Vol. 2, pp: 684-689.

[106] H. Kuzuya and S. Shin, "Development of robust motor servo control for rear steering actuator based on two-degree-of-freedom control system," Mechatronics, 2000, vol. 10, no. 1-2, pp: 53-66.

[107] J. Ackermann and T. Bunte, "Actuator rate limits in robust car steering control," Proceedings of the 36th IEEE Conference on Decision and Control, 1997, vol. 5, pp: 4726-4731.

[108] J. Ackermann, "Robust decoupling, ideal steering dynamics, and yaw stabilization of 4WS cars," Automatica, 1994, vol. 30, pp: 1761-1768.

[109] J. Ackermann, "Robust decoupling of car steering dynamics with arbitrary mass distribution", Proceedings of American Control Conference, 1994, vol. 2, pp: 1964-1968.

[110] R. T. O'Brien, P. A. Iglesias, and T. J. Urban, "Lane change maneuver via H_∞ steering control methods," Proceedings of the 4th IEEE Conference on Control Applications, 1995, pp: 131-136.

[111] N. Sugitani, Y. Fujuwara, and K. Uchida, "Electric power steering with H-infinity control designed to obtain road information," Proceedings of American Control Conference, 1997, vol. 5, pp: 2935-2939.

[112] K.-T. Feng, H.-S. Tan and M. Tomizuka, "Automatic steering control of vehicle lateral motion with the effect of roll dynamics," Proceedings of American Control Conference, 1998, pp: 2248-2252.

[113] J. H. Park and W. S. Ahn, "H_∞ yaw-moment control with brakes for improving driving performance and stability," Proceedings of 1999 IEEE/ASME International Conference on Advanced Intelligent Mechatronics, 1999, pp: 747-752.

[114] J.-Y. Wang and M. Tomizuka, "Robust H_∞ lateral control of heavy-duty vehicles in automated highway system," Proceedings of American Control Conference, 1999, pp: 3671-3675.

[115] S. Brennan and A. Alleyne, "H-infinity vehicle control using nondimensional perturbation measures", Proceedings of American Control Conference, 2002, Vol. 3, pp: 2534-2539.

[116] C. Hatipoglu, H. Ozbay, and U. Ozguner, "H_∞ controller design for automatic steering of vehicles with modeled time delays," Proceedings of IEEE Conference on Intelligent Transportation System, 1997, pp: 260-265.

[117] S. Drakunov and R. DeCarlo, "Sliding mode control design for automated steering via Lyapunov approach", Proceedings of the 34th IEEE Conference on Decision and Control, 1995, Vol. 4, pp: 4086-4088.

[118] J. R. Zhang, A. Rachid, and S. J. Xu, "Velocity controller design for automatic steering of vehicles", Proceedings of American Control Conference, 2001, Vol. 2, pp: 696-697.

[119] R. G. Hebden, C. Edwards, and S. K. Spurgeon, "An application of sliding mode control to vehicle steering in a split-μ maneuver", Proceedings of American Control Conference, 2003, Vol. 5, pp: 4359-4364.

[120] J. R. Zhang, S. J. Xu, and A. Rachid, "Sliding mode controller for automatic path tracking of vehicles", Proceedings of American Control Conference, 2002, pp: 3974-3979.

[121] M. Tai, "Experimental study of lateral control of heavy vehicles for automated highway systems (AHS)," Proceedings of American Control Conference, 2002, vol. 2, pp: 851-856.

[122] C. Hatipoglu, U. Ozguner, and K. A. Redmill, "Automated lane change controller design", IEEE Transactions on Intelligent Transportation Systems, 2003, Vol. 4, 1, pp: 13-22.

[123] S. Brennan and A. Alleyne, "Driver assisted yaw rate control," Proceedings of American Control Conference, 1999, vol. 3, pp: 1697-1701.

[124] K. J. Astrom and B. Wittenmark, Computer controlled systems: theory and

design, Prentice-Hall, 1997.

[125] S. B. Choi, "The design of a look-down feedback adaptive controller for the lateral control of front-wheel-steering autonomous highway vehicles", IEEE Transactions on Vehicular Technology, 2000, Vol. 49, 6, pp: 2257-2269.

[126] A. Halanay, A. Ionita, and V. Rasvan, "Stability and manoeuvrability analysis of vehicle with four wheel steering system," Proceedings of the Third IEEE Conference on Control Applications, 1994, pp: 385-390.

[127] G. G. Lendaris, L. Schultz, and T. Shannon, "Adaptive critic design for intelligent steering and speed control of a 2-axle vehicle," Proceedings of IEEE-INNS-ENNS International Joint Conference on Neural Networks, 2000, vol. 3, pp: 73-78.

[128] D. Liu and H. D. Patino, "Adaptive critic designs for self-learning ship steering control," Proceedings of the 1999 IEEE International Symposium on Intelligent Control/Intelligent Systems and Semiotics, 1999, pp: 46-51.

[129] L. J. Schultz, T. Shannon, and G. G. Lendaris, "Using DHP adaptive critic methods to tune a fuzzy automobile steering controller," IFSA World Congress and 20th NAFIPS International Conference, 2001, vol. 1, pp: 557-562.

[130] G. L. Brown and J.C. Hung, "Vehicle steering assistance in extreme situations using a fuzzy logic controller," Proceedings of the IEEE International Conference on Industrial Technology, 1994, pp: 225-229.

[131] Z. Zalila, F. Bonnay, and F. Coffin, "Lateral guidance of an autonomous

vehicle by a fuzzy logic controller," IEEE International Conference on Systems, Man, and Cybernetics, 1998, vol. 2, pp: 1996-2001.

[132] N. E. Hodge and M. B. Trabia, "Steering fuzzy logic controller for an autonomous vehicle," Proceedings of 1999 IEEE International Conference on Robotics and Automation, 1999, vol. 3, pp: 2482-2488.

[133] A. El Kamel, J.-Y. Dieulot, and P. Borne, "Fuzzy controller for lateral guidance of busses," Proceedings of the 2002 IEEE International Symposium on Intelligent Control, 2002, pp: 110-115.

[134] K. R. S. Kodagoda, W. S. Wijesoma, and E. K. Teoh, "Fuzzy speed and steering control of an AGV," IEEE Transactions on Control Systems Technology, 2002, vol. 10, no. 1, pp: 112-120.

[135] L. Cai, A. B. Rad, and W. L. Chan, et. al, "A robust fuzzy pd controller for automatic steering control of autonomous vehicles," Proceedings of The 12th IEEE International Conference on Fuzzy Systems, 2003, vol. 1, pp: 549-554.

[136] A. B. Will, M. C. M. Teixeira, and S. H. Zak, "Four wheel steering control system design using fuzzy models," Proceedings of the 1997 IEEE International Conference on Control Applications, 1997, pp: 73-78.

[137] O. Pages, A. El Hajjaji, and R. Ordonez, "H_∞ tracking for fuzzy systems with an application to four wheel steering of vehicles," IEEE International Conference on Systems, Man and Cybernetics, 2003, vol. 5, pp: 4364-4369.

[138] A. El Hajjaji and S. Bentalba, "Fuzzy path tracking control for automatic

steering of vehicles," Robotics and Autonomous Systems, 2003, vol. 43, pp: 203-213.

[139] C. S. Kim, J. Y. Choi, and S. P. Hong, et. al, "H_∞ steering control for the unmanned vehicle system," The 27th Annual Conference of the IEEE Industrial Electronics Society, 2001, vol. 3, pp: 2139-2143.

[140] Y. Fujiwara and S. Adachi, "Steering assistance system for driver characteristics using gain scheduling control," European Control Conference, 2003.

[141] L. Li, F.-Y. Wang, G. Lai, "An LMI approach to robust vehicle steering controller design," to be published.

[142] J.-O. Hahn, J.-W. Hur, and K. Yi, et. al "Nonlinear vehicle stability control using disturbance observer", Proceedings of International Conference on Control Applications, 2002, Vol. 1, 2002, pp: 441-446.

[143] S. J. Xu and J. R. Zhang, "Nonlinear automatic steering control of vehicles based on Lyapunov approach," Proceedings of The IEEE 5th International Conference on Intelligent Transportation Systems, 2002, pp: 183-187.

[144] S. Chaib, M. S. Netto, and S. Mammar, "H_∞, adaptive, PID and fuzzy control: a comparison of controllers for vehicle lane keeping", Proceedings of IEEE Intelligent Vehicles Symposium, 2004, pp: 139-144.

[145] P. Raksincharoensak, M. Nagai, and H. Mouri, "Investigation of automatic path tracking control using four-wheel steering vehicle," Proceedings of the IEEE International Vehicle Electronics Conference, 2001, pp: 73-77.

[146] E. H. M. Lim and J. K. Hedrick, "Lateral and longitudinal vehicle control

coupling for automated vehicle operation", Proceedings of American Control Conference, 1999, Vol. 5, pp: 3676-3680.

[147] Y. Jia, "Robust control with decoupling performance for steering and traction of 4WS vehicles under velocity-varying motion", IEEE Transactions on Control Systems Technology, 2000, Vol. 8, 3, pp: 554-569.

[148] A. Alleyne and M. DePoorter, "Lateral displacement sensor placement and forward velocity effects on stability of lateral control of vehicles," Proceedings of American Control Conference, 1997, vol. 3, pp: 1593-1597.

[149] R. A. Hess and A. Modjtahedzadeh, "A control theoretic model of driver steering behavior," IEEE Control Systems Magazine, 1990, vol. 10, no. 5, pp: 3-8.

[150] T. Fujioka, Y. Shirano, and A. Matsushita, "Driver's behavior under steering assist control system," Proceedings of 1999 IEEE/IEEJ/JSAI International Conference on Intelligent Transportation Systems, 1999, pp: 246-251.

[151] T. Miyazaki, T. Kodama, and T. Furuhashi, et. al, "Modeling of human behaviors in real driving situations," Proceedings of IEEE Intelligent Transportation Systems, 2001, pp: 643-646.

[152] Y. Fujiwara and S. Adachi, "Control design of steering assistance system for driver characteristics," Proceedings of the 41st SICE Annual Conference, 2002, vol. 5, pp: 2879-2882.

[153] J. T. Spooner and K. M. Passino, "Fault tolerant longitudinal and lateral control for automated highway systems," Proceedings of American Control

Conference, 1995, vol. 1, pp: 663-667.

[154] V. Krishnaswami and G. Rizzoni, "Model based health monitoring of vehicle steering system using sliding mode observers," Proceedings of American Control Conference, 1995, vol. 3, pp: 1652-1656.

[155] V. Garg, A. E. Lindsey, "Fault detection for combined lateral and longitudinal control of vehicles for AHS," Proceedings of the 35th IEEE Decision and Control, 1996, vol. 2, pp: 2301-2302.

[156] R. Rajamani, A. S. Howell, and C. Chen, et. al, "A complete fault diagnostic system for automated vehicles operating in a platoon", IEEE Transactions on Control Systems Technology, 2001, vol. 9, 4, pp: 553-564.

[157] J. Huang and M. Tomizuka, "H_∞ controller for vehicle lateral control under fault in front or rear sensors," Proceedings of American Control Conference, 2001, vol. 2, pp: 690-695.

[158] A. Shrivastava and R. Rajamani, "Fault diagnostics for GPS-based lateral vehicle control," Proceedings of American Control Conference, 2001, vol. 1, pp: 31-36.

[159] S. Suryanarayanan, M. Tomizuka, and T. Suzuki, "Design of simultaneously stabilizing controllers and its application to fault-tolerant lane-keeping controller design for automated vehicles," IEEE Transactions on Control Systems Technology, 2004, vol. 12, no. 3, pp: 329-339.

[160] F.-Y. Wang, L. Li, and Q. Zhou, Selected topics in Intelligent Vehicles, World

Scientific Publishing Co., Singapore, 2004.

[161] W.-H. Ma and H. Peng, "Worst-case manoeuvres for the roll-over and jackknife of articulated vehicles," Proceedings of American Control Conference, 1998, Vol. 4, pp: 2263-2267.

[162] B.-C. Chen and H. Peng, H., "A real-time rollover threat index for sports utility vehicles," Proceedings of American Control Conference, 1999, Vol. 2, pp: 1233-1237.

[163] S. Takano and M. Nagai, "Dynamics control of large vehicles for rollover prevention," Proceedings of IEEE International Vehicle Electronics Conference, 2001, pp: 85-89.

[164] J. Ackermann and D. Odenthal, "Damping of vehicle roll dynamics by gain scheduled active steering," Proceedings of European Control Conference, 1999.

[165] D. Odenthal, T. Bunte, and J. Ackermann, "Nonlinear steering and braking control for vehicle rollover avoidance," Proceedings of European Control Conference, 1999.

[166] T. Acarman and U. Ozguner, "Rollover prevention for heavy trucks using frequency shaped sliding mode control," Proceedings of 2003 IEEE Conference on Control Applications, 2003, Vol. 1, pp: 7-12.

[167] K. Chen and B. A. Galler, "An overview of intelligent vehicle-highway systems (IVHS) activities in North America," Proceedings of the 5th Jerusalem Conference on Information Technology, 'Next Decade in Information Technology',

1990. pp: 694-701.

[168] R. Larsen, "AVCS: an overview of current applications and technology," Proceedings of the Intelligent Vehicles Symposium, 1995, pp: 152-157.

[169] R. Bishop, "A survey of intelligent vehicle applications worldwide," Proceedings of the IEEE Intelligent Vehicles Symposium, 2000, pp: 25-30.

[170] U. Kiencke and A. Daiß, "Observation of lateral vehicle dynamics," Control Engineering Practice, 1997, vol. 5, no. 8, pp: 1145–1150.

[171] U. Kiencke and L. Nielsen, Automotive Control System, Berlin, Germany: Springer-Verlag, 2000.

[172] P. J. T. Venhovens and K. Naab, "Vehicle dynamics estimation using Kalman filters," Vehicle Systems Dynamics, 1999, vol. 32, pp. 171–184.

[173] K. Huh, J. Kim, and K. Yi, et. al, "Monitoring system design for estimating the lateral tire force", Proceedings of American Control Conference, 2002, vol. 2, pp: 875-880.

[174] J. R. Zhang, S. J. Xu, and A. Rachid, "Robust sliding mode observer for automatic steering of vehicles," Proceedings of IEEE Intelligent Transportation Systems, 2000, pp: 89-94.

[175] W. Perruquetti and J.-P. Barbot, Sliding Mode Control in Engineering, New York: Marcel Dekker, 2002.

[176] J. Stephant, A. Charara, and D. Meizel, "Virtual sensor: application to vehicle sideslip angle and transversal forces," IEEE Transactions on Industrial Electronics,

2004, vol. 51, no. 2, pp: 278-289.

[177] R. E. Fenton and I. Selim, "On the optimal design of an automotive lateral controller," IEEE Transactions on Vehicular Technology, 1988, vol. 37, no. 2, pp: 108-113.

[178] J. Farrelly and P. Wellstead, "Estimation of vehicle lateral velocity," Proceedings of the 1996 IEEE International Conference on Control Applications, 1996, pp: 552-557.

[179] J.-Y. Wang and M. Tomizuka, "Gain-scheduled loop-shaping controller for automated guidance of tractor-semitrailer combination vehicles," Proceedings of American Control Conference, 2000, vol. 3, pp: 2033-2037.

[180] S. Ibaraki and M. Tomizuka, "Taming internal dynamics by mismatched and -optimized state observer," Proceedings of American Control Conference, 2000, vol. 1, no. 6, pp: 715-719.

[181] S. Ibaraki, S. Suryanarayanan, and M. Tomizuka, " optimization of Luenberger state observers and its application to fault detection filter design," Proceedings of the 40th IEEE Conference on Decision and Control, 2001, vol. 2, pp: 1011-1016.

[182] Y. Aoki, T. Inoue, and Y. Hori, "Robust design of gain matrix of body slip angle observer for Electric Vehicles and its experimental demonstration", The 8th IEEE International Workshop on Advanced Motion Control, 2004, pp: 41-45.

[183] S. Saraf and M. Tomizuka, "Slip angle estimation for vehicles on automated

highways," Proceedings of the American Control Conference, 1997, vol. 3, pp: 1588-1592.

[184] J. Ackermann, "Robust car steering by yaw rate control", Proceedings of the 29th IEEE Conference on Decision and Control, 1990, pp: 2033-2034.

[185] J. Ackermann and W. Dareberg, "Automatic track control of a city bus", IFAC Theory Report on Benchmark problems for Control systems design, 1990.

[186] J. Ackermann and W. Sienel, "Robust yaw damping of cars with front and rear wheel steering", IEEE Transactions on Control Systems Technology, 1993, vol. 1, no.1, pp: 15-20.

[187] J. Guldner, W. Sienel, and H.-S. Tan, et. al, "Robust automatic steering control for look-down reference systems with front and rear sensors," IEEE Transactions on Control Systems Technology, 1999, vol. 7, no. 1, pp: 2-11.

[188] W. S. Wijesoma, K. R. S. Kodagoda, and A. P. Balasuriya, et. al, "Road edge and lane boundary detection using laser and vision," Proceedings of 2001 IEEE/RSJ International Conference on Intelligent Robots and Systems, 2001, vol. 3, pp: 1440-1445.

[189] D. M. Bevly, R. Sheridan, and J. C. Gerdes, "Integrating INS sensors with GPS velocity measurements for continuous estimation of vehicle sideslip and tire cornering stiffness," Proceedings of American Control Conference, 2001, vol. 1, pp: 25-30.

[190] S. L. Miller, B. Youngberg, and A. Millie, et. al, "Calculating longitudinal

wheel slip and tire parameters using GPS velocity," Proceedings of American Control Conference, 2001, vol. 3, pp: 1800-1805.

[191] H. Edgar, Inertial measuring systems with fibreoptic gyroscopes, ATZ worldwide, 104, 2002.

[192] S. Boyd, L. El Ghaoui, and E. Feron, et. al, Linear Matrix Inequalities in System and Control Theory, SIAM Studies in Applied Mathematics, Philadelphia, 1994.

[193] K. M. Nagpal and P. P. Khargonekar, "Filtering and smoothing in an setting," IEEE Transaction on Automatic Control, 1992, vol. 36, no. 2, pp: 152-166.

[194] D.-W. Gu and F. W. Poon, "A robust state observer scheme," IEEE Transactions on Automatic Control, 2001, vol. 46, no. 12, pp: 1958-1963.

[195] M. Boutayeb and M. Darouach, "Comments on 'A robust state observer scheme'," IEEE Transactions on Automatic Control, 2003, vol. 48, no. 7, pp: 1292-1293.

[196] D.-W. Gu and F. W. Poon, "Authors' reply [Comment on 'A robust state observer scheme']," IEEE Transactions on Automatic Control, 2003, vol. 48, no. 7, pp: 1293-1294.

[197] K. Chen and B. A. Galler, "An overview of intelligent vehicle-highway systems (IVHS) activities in North America," Proceedings of the 5th Jerusalem Conference on Information Technology, 'Next Decade in Information Technology', 1990. pp: 694-701.

[198] R. Larsen, "AVCS: an overview of current applications and technology," Proceedings of the Intelligent Vehicles Symposium, 1995, pp: 152-157.

[199] R. Bishop, "A survey of intelligent vehicle applications worldwide," Proceedings of the IEEE Intelligent Vehicles Symposium, 2000, pp: 25-30.

[200] J. Ackermann, "Robust car steering by yaw rate control", Proceedings of the 29th IEEE Conference on Decision and Control, 1990, pp: 2033-2034.

[201] J. Ackermann and W. Dareberg, "Automatic track control of a city bus", IFAC Theory Report on Benchmark problems for Control systems design, 1990.

[202] J. Ackermann, J. Guldner, and W. Sienel, et. al, "Linear and nonlinear controller design for robust automatic steering", IEEE Transactions on Control Systems Technology, 1995, Vol. 3, 1, pp:132-143.

[203] J. Ackermann, "Robust decoupling of car steering dynamics with arbitrary mass distribution", Proceedings of American Control Conference, 1994, Vol. 2, pp: 1964-1968.

[204] J. Ackermann, "Robust control prevents car skidding", IEEE Control Systems Magazine, 1997, Vol. 17, 3, pp: 23-31.

[205] J. Ackermann and W, Sienel, "Robust control for automatic steering", Proceedings of American Control Conference, 1990, pp: 795-800.

[206] J. Guldner, W. Sienel, and H.-S. Tan, et. al, "Robust automatic steering control for look-down reference systems with front and rear sensors," IEEE Transactions on Control Systems Technology, 1999, vol. 7, no. 1, pp: 2-11.

[207] B. A. Francis, A course in H_∞ control theory, New York: Springer- Verlag, 1987.

[208] G. Zames, "Feedback and optimal sensitivity: Model reference transformations, multiplicative seminorms, and approximate inverses," IEEE Transactions on Automatic Control, 1981, vol. 26, pp: 301-320.

[209] B. A. Guvenc, T. Bunte, and D. Odenthal, et. al, "Robust two degree-of-freedom vehicle steering controller design," IEEE Transactions on Control Systems Technology, 2004, vol. 12, no. 4, pp: 627-636.

[210] S. Mammar, V. B. Baghdassarian, and L. Nouveliere, "Speed scheduled vehicle lateral control", Proceedings of the 1999 IEEE/IEEJ/JSAI International Conference on Intelligent Transportation Systems, 1999, pp: 80-85.

[211] D. J. N. Limebeer, E. M. Kasenally and J. D. Perkins, "On the design of robust two degree of freedom controllers," Automatica, 1993, vol. 29, no. 1, pp: 157-168.

[212] H. Kuzuya and S. Shin, "Development of robust motor servo control for rear steering actuator based on two-degree-of-freedom control system," Mechatronics, 2000, vol. 10, no. 1-2, pp: 53-66.

[213] J. Ackermann and T. Bunte, "Actuator rate limits in robust car steering control," Proceedings of the 36th IEEE Conference on Decision and Control, 1997, vol. 5, pp: 4726-4731.

[214] S. Drakunov and R. DeCarlo, "Sliding mode control design for automated

steering via Lyapunov approach", Proceedings of the 34th IEEE Conference on Decision and Control, 1995, vol. 4, pp: 4086-4088.

[215] R. G. Hebden, C. Edwards, and S. K. Spurgeon, "An application of sliding mode control to vehicle steering in a split-μ maneuver", Proceedings of American Control Conference, 2003, vol. 5, pp: 4359-4364.

[216] J. R. Zhang, S. J. Xu, and A. Rachid, "Sliding mode controller for automatic path tracking of vehicles", Proceedings of American Control Conference, 2002, pp: 3974-3979.

[217] G. L. Brown and J. C. Hung, "Vehicle steering assistance in extreme situations using a fuzzy logic controller," Proceedings of the IEEE International Conference on Industrial Technology, 1994, pp: 225-229.

[218] L. J. Schultz, T. T. Shannon, and G. G. Lendaris, "Using DHP adaptive critic methods to tune a fuzzy automobile steering controller", IFSA World Congress and 20th NAFIPS International Conference, 2001, vol. 1, pp: 557-562.

[219] L. Cai, A. B. Rad and W. L. Chan, et. al, "A robust fuzzy pd controller for automatic steering control of autonomous vehicles," The 12th IEEE International Conference on Fuzzy Systems, 2003, vol. 1, pp: 549-554.

[220] S. B. Choi, "The design of a look-down feedback adaptive controller for the lateral control of front-wheel-steering autonomous highway vehicles", IEEE Transactions on Vehicular Technology, 2000, vol. 49, 6, pp: 2257-2269.

[221] S. Chaib, M. S. Netto, and S. Mammar, "H_∞, adaptive, PID and fuzzy control:

a comparison of controllers for vehicle lane keeping", Proceedings of IEEE Intelligent Vehicles Symposium, 2004, pp: 139-144.

[222] M. Vidyasagar, "Optimal rejection of persistent bounded disturbances," IEEE Transactions on Automatic Control, 1986, vol. 31, pp: 527-535.

[223] S. Boyd, L. El Ghaoui, and E. Feron, et. al, Linear Matrix Inequalities in System and Control Theory, SIAM Studies in Applied Mathematics, Philadelphia, 1994.

[224] W. S. Wijesoma, K. R. S. Kodagoda, and A. P. Balasuriya, et. al, "Road edge and lane boundary detection using laser and vision," Proceedings of 2001 IEEE/RSJ International Conference on Intelligent Robots and Systems, 2001, vol. 3, pp: 1440-1445.

[225] H. Edgar, Inertial measuring systems with fibreoptic gyroscopes, ATZ worldwide, 104, 2002.

[226] D. M. Bevly, R. Sheridan, and J. C. Gerdes, "Integrating INS sensors with GPS velocity measurements for continuous estimation of vehicle sideslip and tire cornering stiffness," Proceedings of American Control Conference, 2001, vol. 1, pp: 25-30.

[227] S. L. Miller, B. Youngberg, and A. Millie, et. al, "Calculating longitudinal wheel slip and tire parameters using GPS velocity," Proceedings of American Control Conference, 2001, vol. 3, pp: 1800-1805.

[228] U. Kiencke and A. Daiß, "Observation of lateral vehicle dynamics," Control

Engineering Practice, 1997, vol. 5, no. 8, pp: 1145–1150.

[229] U. Kiencke and L. Nielsen, Automotive Control System, Berlin, Germany: Springer-Verlag, 2000.

[230] P. J. T. Venhovens and K. Naab, "Vehicle dynamics estimation using Kalman filters," Vehicle Systems Dynamics, 1999, vol. 32, pp. 171–184.

[231] J. R. Zhang, S. J. Xu, and A. Rachid, "Robust sliding mode observer for automatic steering of vehicles," Proceedings of IEEE Intelligent Transportation Systems, 2000, pp: 89-94.

[232] J. Stephant, A. Charara, and D. Meizel, "Virtual sensor: application to vehicle sideslip angle and transversal forces", IEEE Transactions on Industrial Electronics, 2004, vol. 51, no. 2, pp: 278-289.

[233] J. Abedor, K. Nagpal, and K. Poolla, "A linear matrix inequality approach to peak-to-peak gain minimization," International Journal of Robust and Nonlinear Control, 1996, vol. 6, pp: 899–927.

[234] S. R. Venkatesh and M. A. Dahleh, "Does star norm capture l1 norm?" Proceedings of American Control Conference, 1995, vol. 1, pp: 944-945.

[235] T. Nguyen and F. Jabbari, "Output feedback controllers for disturbance attenuation with bounded control," Proceedings of the 36th IEEE Conference on Decision and Control, 1997, vol. 1, pp: 177-182.

[236] T. Nguyen and F. Jabbari, "Disturbance attenuation for systems with input saturation: An LMI approach," IEEE Transactions on Automatic Control, 1999, vol.

44, no. 4, pp: 852-857.

[237] P. Gahinet, A. Nemirovskii, and A. J. Laub, et. al, "The LMI control toolbox," Proceedings of the 33rd IEEE Conference on Decision and Control, 1994, vol. 3, pp: 2038-2041.

[238] L. El Ghaoui, R. Nikoukhah, and F. Delebecque, "LMITOOL: a package for LMI optimization," Proceedings of the 34th IEEE Conference on Decision and Control, 1995, vol. 3, pp: 3096-3101.

[239] V. B. Kolmanovskii and J.-P. Richard, "Stability of some linear systems with delays," IEEE Transactions on Automatic Control, 1999, vol. 44, no. 5, pp: 984-989.

[240] El-K. Boukas and Z.-K. Liu, Deterministic and stochastic time delay Systems, Birkhäuser, 2002.

[241] L. Li, F.-Y. Wang, "Trajectory generation for driving guidance of front wheel steering vehicles," Proceedings of IEEE Intelligent Vehicles Symposium, 2003, pp: 231-236.

[242] L. Li and F.-Y. Wang, "A design framework for driver/passenger-oriented trajectory planning," Proceedings of the IEEE 6th International Conference on Intelligent Transportation Systems, 2003, pp: 1764-1769

[243] F.-Y. Wang and L. Li, "Optimal guideline design for curve steering and lane change," Proceedings of IEEE International Conference on Networking, Sensing and Control, 2005.

[244] S. Tsugawa, "Inter-vehicle communications and their applications to

intelligent vehicles: an overview," IEEE Intelligent Vehicle Symposium, 2002, vol. 2, pp: 564-569.

[245] S. Tsugawa, T. Saito, and A. Hosaka, "Super smart vehicle system: AVCS related systems for the future," Proceedings of the Intelligent Vehicles 1992 Symposium, 1992, pp: 132-137.

[246] M. Nakamura, H. Kawashima, and T. Yoshikai, et. al, "Road-vehicle cooperation driving system," Proceedings of 1994 Vehicle Navigation and Information Systems Conference, 1994, pp: 425-430.

[247] J. K. Hedrick, M. Tomizuka, and P. Varaiya, "Control issues in automated highway systems," IEEE Control Systems Magazine, 1994, vol. 14, no. 6, pp: 21-32.

[248] A. R. Girard, J. B. de Sousa, and J. A. Misener, et. al, "A control architecture for integrated cooperative cruise control and collision warning systems," Proceedings of the 40th IEEE Conference on Decision and Control, 2001, vol. 2, pp: 1491-1496.

[249] O. Gehring and H. Fritz, "Practical results of a longitudinal control concept for truck platooning with vehicle to vehicle communication," IEEE Conference on Intelligent Transportation System, 1997, pp: 117-122.

[250] S. Kato, S. Tsugawa, and K. Tokuda, et. al, "Vehicle control algorithms for cooperative driving with automated vehicles and intervehicle communications," IEEE Transactions on Intelligent Transportation Systems, 2002, vol. 3, no. 3, pp: 155-161.

[251] A. M. K. Cheng and K. Rajan, "A digital map/GPS based routing and addressing scheme for wireless ad-hoc networks," Proceedings of IEEE Intelligent

Vehicles Symposium, 2003, pp: 17-20.

[252] J.-P. Hubaux, S. Capkun, and J. Luo, "The Security and Privacy of Smart Vehicles," IEEE Security & Privacy Magazine, vol. 2, no. 3, 2004, pp: 49-55.

[253] L. Chisalita and N. Shahmehri, "A peer-to-peer approach to vehicular communication for the support of traffic safety applications," Proceedings of the IEEE 5th International Conference on Intelligent Transportation Systems, 2002, pp: 336-341.

[254] J. Blum, A. Eskandarian, and L. J. Hoffman, "Performance characteristics of inter-vehicle ad hoc networks," Proceedings of 2003 IEEE Intelligent Transportation Systems, 2003, vol. 1, pp: 114-119.

[255] Y. Chang and K. Kurami, "Longitudinal guidance and control for the entry of vehicles onto automated highways," Proceedings of the 32nd IEEE Conference on Decision and Control, 1993, vol.2, pp: 1891-1896.

[256] P. Kachroo and Z. Li, "Vehicle merging control design for an automated highway system," IEEE Conference on Intelligent Transportation System, 1997, pp: 224-229.

[257] J. W. Choi, T. H. Fang, and S. Kwong, et. al, "Remote-controlled platoon merging via coder-estimator sequence algorithm for a communication network," IEEE Transactions on Industrial Electronics, 2003, vol. 50, no. 1, pp: 30-36.

[258] S. Joo, X. Y. Lu, and J. K. Hedrick, "Longitudinal maneuver design in coordination layer for automated highway system," Proceedings of the 2003 American

Control Conference, 2003, vol. 1, pp: 42-47.

[259] S. Arora, A. K. Raina, and A. K. Mittal, "Collision avoidance among AGVs at junctions," Proceedings of the IEEE Intelligent Vehicles Symposium, 2000, pp: 585-589.

[260] R. Lachner, "Collision avoidance as a differential game: real-time approximation of optimal strategies using higher derivatives of the value function," 1997 IEEE International Conference on Systems, Man, and Cybernetics, 'Computational Cybernetics and Simulation', 1997, Vol. 3, pp: 2308-2313.

[261] J. Kaltwasser and J. Kassubek, "A new cooperative optimized channel access for inter-vehicle communication," Proceedings of Vehicle Navigation and Information Systems Conference, 1994, pp: 145-148.

[262] R. Verdone, "Communication systems at millimeter waves for ITS applications," 1997 IEEE 47th Vehicular Technology Conference, 1997, vol. 2, pp: 914-918.

[263] K. Tokuda, M. Akiyama, and H. Fujii, "DOLPHIN for inter-vehicle communications system," Proceedings of the IEEE Intelligent Vehicles Symposium, 2000, pp: 504-509.

[264] I. R. Porche, K. S. Chang, and W. Li, et. al, "Real time task manager for communications and control in multicar platoons," Proceedings of the Intelligent Vehicles Symposium, 1992, pp: 409-414.

[265] N. Reijers, R. Cunningham and R. Meier, et. al, "Using group

communication to support mobile augmented reality applications," Proceedings of the Fifth IEEE International Symposium on Object-Oriented Real-Time Distributed Computing, 2002, pp: 297-306.

[266] L. Chisalita and N. Shahmehri, "A peer-to-peer approach to vehicular communication for the support of traffic safety applications," Proceedings of The IEEE 5th International Conference on Intelligent Transportation Systems, 2002, pp: 336-341.

[267] P. Mohapatra, G. Chao and J. Li, "Group communications in mobile ad hoc networks," Computer, 2004, vol. 37, no. 2, pp: 52-59.

[268] J. P. Singh, N. Bambos, and B. Srinivasan, et. al, "Wireless LAN performance under varied stress conditions in vehicular traffic scenarios," Proceedings of IEEE 56th Vehicular Technology Conference, 2002, vol. 2, pp: 743-747.

[269] W. Kremer, "Vehicle density and communication load estimation in mobile radio local area networks (MR-LANs)," IEEE 42nd Vehicular Technology Conference, 1992, vol. 2, pp: 698-704.

[270] H. Fujii, M. Akiyama, K. Tokuda, "Inter-vehicle communications protocol for group cooperative driving," IEEE VTS 50th Vehicular Technology Conference, 1999, vol. 4, pp: 2228-2232.

[271] A. Uno, T. Sakaguchi, and S. Tsugawa, "A merging control algorithm based on inter-vehicle communication," Proceedings of 1999 IEEE/IEEJ/JSAI International

Conference on Intelligent Transportation Systems, 1999, pp: 783-787.

[272] T. Sakaguchi, A. Uno, and S. Kato, et. al, "Cooperative driving of automated vehicles with inter-vehicle communications," Proceedings of the IEEE Intelligent Vehicles Symposium, 2000, pp: 516-521.

[273] L. Wu, Y. Xu, and F.-Y. Wang, et. al, "Supervised learning of longitudinal driving behavior for intelligent vehicles using neuro-fuzzy networks: initial experimental results," International Journal of Intelligent Control and Systems, 1999, vol. 3, no. 4, pp: 443-463.

[274] Y. T. Lin, F.-Y. Wang, and P. B. Mirchandani, et. al, "Implementing adaptive driving systems for intelligent vehicles by using neuro-fuzzy networks", Transportation Research Record, No. 1774 , 2001, pp: 98-105.

[275] F.-Y. Wang, P.B. Mirchandani, and Z. Wang, "The VISTA project and its applications," IEEE Intelligent Systems, vol. 17, no. 6, pp: 72-75.

[276] F.-Y. Wang, L. Li, and Q. Zhou, Selected topics in Intelligent Vehicles, World Scientific Publishing Co., Singapore, 2004.

[277] F.-Y. Wang, G. Shan, and L. Li, et. al., "The Integrated Triangle Testbed System for Intelligent Tires and the Corresponding Research on its Key Technologies," Tire Industry Sinica, 2003, vol. 23, no. 1, pp: 10-15.

[278] F.-Y. Wang, G. Shan, Y. Ding, and L. Li, et. al., "Research in Intelligent Tire and its Key Technologies," Rubber Industry Sinica, 2002, vol. 50, no. 12, pp: 713-719.

[279] E. Baker, L. Nyborg, and H. Pacejka, "Tire modeling for use in vehicle dynamic

studies," SAE# 870421.

[280] J. Harned, L. Johnston, and G. Scharpf, "Measurement of tire brake force characteristics as related to wheel slip (antiblock) control system design," SAE Transactions, 1969, 78(690214), pp: 909-925.

[281] C. Canudas de Wit, H. Olsson, and K. J. Astrom, et. al, "A new model for control of systems with friction," IEEE Transactions on Automatic Control, 1995, vol.40, no. 3, pp: 419-425.

[282] C. Canudas de Wit and P. Tsiotras, "Dynamic tire friction models for vehicle traction control," Proceedings of the 38th IEEE Conference on Decision and control, 1999, vol. 4, pp: 3746-3751.

[283] C. Canudas-de-Wit and R. Horowitz, "Observers for tire/road contact friction using only wheel angular velocity information, " Proceedings of IEEE Conference on Decision and Control, 1999, pp: 3932-3937.

[284] Y. Jingang, L. Alvarez, and X. Claeys, et. al, "Emergency braking control with an observer-based dynamic tire/road friction model and wheel angular velocity information," Proceedings of American Control Conference, 2001, vol. 1, pp: 19-24.

[285] Young Man Cho，Rajamani, R., "A systematic approach to adaptive observer synthesis for nonlinear systems," IEEE Transactions on Automatic Control, 1997, Vol.42, (4), pp: 534-537.

[286] L. El Ghaoui, R. Nikoukhah, and F. Delebecque, "LMITOOL: a package for LMI optimization," Proceedings of IEEE Conference on Decision and Control, 1997,

vol. 3, pp: 3096-3101.

[287] L. Huang，Stability Theory，Beijing，Beijing University Press，1992.

[288] X. Liao, Stability's theory, method and applications, Wuhan, Huazhong University of Science and Technology Press, 1999.